The Hong Kong Polytechnic University

Department of Applied Biology and Chemical Technology

Properties of fluorophore-labeled derivatives of Class A beta-lactamases

Au Ho Wah

A thesis submitted in partial fulfillment for the requirements for the Degree of Master of Philosophy in The Hong Kong Polytechnic University

Aug 2006

CERTIFICATE OF ORIGINALITY

I hereby declare that this thesis is my own work and that, to the best of my knowledge and belief, it reproduces no material previously published or written, nor material that has been accepted for the award of any other degree or diploma, except where due acknowledgement has been made in the text.

Au Ho Wah

Abstract

The intensive use of beta-lactam antibiotics, such as penicillins and cephalosporins, has led to food contamination and the emergence of antibiotic-resistant bacteria. This is a very serious problem as it may reduce the efficacy of antibiotics and make them no longer able to kill the resistant infectious bacteria. This situation keeps worsening due to the evolution process of the bacteria. As a result, an effective detection method for any residual antibiotics and strategies to discover new effective beta-lactam drugs and beta-lactamase inhibitors are urgently required.

Previously, the novel fluorescence biosensor (PenPC_E166Cf), derived from beta-lactamase I of *Bacillus cereus* 569/H, demonstrated its success in detecting beta-lactam antibiotics and beta-lactamase inhibitors. Its development opened up a new arena for antibiotic detection and novel drug screening. In order to evaluate the feasibility of using other class A beta-lactamases for the biosensor construction, four fluorescence biosensors (PenP_E166Cf, PenP_E166Cb, PenP_E166Cf/N170Q and PenP_E166Cb/N170Q) were developed in this study by a similar approach, using the PenP beta-lactamase of *Bacillus licheniformis* 749/C as the basis. The PenP beta-lactamase is 58% identical to PenPC in the amino acid sequence but is more thermostable. Two PenP beta-lactamase mutants, E166C and E166C/N170Q, were constructed in the project. Mutations of E166C and N170Q were found to cause a dramatic decrease in the activity of the PenP beta-lactamase, in which the catalytic efficiencies of the E166C and E166C/N170Q were approximately 4×10^4-fold and 1.2×10^5-fold lower than that of the wild-type, respectively. The PenP biosensors showed the ability in detecting penicillins

such as penicillin G and penicillin V, and cephalosporins such as cefotaxime and moxalactam. The detection limits of the biosensors for these beta-lactam antibiotics were approximately 10 nM. Biosensors developed from the double mutants gave longer detectable signals than those developed from the single mutants, because of the further suppressed deacylation of enzyme by the N170Q mutation. Apart from the detection of antibiotics, the capability of the PenP biosensors in signal generation in the presence of beta-lactamase inhibitors, such as sulbactam and clavulanate, may allow them to find their applications in drug discovery. However, in terms of developing a sensing system for detecting beta-lactams and screening beta-lactamase inhibitors, PenP biosensors labeled with fluorescein-5-maleimide seem to be more useful than the badan-labeled counterparts, because the formers confer a higher quantum yield with a lower incidence of false results.

In comparison with the PenPC-based biosensors developed previously, the PenPC_E166Cb seems to be the best biosensor in detecting penicillin-type antibiotics because of its ability to generate significant and long detectable signals with a good detection limit. PenP_E166Cf seems to be the best in detecting cephalosporin-type antibiotics as it gave significant stable signals with a fast response time and a low incidence of false results. The PenP-based biosensors, which functioned well at temperature as high as 50 ^{o}C, also demonstrated their high thermostability.

Acknowledgements

I am deeply appreciative to my chief-supervisor, Dr. Thomas Y. C. Leung, for his diligent guidance and support throughout my study. I am also indebted to my co-supervisor, Professor K. Y. Wong, for his helpful advice and constructive critique.

Enormous thanks must go to the teammates of the biosensor research group for their valuable advice and assistance. I would like to thank Kin for performing the ESI-MS analysis. Special thanks are given to Emily for her kind support and patience. She taught me a lot of skills and was always available when I needed her help and advice.

I would like to thank Dr. Johnny Tang and Dr. Bernice Kwok for their encouragement. Thanks are also given to all the staff and technicians in the Biology section of the Department of Applied Biology and Chemical Technology for their generous assistance.

I would also like to express my gratitude to my colleagues in Dr. Leung's laboratory for their help and support throughout the project. I would like to thank all my good friends: Kit Ying, Ka Ka, Phibe, Helen, Shan and Ming for their tremendous support and friendship.

Finally, I would like to thank all my family members for their endless love, encouragement and support.

Table of Contents

CERTIFICATE OF ORIGINALITY
Abstract
Acknowledgements
Abbreviations **i-ii**
List of Figures and Tables **iii-vi**

Chapter One: Introduction **1**
1.1. Beta-lactams and their target enzymes 1
1.2. Beta-lactamases 3
1.3. Class A beta-lactamases and their catalytic mechanism 4
1.4. Problem of antibiotic resistance 9
1.5. Rational design of biosensors 12
1.6. Class A beta-lactamase in novel biosensor development 13
1.7. Aims of study 15

Chapter Two: Materials and Methods **18**
2.1. Subcloning of the PenP_E166C beta-lactamase gene into pMAL-c2X vector 18
2.1.1. Preparation of plasmid DNA 18
2.1.2. PCR amplification of PenP gene 18
2.1.3. Restriction enzyme digestion of DNA and electrophoresis 19
2.1.4. Isolation and purification of DNA fragment 22
2.1.5. Ligation of DNA fragments 22
2.1.6. Preparation of *E. coli* competent cells 22
2.1.7. Transformation 23

2.2. Introduction of N170Q mutation by site-directed mutagenesis 23

2.3. Expression and purification of MBP-beta-lactamase fusion proteins 25
2.3.1. Expression of beta-lactamase mutants from *E. coli* 25
2.3.2. Protein extraction by sonication 25
2.3.3. Protein purification by amylose affinity column 26
2.3.4. Protein gel electrophoresis (SDS/PAGE) 26
2.3.5. Determination of protein concentration 27

2.4. Removal of MBP from MBP-beta-lactamase fusion proteins 28
2.4.1. Cleavage of MBP by Factor Xa 28
2.4.2. Purification of MBP-cleaved protein by DEAE cellulose column 28

2.5. Modification of E166C and E166C/N170Q with fluorophores 29
2.5.1. Protein labeling 29
2.5.2. Refolding of mutant enzymes 29

2.6. Kinetic characterization of PenP mutants and their fluorophore-labeled derivatives 30
2.6.1. Preparation of nitrocefin solution 30
2.6.2. Monitoring the initial rates of substrate hydrolysis 30
2.6.3. Calculation of kinetic parameters of PenP mutants 31

2.7. Protein structural and thermostability studies 32
2.7.1. Study of protein secondary structure by circular dichroism spectrometry 32
2.7.2. Thermal-denaturation study 32
2.7.3. Thermal-inactivation study 32

2.8. Fluorescence studies of fluorophore-labeled beta-lactamases 33
2.8.1. Fluorescence spectra scanning 33
2.8.2. Time-resolved fluorescence measurement 33

2.9. Detection of acyl-enzyme intermediate in the hydrolysis of penicillin G by fluorophore-labeled beta-lactamases 34
2.9.1. Time-resolved fluorescence measurement by stopped-flow study 34
2.9.2. Quench-flow experiment combined with ESI-MS 34

Chapter Three: Results **36**
3.1. Expression of MBP-beta-lactamase fusion proteins 36

3.2. Purification of MBP-beta-lactamase fusion proteins 39

3.3 Removal of MBP from MBP-beta-lactamase fusion proteins 43
3.3.1 Cleavage of MBP by Factor Xa 43

3.3.2 Purification of cleavage product by DEAE ion-exchange chromatography 45

3.4. Modification of E166C and E166C/N170Q with fluorophores 49

3.5. Kinetic characterization of PenP mutants and their fluorophore-labeled derivatives 51

3.6. Protein structural and thermostability studies 55
3.6.1. Study of protein secondary structure 55
3.6.2. Thermal-denaturation of PenP and PenPC beta-lactamases 58
3.6.3.. Thermal-inactivation of PenP and PenPC beta-lactamases 60

3.7. Fluorescence studies of fluorophore-labeled beta-lactamases 62
3.7.1. Fluorescence spectra scanning upon addition of antibiotics 62
3.7.2. Time-resolved fluorescence measurement 64
3.7.3. Fluorescence spectra scanning upon addition of inhibitors 71

3.8 Detection of acyl-enzyme intermediate in the hydrolysis of penicillin G by fluorophore-labeled beta-lactamases 74
3.8.1. Time-resolved fluorescence measurement by stopped-flow study 74
3.8.2. Detection of reaction species by ESI-MS 76

Chapter Four: Discussion **78**
4.1. Preparation of MBP-PenP fusion proteins using a *E. coli* expression system 78
4.1.1. *E. coli* expression system 79
4.1.2. Maltose binding protein as a fusion partner 79
4.1.3. Expression and purification of MBP-PenP mutants 80

4.2. The use of MBP in biosensor development 81
4.2.1. Poor recovery of MBP-cleaved beta-lactamases 81
4.2.2. Negligible effects of MBP on biosensing system 82

4.3. Catalytic deficiency of E166C and E166C/N170Q mutants 83
4.3.1. Sites of mutations 83
4.3.2. Kinetic properties of MBP-PenP mutants and their 84

fluorophore-labeled derivatives

4.4. Studies of the protein secondary structure 87
4.4.1. Effects of mutation(s) 88
4.4.2. Effects of fluorophore-labeling reaction 88

4.5. Characterization of fluorophore-labeled PenP mutants 90
4.5.1. Spectral properties of fluorophore-labeled mutants 90
4.5.2. Detection of beta-lactam antibiotics 100
4.5.3. Detection of beta-lactamase inhibitors 104

4.6. Biosensing process of PenP biosensors 105
4.6.1. Detection of acyl-enzyme intermediate in penicillin G hydrolysis 106
4.6.2. Correlation between fluorescence spectra and enzyme kinetics 106

4.7. Comparison between PenPC and PenP biosensors 109
4.7.1. Detection limit 109
4.7.2. Sensitivity 111
4.7.3. Response time 112
4.7.4. Signal stability 112
4.7.5. Specificity 114
4.7.6. Protein thermostability 115

Chapter Five: Conclusion **118**

APPENDIX I : Amino acid sequence of MBP_PenP_E166C and MBP_PenP_E166C/N170Q. 120
APPENDIX II : Mass spectra of fluorophore-labeled PenP beta-lactamases. 122
APPENDIX III : Plot of change in fluorescence intensity (at the maxima) of PenP-based biosensors as function of log [antibiotic, M]. 124
APPENDIX IV : Chemical structures of beta-lactam antibiotics and inhibitors. 128
APPENDIX V : Time-resolved fluorescence spectra of PenPC-based biosensors. 130
APPENDIX VI : Reagents and Solutions. 132

References **134**

Abbreviations

A_X	Absorbance at x nm wavelength
Badan	6-bromoacetyl-2-dimethylaminonaphthalene
B. cereus	*Bacillus cereus*
B. licheniformis	*Bacillus licheniformis*
CD	Circular dichroism
△ (Delta)	Change of
Da	Dalton(s)
ddH_2O	Double distilled water
DD-transpeptidase	D-alanyl-D-alanine transpeptidase
DEAE	Diethylaminoethyl
DNA	Deoxyribonucleic acid
DMF	Dimethyl formamide
E	Enzyme
EC	Non-covalent enzyme-substrate complex
EC*	Covalent acyl-enzyme intermediate
E. coli	*Escherichia coli*
EDTA	Ethylenediamine tetra acetic acid
Fluorescein	Fluorescein-5-maleimide
h	Hour(s)
HPLC	High performace liquid chromatography
IAF	6-iodoacetamidofluorescein
IPTG	Isopropyl beta-D-thiogalactoside

Kan^r	Kanamycin resistance
mAU	Milli absorption unit
MBP	Maltose binding protein
min	Minute(s)
OD_X	Optical density at x nm wavelength
PBP	Penicillin-Binding protein
PCR	Polymerase Chain Reaction
PC1 beta-lactamase	Beta-lactamase of *Staphylococcus aureus*
PenPC beta-lactamase	Beta-lactamase I of *Bacillus cereus* 569/H
PenP beta-lactamase	Beta-lactamase of *Bacillus licheniformis* 749/C
ppb	Parts per billion
rpm	Revolutions per minute
s	Second
SAA	Solvent accessible area
SDS/PAGE	Sodium dodecyl sulphate polyacrylamide gel electrophoresis
T_m	Melting temperature
TBE	Tris-borate-EDTA
TEM-1 beta-lactamase	Beta-lactamase of *Escherichia coli*
Tris-HCl	Tris(hydroxymethyl)aminomethane with pH adjusted by hydrochloric acid
TY	Tryptone with yeast extract
UV/VIS	Ultra violet light/ Visible light

List of Figures and Tables

Figures	Descriptions
1.1	Structures of some beta-lactam antibiotics.
1.2	General catalytic pathway of active site serine beta-lactamase and the enzymatic reaction model.
1.3	X-Ray crystal structure of beta-lactamase of *Bacillus licheniformis* 749/C.
2.1	Plasmid map of pMAL-c2X.
3.1	Growth curves of *E. coli* BL-21 transformed with MBP_PenP_E166C and MBP_PenP_E166C/N170Q.
3.2	12% SDS/PAGE analysis of the expression profile for MBP_PenP_E166C and MBP_PenP_E166C/N170Qin *E. coli* at different time points.
3.3	Elution profiles of MBP_PenP_E166C and MBP_PenP_E166C/N170Q from amylose affinity chromatography.
3.4	12% SDS/PAGE analysis of the column fractions from amylose affinity chromatography for MBP_PenP_E166C and MBP_E166C/N170Q.
3.5	12% SDS/PAGE analysis of MBP-cleaved beta-lactamases by Factor Xa at different incubation time points.
3.6	Elution profiles of MBP-cleaved PenP_E166C and MBP-cleaved PenP_E166C/N170Q from DEAE ion exchange chromatography.
3.7	12% SDS/PAGE analysis of the column fractions from the DEAE ion-exchange chromatography for MBP-cleaved E166C and MBP-cleaved E166C/N170Q.
3.8	12% SDS/PAGE analysis of MBP_PenP_E166C, MBP_PenP_E166C/N170Q and their fluorophore-labeled derivatives; and its corresponding fluorescence image under UV.
3.9	Far-UV circular dichroism spectra of PenP beta-lactamase, E166C and E166C/N170Q; E166C, E166Cb and E166Cf; E166C/N170Q, E166Cb/N170Q and E166Cf/N170Q.

3.10 Thermal denaturation curves for PenP beta-lactamases, PenPC beta-lactamase and their fluorophore-labeled derivatives.

3.11 Relative activities of PenP beta-lactamases, PenPC beta-lactamase and their fluorophore-labeled derivatives as a function of incubation time.

3.12 Fluorescence scanning spectra of PenP_E166Cf, PenP_E166Ciaf and PenP_E166Cb upon addition of penicillin G and cefotaxime.

3.13 Time-resolved fluorescence spectra of MBP_PenP_E166Cf in different beta-lactam antibiotics in 50 mM potassium phosphate buffer (pH 7.0).

3.14 Time-resolved fluorescence spectra of MBP_PenP_E166Cf/N170Q in different beta-lactam antibiotics in 50 mM potassium phosphate buffer (pH 7.0).

3.15 Time-resolved fluorescence spectra of MBP_PenP_E166Cb in different beta-lactam antibiotics in 50 mM potassium phosphate buffer (pH 7.0).

3.16 Time-resolved fluorescence spectra of MBP_PenP_E166Cb/N170Q in different beta-lactam antibiotics in 50 mM potassium phosphate buffer (pH 7.0).

3.17 Fluorescence spectra of different fluorophore-labeled beta-lactamases in 50 mM potassium phosphate buffer (pH 7.0) in the presence of 10^{-4} M of sulbactam and tazobactam.

3.18 Fluorescence spectra of different fluorophore-labeled beta-lactamases in 50 mM potassium phosphate buffer (pH 7.0) in the presence of 10^{-4} M of clavulanate.

3.19 Time-resolved fluoresecence spectra of MBP_PenP_E166Cf/N170Q upon addition of penicillin G, with enzyme to substrate ratio of 1:1 at concentration of 5×10^{-7} M.

3.20 Mass spectrometry spectra of the reaction between MBP_PenP_E166Cf/N170Q and penicillin G at different time intervals.

4.1 Reaction of a thiol with 6-iodoacetamidofluorescein, fluorescein-5-maleimide and badan.

4.2 Molecular models for E166Cf before and after binding with penicillin G.

4.3 Molecular models for E166Ciaf before and after binding with penicillin G.

4.4 Molecular models for E166Cb before and after binding with penicillin G.

4.5 Sequence alignment of the PenPC and PenP beta-lactamase numbered according to the ABL scheme.

4.6 Fluorescence scanning spectra of various badan-labeled biosensors in the presence of 10^{-4} M of penicllin G.

5.1 Amino acid sequence of MBP_PenP_E166C.

5.2 Amino acid sequence of MBP_PenP_E166C/N170Q.

5.3 Mass spectra of MBP_PenP_E166Cf and MBP_PenP_E166Cf/N170Q.

5.4 Mass spectra of MBP_PenP_E166Cb and MBP_PenP_E166Cb/N170Q.

5.5 Plot of change in fluorescence intensity (at the maxima) of MBP_PenP_E166Cf as function of log [antibiotic, M].

5.6 Plot of change in fluorescence intensity (at the maxima) of MBP_PenP_E166Cf/N170Q as function of log [antibiotic, M].

5.7 Plot of change in fluorescence intensity (at the maxima) of MBP_PenP_E166Cb as function of log [antibiotic, M].

5.8 Plot of change in fluorescence intensity (at the maxima) of MBP_PenP_E166Cb/N170Q as function of log [antibiotic, M].

5.9 Chemical structures of the beta-lactam antibiotics used in the study.

5.10 Chemical structures of the beta-lactam inhibitors used in the study.

5.11 Time-resolved fluorescence spectra of PenPC_E166Cf in different beta-lactam antibiotics in 50 mM potassium phosphate buffer (pH 7.0).

5.12 Time-resolved fluorescence spectra of PenPC_E166Cb in different beta-lactam antibiotics in 50 mM potassium phosphate buffer (pH 7.0).

List of Figures and Tables

Tables	Descriptions
1.1	The tolerance levels towards beta-lactam residues in milk.
2.1	Information of primers used in the study.
2.2	Settings of parameters in fluorescence measurement.
3.1	Purification table of MBP_PenP_E166C beta-lactamase.
3.2	Purification table of MBP_PenP_E166C/N170Q beta-lactamase.
3.3	Purification table of MBP-cleaved PenP_E166C beta-lactamase.
3.4	Purification table of MBP-cleaved PenP_E166C/N170Q beta-lactamase.
3.5	Kinetic parameters of wild-type PenP beta-lactamase, E166C and E166C/N170Q.
3.6	Specific activities of PenP E166C and its fluorophore-labeled derivatives; PenP E166C/N170Q and its fluorophore-labeled derivatives.
3.7	The calculated secondary structure of different PenP beta-lactamases and their fluorophore-labeled derivatives.
4.1	Calculated solvent accessible areas of different fluorescence reporter groups covalently linked to E166C before and after penicillin G binding.

Chapter One: Introduction

1.1. Beta-lactams and their target enzymes

Beta-lactam antibiotics are antibacterial agents that are commonly used in human and animal therapy. They are popularly used because of their high specificity and clinical efficacy, broad-spectrum activity and absence of secondary effects in higher organisms. The beta-lactams kill bacteria by inactivating a set of bacterial transpeptidase enzymes (penicillin-binding proteins, PBPs), which are important for cell wall biosynthesis and repair. This group of antibiotics is called "beta-lactam" because of the common core structure of the 4-membered-beta-lactam ring. Two common examples of beta-lactams are the penicillins and cephalosporins (Figure 1.1).

Although beta-lactams exert high antibacterial efficiency, intensive use of it causes the emergence of resistant bacteria. These bacteria have developed various strategies for escaping the lethal actions of the beta-lactams, for example, through the generation of resistant DD-transpeptidase, or the modification of the diffusion barriers and upregulation of the active efflux systems. However, the most common and efficient resistance mechanism is the destruction of the beta-lactams by the synthesis of beta-lactamases (Matagne *et al.*,1999).

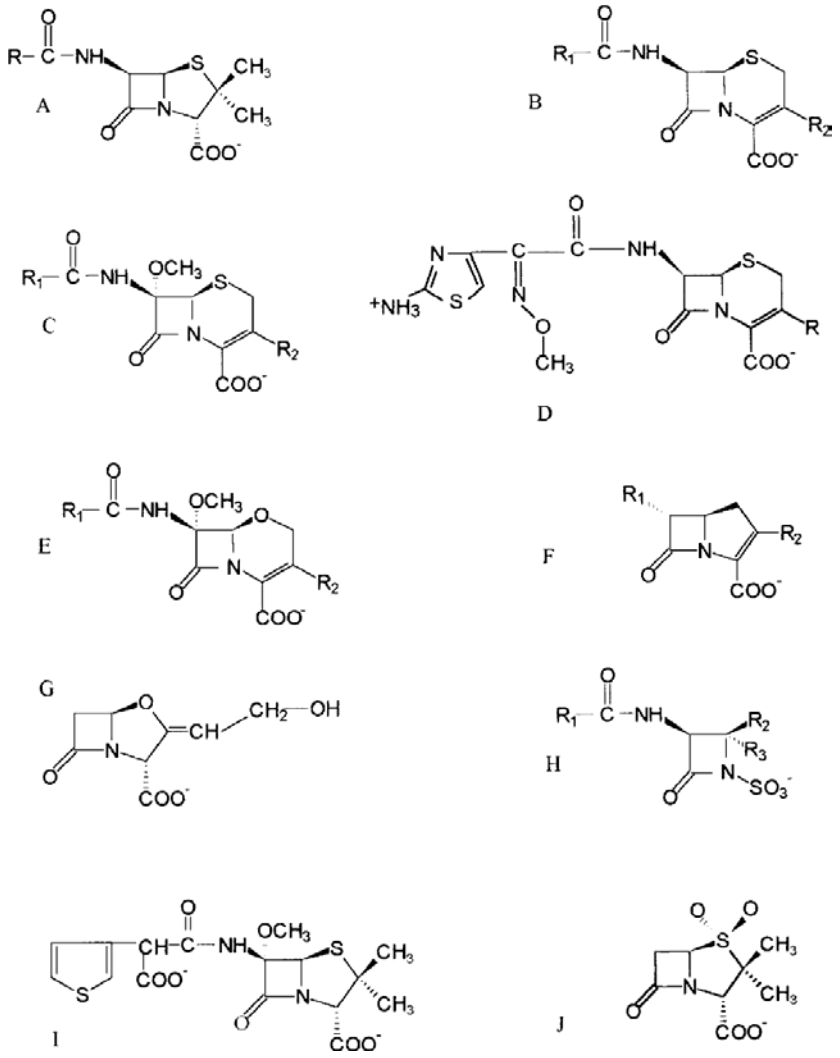

Figure 1.1. Structures of some beta-lactam antibiotics (Matagne *et. al.*, 1998). (A) Penicillins (e.g. benzylpenicillin, ampicillin, amoxycillin), (B) Cephalosporins, (C) cephamycins (e.g. cefoxitin), (D) cefotaxime, (E) oxacephamycins (e.g. moxalactam), (F) carbapenems (e.g. imipenem), (G) clavulanate (H) monobactams (e.g. aztreonam), (I) temocillin and (J) sulbactam.

1.2. Beta-lactamases

Beta-lactamases (E.C.3.5.2.6, systematic name: beta-lactam hydrolases) are enzymes that disrupt the antibacterial action of beta-lactam antibiotics. They are the main cause of bacterial resistance to the beta-lactams, which act by irreversibly hydrolyzing the amide bond of beta-lactam ring and leaving an inactive carboxylic acid product. These enzymes which can be chromosome or plasmid encoded and produced in a constitutive or inducible manner, are usually secreted into the outer medium by Gram-positive species and into the periplasm by the Gram-negative counterparts. There are over 470 of known beta-lactamases to date and the continued use of beta-lactams may lead to selection of newer variants (Fisher *et al.*, 2005).

Beta-lactamases are highly diversified in terms of their structures and substrate specificity. Various classification systems have been used to group the enzymes into different classes. For instance, they are grouped according to the bacterial sources, location of genes, substrate profiles and inhibition properties. However, such classification systems were soon found to be inadequate and unhelpful.

In 1980, Ambler proposed the first molecular structure classification, which remains totally valid to date (Ambler, 1980; Ambler *et al*., 1991). This classification scheme divides the enzymes into 4 molecular classes, Class A, B, C and D, on the basis of the homology in their amino acid sequences. In 1992, Waley further grouped the beta-lactamases on the basis of the catalytic mechanisms, and distinguished serine enzymes from zinc enzymes (Waley, 1992). Class A, C and D are serine enzymes which

display an active-site serine residue and act through a covalent acyl-enzyme mechanism, whereas class B enzymes belong to the zinc enzymes that are metalloenzymes, and appear to involve non-covalent intermediates in their actions. Class A and C enzymes represent the most clinically important beta-lactamases and are responsible for numerous failures in the treatment of infectious diseases. Class A prefers penicillins as substrates but class C hydrolyze cephalosporins better. Of all the beta-lactamases, class A is the most numerous and the best studied.

1.3. Class A beta-lactamases and their catalytic mechanism

The class A beta-lactamases are medium-sized proteins with molecular weights around 29,000 Da. The enzymes show a wide distribution of the pI values, which range from 3.5 to 10. A very large number of enzymes have been reported and more than 45 sequences were determined (Matagne *et al.*, 1999). The varying catalytic properties and primary structures of class A explain the high diversity of the enzymes in this class.

Sequence alignments of different class A beta-lactamases suggest that only 9 residues, out of the 260-280 residues, are highly conserved (Matagne *et al.*, 1999). The functions of these conserved residues have also been probed and studied by site-directed mutagenesis. Four of the conserved residues, including Ser-70, Lys-73, Ser-130, Glu-166, are found to be essential for catalysis, whereas the other five (Gly-45, Pro-107, Asp-131, Ala-134 and Gly-236) are probably responsible for structural functions. In addition, residues at position 132 (Asn in most sequences), 234 (Lys or Arg) and 235 (Ser or Thr) have also been shown to be important for the enzyme activity (Matagne *et al.*, 1999).

Class A beta-lactamases are efficient active-site serine enzymes and they function by a three-step mechanism similar to that of the DD-peptidases, except with a more rapid deacylation step (Ghuysen, 1991). Their catalytic pathways are thus characterized by the transient formation of a covalent acyl-enzyme intermediate (EC*), which is extremely unstable and is rapidly hydrolyzed.

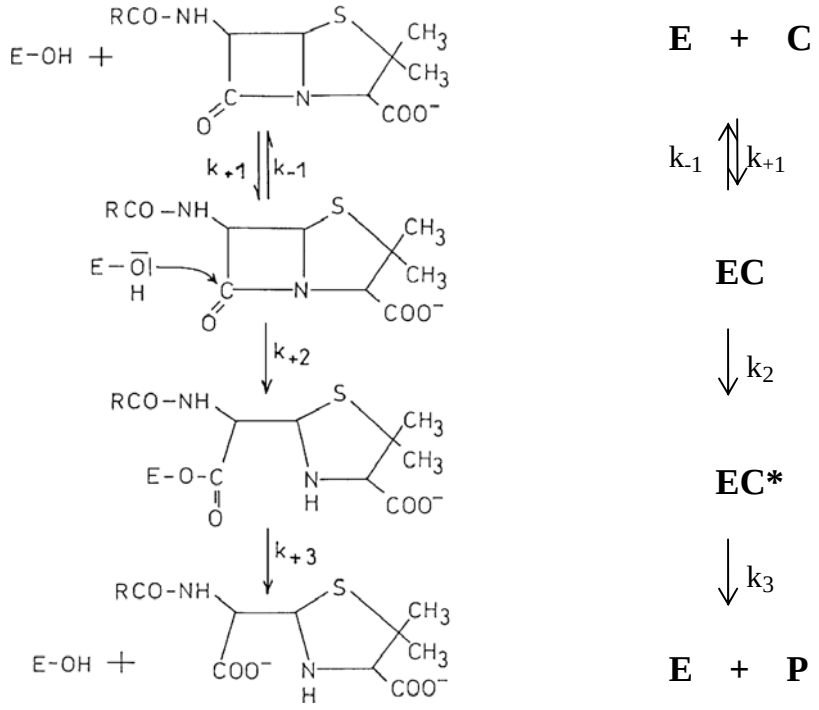

(a) (b)

Figure 1.2. General catalytic pathway of active site serine beta-lactamase (Matagne *et. al.*, 1998) (a), and its corresponding enzymatic reaction model (b) , where E is the beta-lactamase, C is an antibiotic substrate, EC is the enzyme-substrate non-covalent complex, EC* is the acyl-enzyme adduct and P is the hydrolyzed product.

According to the three-step mechanism shown in Figure 1.2, the beta-lactamase (E) firstly associates with the antibiotic (C) to form a non-covalent Heri-Michaelis complex (EC). Undergo acylation, the hydroxyl group of the active-site serine residue (Ser-70) attacks the carbonyl carbon of the beta-lactam nucleophilically and forms a tetrahedral covalent acyl-enzyme intermediate (EC*). At the same time, the amide bond of the beta-lactam ring is hydrolyzed and cleaved. Upon the deacylation step with the presence of a water molecule, the ester-linkage of the acyl-enzyme is hydrolyzed, a free enzyme (E) is hence regenerated and an inactive carboxylic acid product (P) is resulted.

On the basis of the above catalytic mechanism, the active site of the class A beta-lactamases are expected to contain both an oxyanion hole, for stabilization of the tetrahedral intermediates, and a general base, for proton abstraction from the active site serine hydroxyl group (Matagne *et al.*, 1999). Although it is now quite certain that the oxyanion hole, which interacts with the oxygen of the beta-lactam carbonyl group, is formed by the main chain amino group of Ser-70 and Ala-237 in the class A enzymes (Diaz *et al*., 2003), the exact residue(s) which enhance the nucelophilicity of the serine hydroxyl group in the acylation remains unclear. This question becomes the most controversial topic for class A enzymes and 2 distinct residues have been proposed as the potential general bases.

In one hypothesis (Matagne *et al.*, 1999; Gibson *et al*., 1990) the conserved Glu-166 is suggested to play the role of general bases in both acylation and deacylation in a symmetrical mechanism. Though the Glu-166 and Ser-70 side chains are too distant for

direct proton transfer, some crystallographic and molecular modeling data have suggested that a conserved water molecule (W1) could form a bridge between the Ser-70 hydroxyl group and Glu-166 carboxylate side chain which acts as a replay in the transfer of proton (Knox and Moews, 1991; Herzberg, 1991; Minasov *et al.*, 2002 Diaz *et al*., 2002). On the other hand, the flexibility of the omega-loop may also help to reduce the distance and facilitate the transfer. Once the Ser-70 residue is activated, it attacks the carbonyl carbon of the beta-lactam and proton will be delivered back to the leaving nitrogen atom of the beta-lactam via a network of hydrogen bonds. Hydrolysis of the acyl-enzyme intermediate will subsequently occur in a symmetrical mechanism, in which the Glu-166 interacts and activates a hydrolytic water molecule to attack the carbonyl carbon of the acyl-enzyme, and ensure back-delivery of the abstracted proton to the Ser-70, finally regenerating a free enzyme.

The second hypothesis (Lys-73 hypothesis) assumes a non-symmetrical mechanism and two different general bases, Lys-73 and Glu-166, are suggested to be involved in the acylation and deacylation respectively (Escobar *et al.*, 1991, Strynadka *et al.*, 1992). In this case, the active site of the enzyme may provide a favorable local environment, namely a very positive electric field that strongly reduces the p*K*a value of the alkyl-ammonium group of Lys73, which enables the lysine to remain unprotonated at neutral pH and activate the Ser-70 by direct proton abstraction. The subsequent deacylation processes are similar to that of the first hypothesis, which agrees that the Glu-166 carboxylate acts as the general-base catalyst in the deacylation step.

To find out which hypothesis is true, site-directed mutagenesis experiments and structural studies have been carried out (Gibson *et al.*, 1990; Leung *et al.*, 1994; Guillaume *et al.*, 1997; Damblon *et al.*, 1996; Escobar *et al.*, 1994; Raquet *et al.*, 1997). However, it seems that the present evidence substantiates the view of the first hypothesis, which describes the symmetrical mechanism, but without ruling out the importance of Lys-73.

Some Glu-166 mutants have been prepared with different class A beta-lactamases and detailed kinetic studies were performed (Gibson *et al.*; 1990; Escobar *et al.*, 1994; Leung *et al.*, 1994; Guillaume *et al.*, 1997). Results from the Glu-166 mutants of beta-lactamase I from *B. cereus* 569/H and TEM-1 showed that both acylation and deacylation rates appeared to be suppressed by the disappearance of Glu-166, but deacylation was generally more impaired (Gibson *et al.*; 1990; Leung *et al.*, 1994; Guillaume *et al.*, 1997). These observations hence tend to agree with the first hypothesis, however, suggesting that the acylation and deacylation are not necessarily “mirror” images of each other, and Glu-166 seems to have a more crucial role in deacylation than in the acylation. In contrast, a NMR titration of the Lys-73 residue in the TEM-1 beta-lactamase failed to provide evidence to support the Lys-73 hypothesis (Damblon *et al.*, 1996; Raquet *et al.*, 1997). For Lys-73 to act as a catalytic base, it would have to be deprotonated at physiological pH. However, according to Escobar *et al.* (1994) and Raquet *et al.* (1997), the p*K*a values for Lys-73 of the *Bacillus licheniformis* beta-lactamase and TEM-1 were found to be greater than 10. Similar finding was further illustrated by the molecular dynamics (MD) simulations of the TEM-1 complexed with benzylpenicillin (Diaz *et al.*, 2002). In addition, a study (Gibson *et al.*, 1990) also found that the K73R mutant of the beta-lactamase I was more active than its

E166D counterpart. In light of these results, Lys-73 is unlikely to be actively involved in the proton abstraction of the acylation but does play a role in the process.

1.4. Problem of antibiotic resistance

Beta-lactam antibiotics, such as the penicillins and cephalosporins, have been used extensively in the treatment of bacterial infections in both livestock and humans. Nevertheless, the intensive use and sometimes abuse of antibiotics in veterinary and farming industries have lead to contamination in food and in the environment. For example, the US Food and Drug Administration (FDA) recognizes that six beta-lactams are widely used in treating disease in lactating dairy cattle and are the most likely to cause a residue in milk if misused (NCIMS, 2004). Such contamination has raised much concern from the public as it may cause severe allergic reactions. More importantly, the over-prescription of antibiotics by doctors has also lead to emergence of antibiotic-resistant bacteria. Clearly, this is a very serious problem as this may reduce the efficacy of antibiotics and make them no longer kill the resistant infectious bacteria. According to a report published in 2000 by Hospital Authority, the antibiotics in Hong Kong are less effective than anywhere else in the world and the situation keeps worsening due to the evolution process of the bacteria.

In the face of the antibiotic contamination problems, some food-regulatory bodies have set measures and standards to monitor the antibiotic residue levels in food. Some food quality assurance programs, such as the *Grade A Pasteurized Milk Ordinance* (PMO), are also in place to promote food safety (U.S. Food and Drug Administration, 2003). The PMO, which is published by the FDA, outlines the minimum standards and requirements

for Grade A milk production and processing. It aims to encourage a greater uniformity and a higher level of excellence of milk sanitation practice in the United States. Table 1.1 shows the tolerance levels towards six beta-lactam residues in milk, which is established by the FDA.

A number of screening tests have been developed to help detecting the residual antibiotics in food. Conventional screening tests such as the Charm test and Penzym test have been widely used and approved by the FDA (Charms Sciences, Inc.). However, these tests are not fully perfect as they are largely semiquantitative. Other developments, such as the analysis of antibiotics by HPLC (Niessen, 1998), may not be very convenient as tedious sample pre-treatments and separation steps were required. Whereas the uses of fiber optics (Kulp *et al.*, 1987; Healey and Walt, 1995) and electrochemical beta-lactam sensors (Papariello et al, 1973; Nishizawa, 1992) may also unsatisfactory as the measurements are easily interfered by the change of the environmental pH. Therefore, in order to allow more rapid and reliable detections for intensifying the testing of food for beta-lactam residues, a specific and sensitive detection method for beta-lactams is a must.

Development of beta-lactamase inhibitors, such as sulbactam and clavulanate, have also been proved to be successful in the treatment of infections due to the beta-lactamase-producing pathogens, in which the inhibitors are administered in combination with classical beta-lactam antibiotics (Matagne *et al.*, 1999). However, in the past two decades, the clinical use of such drugs has also been responsible for the appearance of strains exhibiting resistance to the inhibitors. These inhibitors, therefore,

become less effective for the combination therapies. As a result, apart from the development of more effective antibiotics, there is also an urgent need to develop new strategies to discover new beta-lactamase inhibitors. In this way, new drugs can be developed and can be applied to kill those resistant infectious bacteria.

Table 1.1. The tolerance levels towards six beta-lactam residues in milk, which is established by the US Food and Drug Administration (FDA). These beta-lactams are widely used in treating disease in lactating dairy cattle and are the most likely to cause a residue in milk if misused.

Beta-lactam Drugs	**Tolerance or Safe Level (ppb)**	**Tolerance or Safe Level (nM)**
Amoxicillin	10	2.7
Ampicillin	10	2.9
Ceftiofur	50	9.4
Cephapirin	20	4.7
Cloxacillin	10	2.2
Penicillin	5	1.5

1.5. Rational design of biosensors

According to Thevenot *et al.* (2001) and De Lorimier *et al.* (2002), biosensor is a self-contained analytical tool that measures the presence of a single molecular species in complex mixtures using a biological recognition element which is in direct spatial contact with a transducer element. It combines the exquisite molecular recognition properties of the biological molecule with signal transduction function that couples ligand binding to readily detectable physical changes. Recently, molecular engineering techniques have been explored to construct biosensors based on the induced conformational changes of simple allosteric proteins. The sensing system strategy is based on the fluorescence changes of the probe as the protein undergoes structural changes on binding (De Lorimier *et al.,* 2002). Such sensing systems have been applied for the detection of different ligands, such as sugar (Salins *et al.*, 2001), protein (Doi and Yanagawa, 1999), DNA (Tsoi and Yang, 2004) and ions (Salins *et al.*, 2004). This rational biosensor design is also well illustrated by a family of bacterial periplasmic binding proteins (bPBPs) , in which the natural ligand-binding properties coupled with generic, reagentless and engineered signal transduction mechanisms, have successfully turned this group of proteins into a versatile biosensor system (De Lorimier *et al.,* 2002). It is important to note that these biosensors are often pure binding proteins capable of ligand binding without hydrolysis. In that case, protein conformational change created upon the binding of ligand will induce stable analytical signals for analysis. In this project, a class A beta-lactamase is tested and engineered for developing biosensors to detect beta-lactam antibiotics and beta-lactamase inhibitors. However, such novel development is extremely challenging as beta-lactamases are not allosteric proteins but enzymes with excellent hydrolytic abilities.

1.6. Class A beta-lactamase in novel biosensor development

Class A beta-lactamases are excellent catalytic enzymes because of their broad substrate spectrum, high specificity and catalytic efficiency. Their superior selectivity towards beta-lactam antibiotics and beta-lactamase inhibitors meet an important criterion to be engineered for developing biosensors to detect beta-lactam antibiotics and to screen the related drugs. Although beta-lactamases are very active hydrolytic enzymes, they can be turned into more “binding” like by molecular engineering techniques, i.e. the construction of catalytically defective beta-lactamase mutants by site-directed mutagenesis.

Site-directed mutagenesis is one of the most powerful tools for understanding structure-function relationships of enzymes and creating enzymes with novel properties (Guillaume *et al.*, 1997; Miyanaga *et al.*, 2004; Datta *et al.*, 2005). By removing the catalytically important residues of the beta-lactamases by this technique (Gibson *et al.*, 1990; Escobar *et al.*, 1994; Guillaume *et al.*, 1997), the catalytically-defective beta-lactamase can behave as a pure binding protein and become an ideal basis for the construction of biosensors.

Structural studies of beta-lactamases have shown that this group of enzymes, although not allosteric proteins, possesses a conserved potentially flexible omega-loop (Banerjee *et al*., 1998, Castillo *et al.*, 2002). The omega-loop in class A enzymes is a loosely packed 16-residue segment. It spans residues 164 to 179, which form a portion of the active-site pocket of the enzyme. The flexibility of this loop would allow conformational changes

upon the substrate binding. Therefore, if we make good use of this induced conformational property with an external environmentally sensitive reporter group placed at specific region on the loop, a catalytic-defective beta-lactamase can be turned into new enzyme-based biosensor.

A novel fluorescence biosensor (PenPC_E166Cf), derived from beta-lactamase I of *Bacillus cereus* 569/H, has been constructed successfully (Chan *et al.*, 2004). By generating the PenPC_E166C mutant, in which the catalytic efficiency is 1800-fold lower than the wild-type, the sufficiently stable enzyme-substrate complex can accumulate and allow the enzyme to function as a biosensor. Since the residue 166 locates at the flexible omega loop, by site-selectively labeling this residue with a fluorescent reporter group, binding of substrate will induce conformational change of the loop, hence move the reporter group. As a result, the fluorescence properties will change accordingly and serve as the basis of the signal. Apart from the development of PenPC_E166Cf, PenPC_E166Cb was also constructed, by labeling the enzyme with a different fluorophore. The exciting data of this biosensor are going to be published. Nevertheless, the PenPC-biosensors have demonstrated the ability to generate detectable fluorescence signals upon the binding of various beta-lactams, including penicillins such as pencillin G, penicillin V and ampicillin, as well as cephalosporins such as cefoxitin and moxalactam. Experiments have also indicated that they can detect beta-lactam antibiotics as low as 5-10 nM in water and work for detecting beta-lactamase inhibitors such as sulbactam. Apart from exploring new potential method for antibiotic detection and drug screening, a breakthrough has been achieved as hydrolytic enzymes are seldom used in biosensor construction.

1.7. Aims of study

The previously developed PenPC_E166Cf biosensor has demonstrated its ability in detecting beta-lactam antibiotics and beta-lactamase inhibitors. However, it suffers from short half-life of the fluorescence signal when detecting penicillins. In order to evaluate the feasibility and possibility of constructing better biosensors by using other class A beta-lactamases, PenP beta-lactamase of *Bacillus licheniformis* 749/C was modified into biosensors in this study by similar approach. This beta-lactamase was chosen because of its high thermostability and availability of the X-ray crystal structure (Figure 1.3) (Knox and Moews, 1991; Moews *et al*., 1990). Thermal unfolding results showed that the melting temperature of PenP beta-lactamase was 63 ^{o}C, which was higher than that of other beta-lactamases (Vanhove *et al.*, 1995). This property may hence facilitate the storage and handling of the biosensors. In addition, the well-known three dimensional structure of PenP beta-lactamase may also provide valuable information in studying the biosensing process of the biosensors in the project. Also, reports have showed that the E166A mutant of PenPC was about 200-fold more active than the E166A mutant of PenP (Leung *et al.*, 1994). Therefore, it is predicted that biosensors developed from the PenP mutants may be catalytically more defective than the PenPC counterparts, and may generate more stable signals.

Apart from applying the PenP_E166C mutant in the biosensor construction, double mutants (E166C/N170Q) with further suppressed deacylation were also generated (Zawadzke *et al.*, 1996; Chen *et al*., 2001), aiming to improve the stability of the fluorescence signal from the sensor in detecting penicillins. In the project, a total of 4

biosensors were developed: E166Cb, E166Cf, E166Cb/N170Q and E166Cf/N170Q. Their properties and performance in detecting various beta-lactam antibiotics were investigated and studied. Evaluation of the PenP and PenPC beta-lactamases in terms of developing the sensing system for beta-lactam antibiotics and beta-lactamase inhibitors were also made.

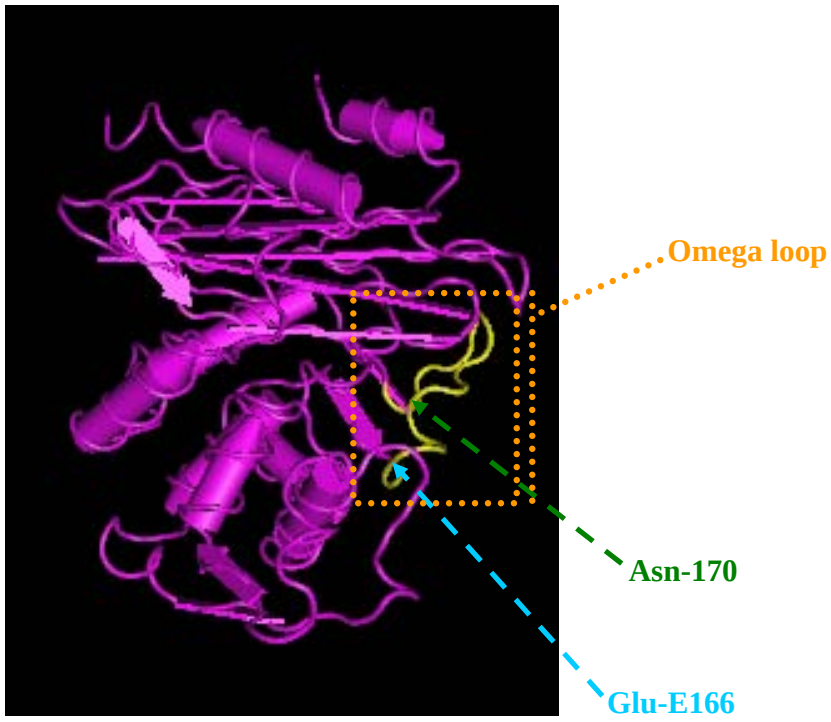

Figure 1.3. X-Ray crystal structure of beta-lactamase of *Bacillus licheniformis* 749/C (Moews *et al*., 1990). The region shown in yellow refers to the omega loop. Pale blue and green arrows indicate the positions of Glu-166 and Asn-170, respectively.

Chapter Two: Materials and Methods

2.1. Subcloning of the PenP_E166C beta-lactamase gene into pMAL-c2X

2.1.1. Preparation of plasmid DNA

The bacterial stock of *E. coli* XL1-Blue containing pQE31 plasmid carrying the PenP E166C mutant gene was provided by Dr. H. B. Liu. Single colony of *E. coli* XL-1 Blue was transferred from an agar plate to a universal bottle containing 5 ml 2xTY medium and grown at 37 ^{o}C, 300 rpm for 14-16 h. The overnight culture was then collected and cells were pelleted by centrifugation at bench top speed for around 3 min. The plasmid DNA was then isolated by the Miniprep DNA Purification Kit (Roche).

2.1.2. PCR amplification of PenP gene

The PenP_E166C mutant gene (798 bp) was amplified by Polymerase Chain Reaction (PCR). Two primers (named “BamHI-start” and “HindIII-end”), flanked by the sequences of BamHI and HindIII restricition sites respectively (Table 2.1), were designed to carry out PCR amplification. The reaction was prepared by mixing the following reagents: 10 µl of 10X reaction buffer, 300 nM of the two PCR primers, 0.1-0.75 ng of template DNA, 2 µl of 10 mM dNTP mix, 0.75 µl of DNA polymerase (2.6 U) and appropriate volume of sterile dd$H_2$0 which make up to a final volume of 100 µl. The mixture was then used for PCR reaction. The reaction mixture was denatured at 94 ^{o}C for 5 min, 25 cycles of amplification were performed with the following temperatures and reaction time: 94 ^{o}C for 1 min, 60 ^{o}C for 1 min, 72 ^{o}C for 1 min. Finally, the ragged ends were filled at 72 ^{o}C for 7 min. The PCR product would then be purified by HP PCR Product Purification Kit (Roche), according to the manufacturer’s instruction.

2.1.3. Restriction enzyme digestion of DNA and electrophoresis

The vector used for expression of MBP-beta-lactamase fusion proteins in this project was pMAL-c2X (Figure 2.1), which was purchased from the New England Biolabs. However, to avoid the contamination of TEM-1 beta-lactamases encoded from the *bla* gene for ampicillin resistance, the *bla* gene was replaced by kanamycin resistance-encoding gene before the cloning steps, which was performed by Dr. H. K. Yap. The purified PCR product and pMAL-c2X vector were then subjected to restriction digestion by BamHI and HindIII restriction enzymes. Digestions were performed according to the instruction provided from the manufacturer. The map of pMAL-c2X vector was shown in Figure 2.1. Digested DNA fragments were then analyzed by gel electrophoresis (with 0.8% agarose, 0.008% ethidium bromide and 1X TBE running buffer). The DNA was visualized under UV light from the UV transilluminator of Lumi-Imager^{TM} (Boehringer). The 1 kb DNA Ladder (Promega) was used as the marker for the estimation of the sizes of DNA fragments.

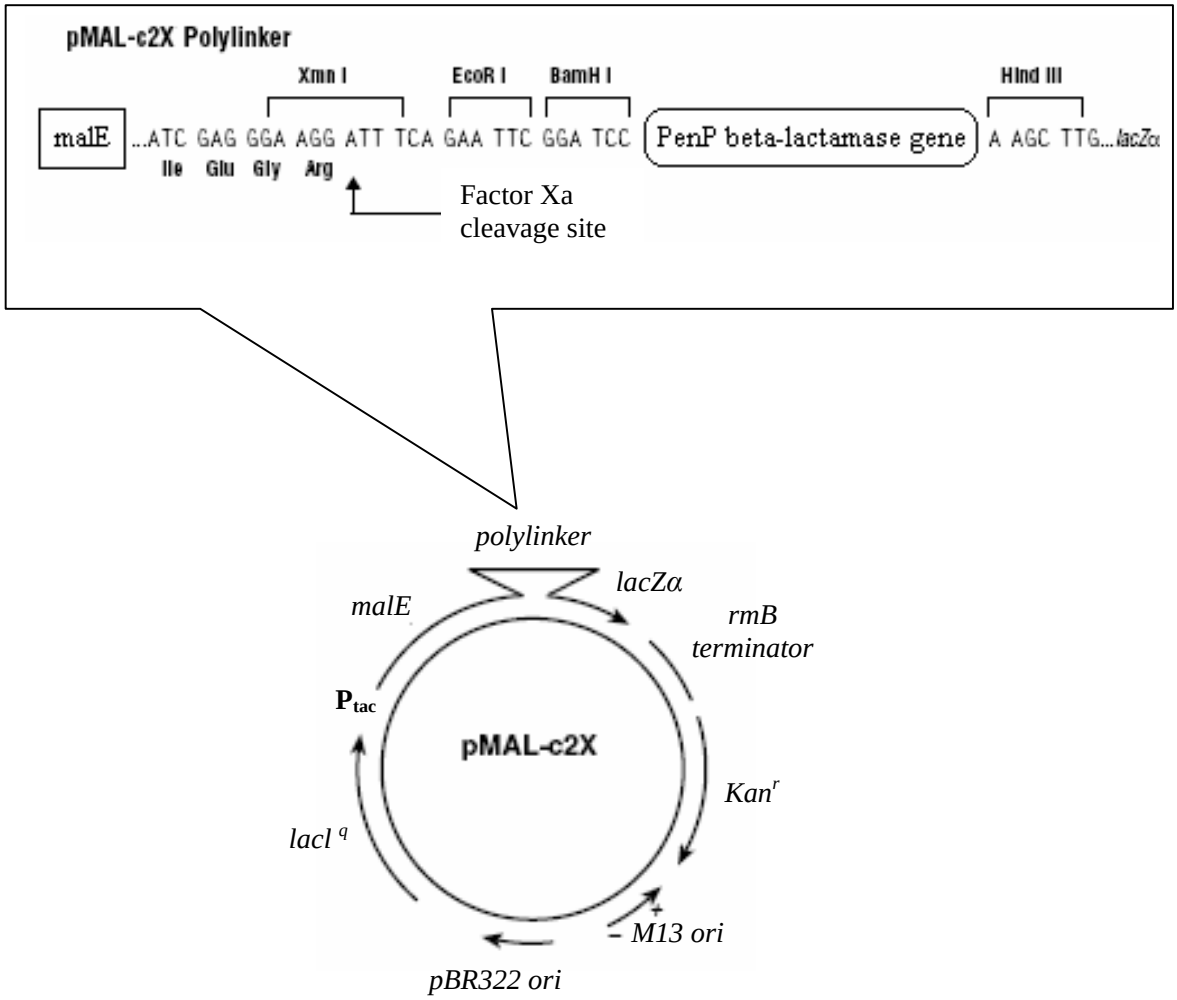

Figure 2.1. Plasmid map of pMAL-c2X (6648 base pairs). The vector has an exact deletion of the *malE* signal sequence and the *bla* gene for ampicillin resistance has been replaced by kanamycin resistance-encoding gene. Arrows indicate the direction of transcription. Unique restriction sites are indicated with the PenP beta-lactamase gene inserted downstream from the *malE* gene and flanked by the BamHI and HindIII restriction sites.

Table 2.1. Information of primers used in the study.

Primers	Sequence	Size (base)	Tm (^{o}C)
Mutagenic primers			
E166C/N170Q_F	5’-cgattctgcccagagttacaggaagtgaatccgggtgaa-3’	39	76
E166C/N170Q_R	5’-ttcacccggattcacttcctgtaactctgggcagaatcg-3’	39	76
Cloning primers			
BamHI_start	5'- cgatgaggatccaagacggagatgaaag -3'	28	65
HindIII_end	5'- taccgtaagcttttatttgccgccgttcatgtttaaggc -3'	36	68
Sequencing Primers			
MalE	5’- ggtcgtcagactgtcgatgaagcc -3’	24	76
PenP_Seq_1	5'- caaattggcggacctgaaag -3’	20	60
PenP_Seq_2	5’- ggcttgtgacaagtgctcttgc -3’	22	56

2.1.4. Isolation and Purification of DNA fragment

Following the agarose gel electrophoresis, the gel containing the desired DNA fragments were excised by a scalpel and DNA was then extracted by using the Agarose Gel DNA Extraction Kit (Roche). Quality of the extracted DNA could then be analyzed by agarose gel electrophoresis.

2.1.5. Ligation of DNA fragments

After purification of the digested DNA, appropriate amount of digested vector and DNA insert (normally in a molar ratio 1:3) were subjected to ligation. The T4 DNA Ligase and ligation buffer were provided from the Quick Ligation^{TM} Kit (New England Biolabs) and reaction was performed according to the instruction from the manufacturer.

2.1.6. Preparation of *E. coli* competent cells

Both *E. coli* TOP10 and *E. coli* BL21(DE3) competent cells were prepared by the following methodology. Overnight culture of *E. coli* was inoculated into 2xTY medium by 1:100 dilution, the fresh culture was then incubated at 37 ^{o}C with shaking at 300 rpm for 2-3 h, until A_{600} reached 0.3-0.4. The culture was then collected and cells were pelleted by centrifugation at 4000 rpm for 25 min at 4 ^{o}C. Cell pellet was then resuspended in 10 ml of ice-cold sterile 100 mM $CaCl_2$ solution and kept on ice for 25 min. Afterwards, the cell was pelleted again by centrifugation and the cell pellet was once again resuspended in 1-2 ml of $CaCl_2$ and stored at 4 ^{o}C overnight. Lastly, sterile glycerol was then added into the cells (make up to 15%) and stored at –80 ^{o}C.

2.1.7. Transformation

Approximately 10-20 µl ligation product was added into 50 µl semi-thawed competent cells (*E. coli* TOP10) and it was then incubated on ice for 25 min. The cell mixture was heated shocked at 42 ^{o}C for exactly 2 min and chilled on ice for another 2 min. A 200 µl portion of 2xTY medium was then added into the cells and cells were grown at 37 ^{o}C, 300 rpm for 1.5 h. Transformed cells were then plated on nutrient agar plate containing 50 µg/ml kanamycin and incubated at 37 ^{o}C overnight. Cells transformed with the desired plasmid (with the selective marker) could grow on the kanamycin-containing-agar plate and single colony could be transferring into a universal bottle with 2xTY medium for preparation of bacterial stock. The recombinant plasmids were screened by restriction enzyme digestion and further confirmed by DNA sequencing by ABI PRISM BigDye Terminator Cycle Sequencing Kit (PE Applied Biosystem). A total of 3 sequencing primers were used in the sequencing reactions and the design of their sequences was based on either the sequence of beta-lactamase gene or the downstream sequence of the mal-E gene (Table 2.1). The successfully subcloned plasmid were then transformed into *E. coli* BL21(DE3), expressed in a large scale and used for protein expression.

2.2. Introduction of N170Q mutation by site-directed mutagenesis

Site-directed mutagenesis was carried out by the use of QuickChange II Site-directed Mutagenesis Kit (Strategene). This method allows the rapid introduction of point mutation into sequences of interest, using a pair of complementary mutagenic primers to amplify the entire plasmid in a single PCR reaction. Destruction of the parental template plasmid by DpnI digestion, followed by transformation into *E. coli* cells, allows introduction of the

desired mutation with high efficiency (70-90%).

Two mutagenic primers (Table 2.1), which contain the desired mutation and anneal to the same sequence on opposite strands of the plasmid, were designed to make sure that the melting temperature (T_m) was greater than or equal to 78 ^oC according to the following formula: $T_m = 81.5 + 0.41$ (% GC) - 675/N - % mismatch (where N us the primer length in base pairs). The reaction was prepared by mixing the following reagents: 5 µl of 10X reaction buffer, 125 ng of the two primers, 10-100 ng of template DNA (PenP_E166C beta-lactamase gene subcloned into the pMAL-c2X), 1 µl of dNTP mix, 1 µl of *PfuTurbo* DNA polymerase (2.5 U/µl) and appropriate volume of sterile ddH_20 which make up to a final volume of 50 µl. The mixture was then used for PCR reaction. The reaction mixture was denatured at 95 ^oC for 5 min, 16 cycles of amplification (for single amino acid change) were performed with the following temperatures and reaction time: 95 ^oC for 30 s, 55 ^oC for 1 min, 68 ^oC for 8 min.

During the thermal cycling, Pfu DNA polymerase extended and incorporated the mutagenic primers and resulted in nicked circular double stranded. After that, 1 µl of DpnI (10 U/µl) was added to the PCR amplification product and incubated at 37 ^oC for 1 h to digest the parental supercoiled dsDNA. The product mixture was then transformed into the competent *E. coli* TOP10 bacterial cells and sequence of successful clone was confirmed by DNA sequencing. The successfully subcloned plasmid were then transformed into *E. coli* BL21(DE3) for protein expression at later stage.

2.3. Expression and purification of MBP-beta-lactamase fusion proteins

2.3.1. Expression of beta-lactamase mutants from *E. coli*

A single colony of *E. coli* BL21(DE3) transformed with the desired pMAL-c2x plasmid was inoculated into 5 ml 2xTY medium with 50 µg/ml kanamycin in a universal bottle. The culture was then grown at 37 ^{o}C, 300 rpm for 14-16 h. The 2 ml overnight culture was then diluted 1:100 into a 1 L non-baffled flask containing fresh 200 ml 2xTY medium (Flask was filled with 20% capacity in order to ensure adequate aeration). The culture was then grown at 37 ^{o}C with shaking speed at 300 rpm. Filtered IPTG (isopropylthiogalactoside) was added to the culture (to a final concentration of 0.3 mM) to induce protein production when A_{600} reached 0.5-0.7. The culture was then continually incubated for additional 4 h and transferred into appropriate centrifuge bottles for centrifugation at 6500 rpm and 4 ^{o}C for 25 min. Cells was hence pelleted and supernatant was discarded. The cell pellet could then be stored at –80 ^{o}C for subsequent protein extraction and purification.

2.3.2. Protein extraction by sonication

For protein extraction, the harvested cell pellet was resuspended in appropriate amount of solubilization buffer (20 mM Tris-HCl, 0.2 M sodium chloride and 1 mM EDTA, pH 7.4) (10 ml buffer for cell pellet of 100 ml culture). Lysozyme was added (to a final concentration of 0.075 mg/ml) into the cell suspension and incubated at 30 ^{o}C for 30-60 min. The suspended cells were then lysed on ice by a probe sonicator in short pulses of 30 s for around 5 cycles. The cell debris in the lysate was then removed by centrifugation at 10000 rpm and 4 ^{o}C for 1 h. Supernatant was hence collected and going

to be purified by amylose affinity chromatography.

2.3.3. Protein purification by amylose affinity column

After sonication, supernatant was first clarified by filtration through 0.45 μm filter before loading onto a column packed with amylose affinity gel (New England Biolabs), which was pre-equilibrated with binding buffer (20 mM Tris-HCl, 0.2 M sodium chloride and 1 mM EDTA, pH 7.4). The column was then washed with 2.5-column volume of the binding buffer in order to remove the unbound proteins. Elution was performed with a maltose gradient of 2 segments (0-4 mM and 4-10 mM). All the steps were conducted at 4 ^{o}C and fractions of 8 ml were collected. Eluates showing UV absorbance were analyzed by SDS-PAGE to estimate the yield and purity, and fractions containing the target enzyme were pooled and concentrated by ultrafiltration. Buffer exchange was then carried against 20 mM ammonium bicarbonate and protein sample could be freeze-dried and to be stored at –20 ^{o}C for future use.

2.3.4. Protein gel electrophoresis (SDS/PAGE)

Proteins were separated by polyacrylamide gel electrophoresis (PAGE) in the presence of sodium dodecyl sulphate (SDS) in a Mini-PROTEIN III dual slab cell (Bio-Rad Laboratories). Protein sample was mixed with 10 μl loading buffer with contained the reducing agent beta-mercaptoethanol and SDS. Each polyacrylamide gel was a discontinuous composite gel containing a short stacking gel of 12% layered on top of a long resolving gel of 12% and was subjected to electrophoresis in running buffer at 200 volts for about 1 h. The low-range or broad-range protein marker from Bio-Rad was run

with the samples at the same time and was used to estimate the molecular weight of the protein bands. When the electrophoresis was finished, the gel was stained in Coomassie Blue R-250 staining solution (25% methanol, 10% acetic acid and 0.06% Coomassie Blue R-250) for about 5-15 min with agitation. Then the gel was destained in destaining solution (10% acetic acid and 10% methanol) with agitation, until the background of the gel was clear. After soaking in water for a while, the gel was dried by the use of gel drying films (Promega).

2.3.5. Determination of protein concentration

In this study, the concentrations of the protein samples were estimated by the Bradford assay (Zor *et al.*, 1996). A 800 µl portion of the diluted protein samples were incubated with 200 µl Bradford Reagent Dye (Bio-Rad Laboratories) for 10 min at room temperature. The protein concentration was measured spectrophotometically at 595 nm against a standard protein curve. The bovine serum albumin (sigma) was used as the standard protein and a straight standard curve was obtained with protein concentration range of 0-20 µg/ml.

2.4. Removal of MBP from MBP-beta-lactamase fusion proteins

2.4.1. Cleavage of MBP by Factor Xa

As recommended by the manufacturer's instruction, fusion protein cleavage was carried out by adding Factor Xa into the fusion protein solution at a w/w ratio of 1% the amount of fusion protein (e.g. 1 mg Factor Xa for a reaction containing 100 mg fusion protein). Appropriate amount of MBP-beta-lactamase was first dissolved in the buffer containing 20 mM Tris-HCl and 25 mM NaCl at pH 8.0, making a protein solution with a concentration of around 1 mg/ml. One percent of the amount of fusion protein of Factor Xa was then added into the protein solution and the mixture was gently stirred at either 4 ^{o}C or room temperature for 24 h.

2.4.2. Purification of MBP-cleaved protein by DEAE cellulose column

Following the incubation with Factor Xa, the protein cleavage mixture was loaded onto a DEAE cellulose column to purify the beta-lactamase away from MBP and the protease. The column was pre-equilibrated with binding buffer (20 mM Tris-HCl, 25 mM NaCl at pH 8.0). After loading the protein cleavage mixture onto the column, it was washed with 13-column volume of the binding buffer to remove the unbound proteins. Elution was performed with a gradient of 25 mM NaCl to 500 mM NaCl in 25-column volume of buffer. Eluates showing UV absorbance were analyzed by SDS-PAGE to estimate the yield and purity, and fractions containing the target enzyme were pooled and concentrated by ultrafiltration. Buffer exchange was then carried against 20 mM ammonium bicarbonate and protein sample could be freeze-dried and to be stored at –20 ^{o}C for future use.

2.5. Modification of E166C and E166C/N170Q with fluorophores

2.5.1. Protein labeling

Approximately 2 mg mutant was dissolved in 4 ml of 6 M guanidinium hydrochloride (GuHCl). The protein solution was then incubated at room temperature for 30 min to unfold the mutant. The pH of the solution was then adjusted to 7.5 with 0.2 M sodium hydroxide. A 20 mM stock solution of fluorescence label was prepared by dissolving the fluorophore in DMF. A ten-fold molar excess of the label from stock solution was then added into the protein solution. This mixture was then stirred at room temperature for 2 to 4 h in the dark to allow mutant labeling.

2.5.2. Refolding of mutant enzymes

Following the labeling reaction, excess label was then removed by dialyzing the labeling mixture against 1 L of 50 mM potassium phosphate buffer (pH 7.0) at 4 ^{o}C with a dialysis bag of 12 kDa cut-off size. Buffer exchanges were carried out regularly for at least 6 times (around 2 times per day). Upon the removal of GuHCl from the reaction mixture, enzymes were allowed to refold into their native structures (to be confirmed by circular dichroism spectrometry). The enzymes were now ready for fluorescent measurement and were stored at –20 ^{o}C.

2.6. Kinetic characterization of PenP mutants and their fluorophore-labeled derivatives

2.6.1. Preparation of nitrocefin solution

Nitrocefin was used as the substrate for monitoring the activities of the beta-lactamases in this project. Since nitrocefin is difficult to dissolve in the 50 mM potassium phosphate assay buffer, a stock solution was firstly prepared by dissolving 0.0015 g nitrocefin powder in 200 µl of DMF. This stock solution could be kept at -20 ^{o}C for one month. Before carrying the activity assay, 210 µl of the nitrocefin stock solution was added slowly (drop by drop) into 5.79 ml of the assay buffer with constant stirring. The concentration of nitrocefin for use would then be calculated from the measurement of its absorbance at A_{386} (ε = 19.2 $mM^{-1}cm^{-1}$). This nitrocefin solution could only be kept for a day and have to be freshly prepared from the stock solution each time.

2.6.2. Monitoring the initial rates of substrate hydrolysis

Kinetic measurements were carried in a Perkin-Elmer Lambda Bio20 UV/visible spectrometer. All assays were performed at 20 ^{o}C in 50 mM potassium phosphate buffer at pH 7.0. Initial velocities of substrate hydrolysis were monitored by gain in UV absorbance at 500 nm for nitrocefin ($\triangle\varepsilon_{500}$= 15900 $M^{-1}cm^{-1}$). The wavelength for measuring the enzyme activity for specific substrate is the wavelength at which the difference in absorbance between substrate and product is maximum. The initial rate was taken from the first 5 min of the reaction.

2.6.3. Calculation of kinetic parameters of PenP mutants

Rate constants were determined by fitting the initial rates of nitrocefin hydrolysis to the program of Stanislawski by non-linear regression analysis (Stanislawski, 1991). The initial rate of hydrolysis occurring in the first 5 min was determined in duplicate at each of the 6 to 7 different nitrocefin concentrations. The values of K_m and k_{cat} were then calculated assuming that Michaelis-Menten kinetics was obeyed, using mainly non-linear regression analysis (Equation 1 and 2).

Equation 1: $V_0 = (V_{max} \times [S])/ (K_m + [S])$

Equation 2: $k_{cat} = V_{max}/ [E]$

where V_0 is the initial rate of the reacton;

V_{max} is the maximum rate of reaction;

[S] is the initial substrate concentration;

K_m is the Michaelis constant;

k_{cat} is the turnover number;

[E] is the enzyme concentration.

2.7. Protein structural and thermostability studies

2.7.1. Study of protein secondary structure by circular dichroism spectrometry

Circular dichroism (CD) spectra were measured by the Jasco 810 spectropolarimeter using a water-jacketed cylindrical cell with a path length of 1.0 mm. Temperature control was provided by a Neslab RTE-211 circulating water bath interfaced with a MTP-6 programmer. Protein samples were dissolved in 5 mM potassium phosphate buffer at pH 7.0 and the concentrations were in the range of 150-200 μg/ml. Scanning were carried at a scan speed of 50 nm/min at 25 ^{o}C over the range of 185-250 nm (far-UV region).

2.7.2. Thermal-denaturation study

Thermal denaturation of the MBP-beta-lactamase was studied by monitoring the far-UV molar ellipticity at 222 nm at a scan rate of 50 nm/min in 5 mM potassium phosphate buffer at pH 7.0. Data was recorded as a function of increasing temperature with a rate of 1 ^{o}C/min over the range of 20-85 ^{o}C. The protein concentrations of the samples were in the range of 150-200 μg/ml.

2.7.3. Thermal-inactivation study

The enzymes were incubated at 50 ^{o}C in 50 mM potassium phosphate buffer at pH 7.0. Sample was withdrawn after various periods of time and immediately cooled on ice. The residual activities of the enzymes in hydrolyzing nitrocefin at 20 ^{o}C were then measured in duplicate by the method described in Section 2.6.

2.8. Fluorescence studies of fluorophore-labeled beta-lactamases

All measurements were performed by a Perkin-Elmer LS50B spectrofluorimeter at 20 ^{o}C in 50 mM potassium phosphate buffer at pH 7.0.

2.8.1. Fluorescence spectra scanning

Appropriate volume of labeled mutant (with working concentration of 1.0 x 10^{-7} M) was mixed with 50 mM potassium phosphate buffer (pH 7.0) to make up a total volume of 450 µl in a quartz cuvette with a 1-cm excitation path length. A 50 µl portion of antibiotic solution was then added to the enzyme mixture (make up to the correct working concentrations) and inverted for several times. This reaction mixture was then scanned for fluorescence emission at a range of wavelength. Excitation and emission parameters for corresponding fluorophores used were set according to Table 2.2.

2.8.2. Time-resolved fluorescence measurement

Procedures involved were similar to the description in Section 2.8.1. However, an hour fluorescence spectra was traced at a fixed emission wavelength (wavelength at which maximum change in fluorescence intensity was observed) after the addition of the antibiotic. Excitation and emission parameters for corresponding fluorophores used were listed in Table 2.2.

Table 2.2. Settings of parameters in fluorescence measurement.

		Fluorescein	Badan
Excitation wavelength		494 nm	380 nm
Emission wavelength	Scanning	500-600 nm	410-600 nm
	Time-resolved measurement	515 nm	500 nm
Slit width		5 nm	10 nm
Scan speed		250 nm/min	250 nm/min

2.9. Detection of acyl-enzyme intermediate in the hydrolysis of penicillin G by fluorophore-labeled beta-lactamases

The enzyme and antibiotic solutions used in this experiment was prepared in 20 mM ammonium acetate buffer at pH 7.0. The stopped-flow study and quench-flow experiment (combined with ESI-MS) were done in parallel with identical mutant and substrate concentrations of 5×10^{-7} M. All measurements were carried out at 20^{o}C.

2.9.1. Time-resolved fluorescence measurement by stopped-flow study

Enzymatic reactions were initiated by mixing the enzyme solution with equal concentration of antibiotic, which was done mechanically by SX.18MV-R stopped flow instrument (Applied Photophysics Ltd., Leatherhead, UK). 1000 data points were acquired in each fluorescence spectrum.

2.9.2. Quench-flow experiment combined with ESI-MS

This part was performed by Mr. So Pui Kin. The enzymatic reactions were initiated by mixing the enzyme solution with equal concentration of antibiotic, which was done mechanically by a quench-flow device (Biologic SFM/400). The reaction was quenched at various times by adding formic acid at the final concentration of 4% (v/v). The final pH of the quenched solution was approximately 2. Reaction times were computer-controlled by varying the flow rate of reactants. The quenched samples were then injected into the mass spectrometer (ESI-Q-TOF 2, waters) for spectral scannings. The mass spectrometer was scanned over a m/z range of 700-1600 m/z and the multiply charged spectra were de-convoluted by the transform program (MassLynx 4.1, waters). The m/z was calibrated

externally with Horse Heart Myoglobin (M.W=16950). The ratio of covalently – bound acyl-enzyme intermediates to total enzyme concentration ([ES*] / [E_{total}]) at different times were determined based on peak areas in the mass spectra.

Chapter Three: Results

3.1. Expression of MBP-beta-lactamase fusion proteins

Details of the expression and purification procedures were described in Sections 2.3 and 2.4. The growth curves of *E. coli* BL-21 transformed with MBP_PenP_E166C and MBP_PenP_E166C/N170Q are shown in Figure 3.1. Protein production was induced by adding IPTG when A_{600} reached 0.5-0.7. Followed by induction, sample was withdrawn at each h and the protein content was analyzed by SDS-PAGE analysis (Figure 3.2). From the SDS-PAGE, protein bands showing the molecular size approximately 75,000 Da corresponded to our target protein. The amount of target proteins increased with the culturing time and the maximum was reached after incubation of 3-4 h. Since the production of MBP-PenP took place inside the cells (cytoplasmic expression), many other protein bands were also seen in the SDS-PAGE and they corresponded to other cellular proteins present in the cell lysate. The intensity of the band corresponded to MBP-beta-lactamase indicated that MBP-beta-lactamase constituted approximately 50% of the total protein.

(a)

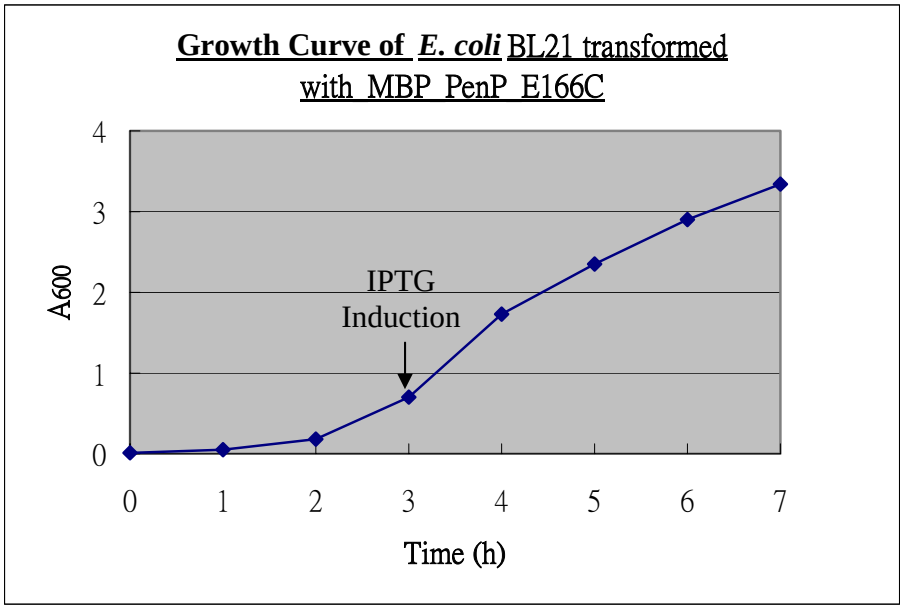

(b)

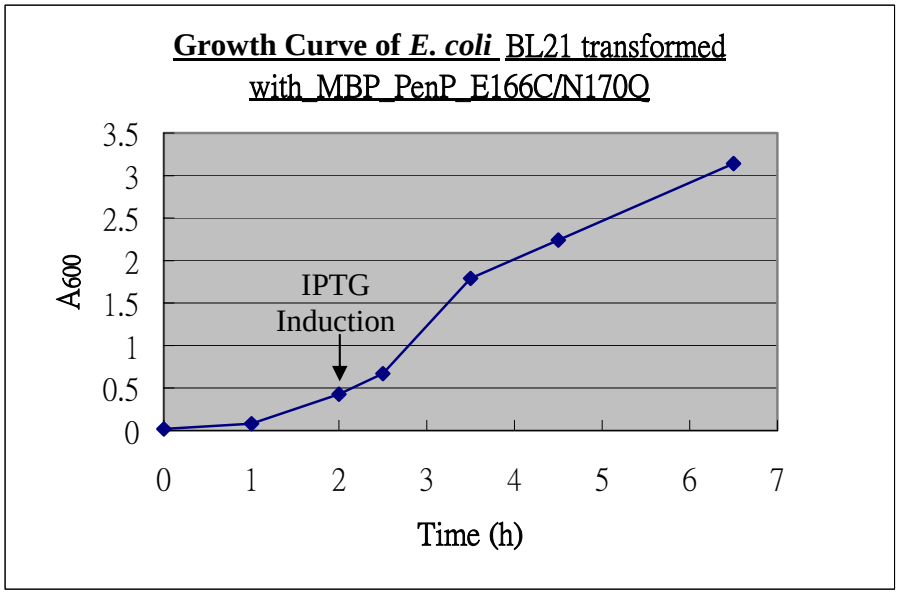

Figure 3.1. Growth curves of *E. coli* BL-21 transformed with MBP_PenP_E166C (a) and MBP_PenP_E166C/N170Q (b), respectively. The growth of bacteria was monitored by measuring the absorbance at 600 nm wavelength (A_{600}). Beta-lactamase production was induced by IPTG addition (to a final concentration of 0.3 mM) when A_{600} reached 0.5-0.7.

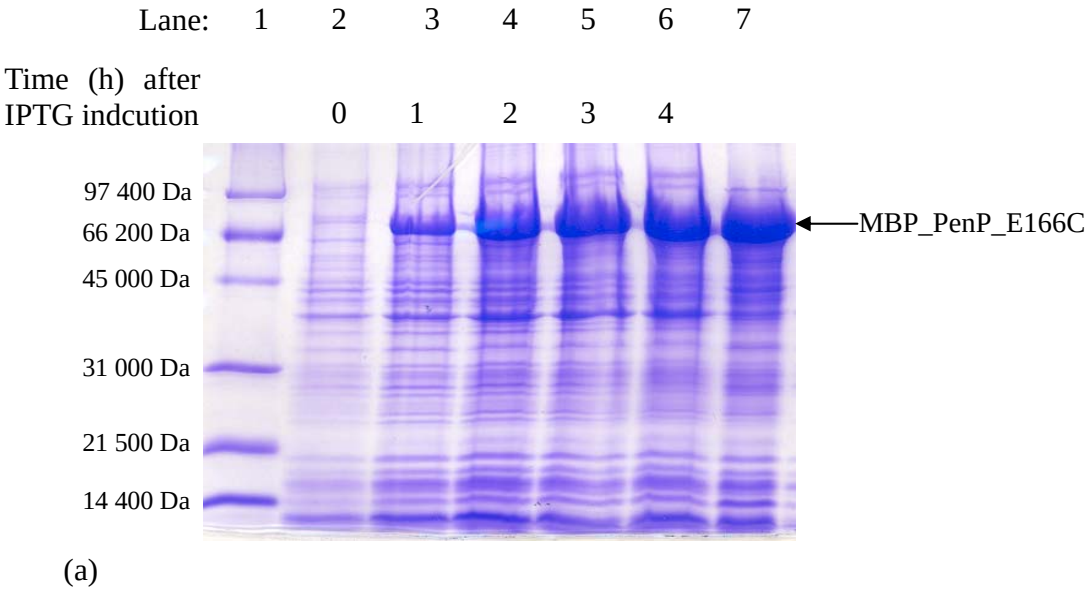

(a)

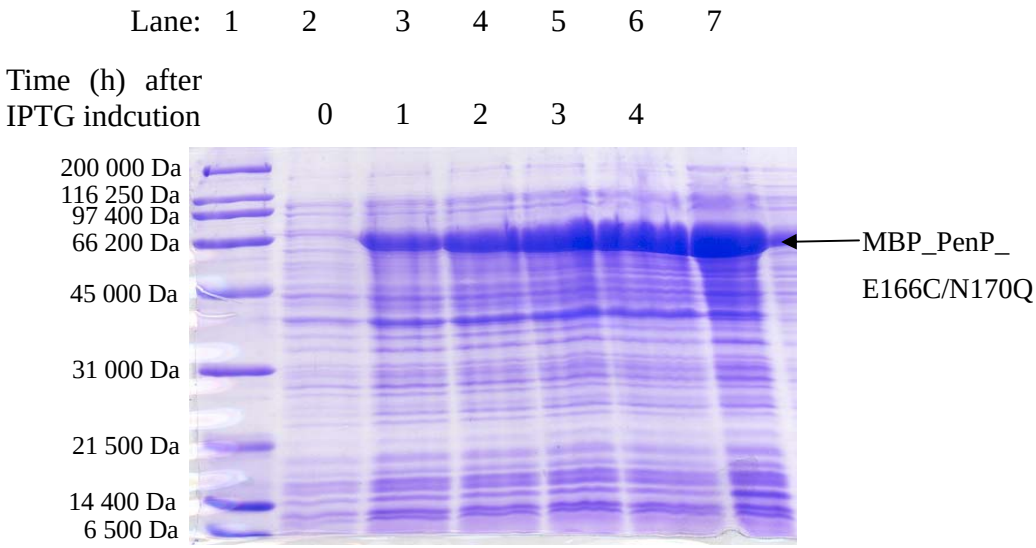

(b)

Figure 3.2. 12% SDS/PAGE analysis of the expression profile for MBP_PenP_E166C (a) and MBP_PenP_E166C/N170Q (b), in *E. coli* at different time points after IPTG induction. Lane 1 is the low range molecular weight marker; lanes 2-6 represent the sample withdrawn at 0, 1, 2, 3 and 4 h after IPTG induction, respectively; lane 7 refers to the sample just prior to the purification by affinity chromatography.

3.2. Purification of MBP-beta-lactamase fusion proteins

The MBP-beta-lactamase fusion proteins were purified by one-step affinity chromatography using an amylose column. Purification profiles of the fusion proteins in amylose affinity column are shown in Figure 3.3. A single peak was resulted from both purifications of single and double mutants. Samples in fractions of the elution peaks were analyzed by SDS/PAGE (Figure 3.4). Bands showing molecular size at approximately 75,000 Da corresponded to our target protein. Fractions showing target protein were pooled and concentrated. SDS/PAGE analysis of the concentrated sample indicated more than 95% pure MBP fusion protein was obtained (refer to lane 2 of Figure 3.5). Purification tables for the mutants are shown in Tables 3.1 and 3.2, respectively. Only approximately 20% of the total protein was recovered, which was not in agreement with the yield of MBP-beta-lactamase estimated from the SDS/PAGE analysis (approximately 50% of the total protein). The great protein loss might be due to the overloading of the amylose column, indicated by the presence of MBP-beta-lactamase in the flow-through (SDS/PAGE not shown). Enzyme activities were not shown in the purification tables as the sample of crude exhibited a very high enzyme activity, which was believed to be due to the enzymes of the host strain (*E. coli* BL21). However, as indicated by the low enzyme activity of our purified beta-lactamase, the contaminating enzymes from the host strain were removed completely after the purification by amylose column. The production yield for MBP_PenP_E166C fusion protein was approximately 160 mg/L of culture and that of MBP_PenP_E166C/N170Q was approximately 104 mg/L of culture.

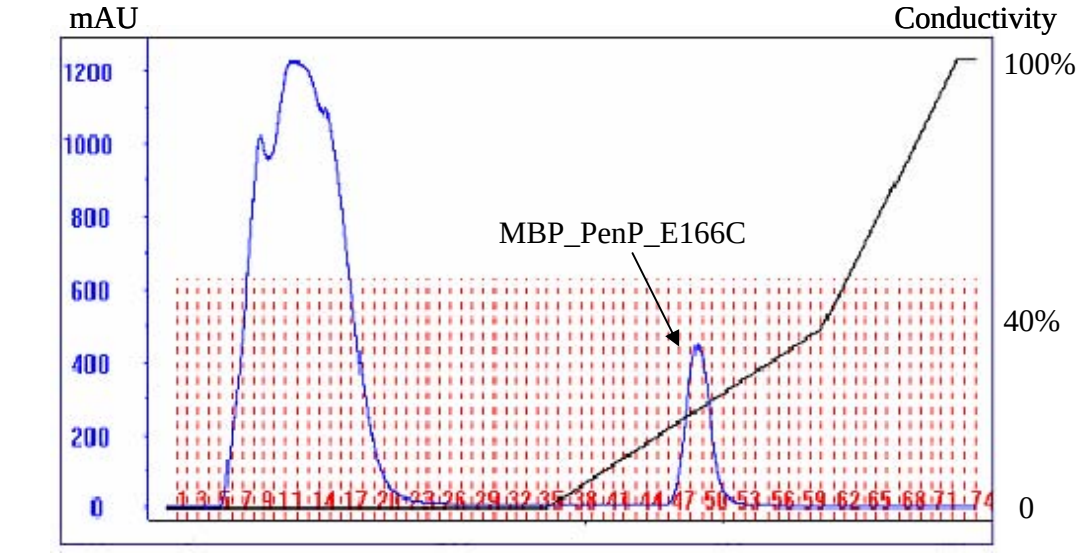

(a)

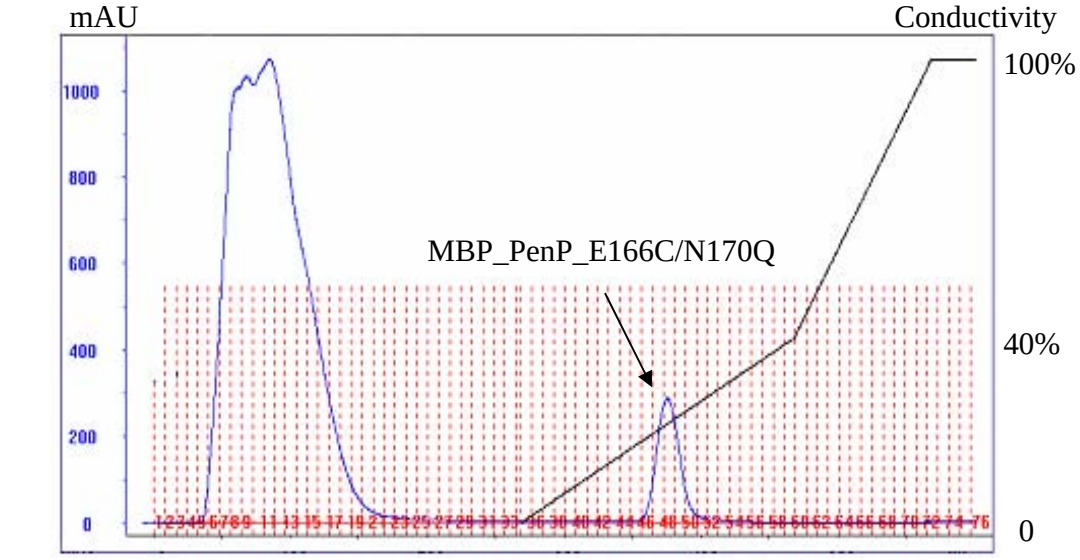

(b)

Figure 3.3. Elution profiles of MBP_PenP_E166C (a) and MBP_PenP_E166C/N170Q (b) from amylose affinity chromatography. Column was washed with 2.5-column volume of Tris-HCl buffer to remove unbound proteins. Elution was performed with a maltose gradient of 2 segments (0-4 mM and 4-10 mM). All the steps were conducted at 4 ^{o}C and fractions of 8 ml were collected. Protein concentration was determined by absorbance at 280 nm and the unit was mAU (milli absorption unit). Elution salt concentration was determined by the conductivity flow cell, and it was represented by conductivity, i.e. 100% =10 mM maltose.

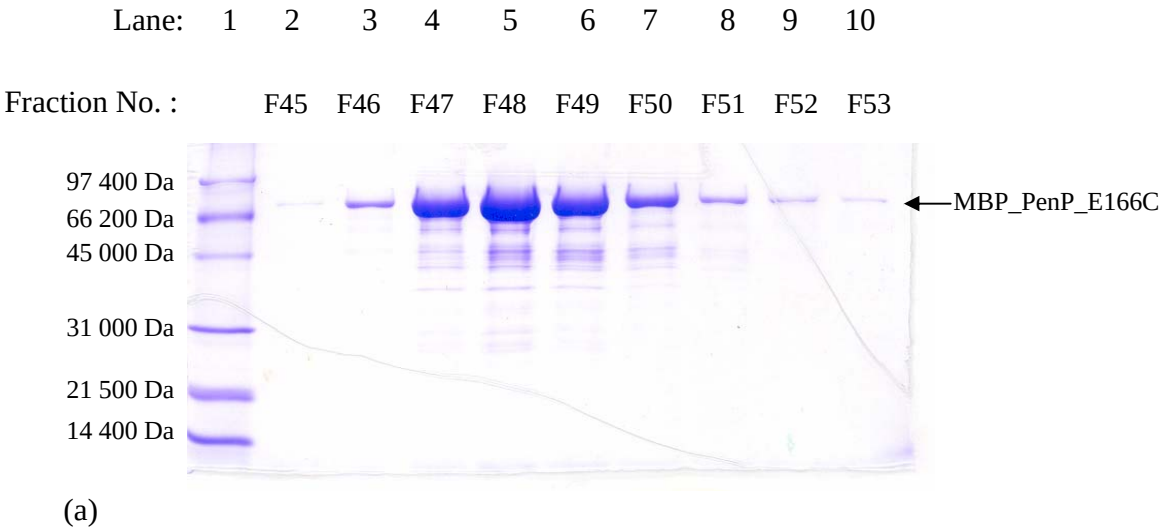

(a)

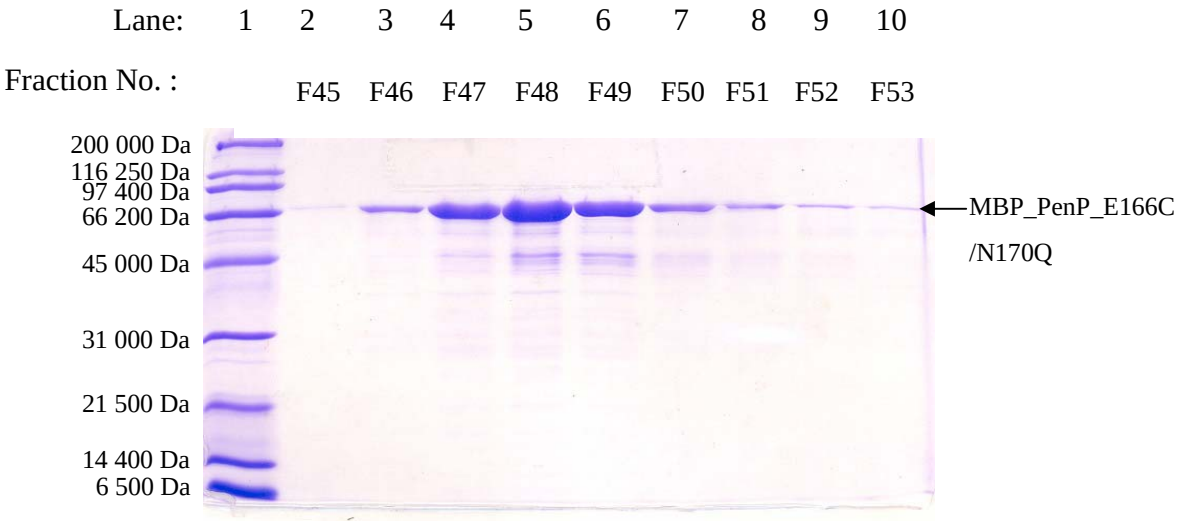

(b)

Figure 3.4. 12% SDS/PAGE analysis of the column fractions from amylose affinity chromatography for MBP_PenP_E166C (a) and MBP_E166C/N170Q (b). Lane 1 is the low range molecular weight marker; lanes 2-10 represent different column fractions as indicated by the numbers with the letter “F”.

Table 3.1. Purification table of MBP_PenP_E166C beta-lactamase. Data was based on 200 ml of bacterial culture.

Purification Step	Protein Concentration (mg/ml)	Total Volume (ml)	Total Protein (mg)	Percentage Protein Recovery (%)
Crude	5.86	24	140.64	100
Amylose Affinity Column	0.53	64	33.92	24.12
Concentration by Ultra-Amicon	5.98	5.4	32.29	22.96

Yield of purified protein = 32.29 mg x 1000ml/ 200ml

= **161.45 mg/L of culture**

Table 3.2. Purification table of MBP_PenP_E166C/N170Q beta-lactamase. Data was based on 200 ml of bacterial culture.

Purification Step	Protein Concentration (mg/ml)	Total Volume (ml)	Total Protein (mg)	Percentage Protein Recovery (%)
Crude	5.88	18	105.84	100
Amylose Affinity Column	0.35	64	22.40	21.16
Concentration by Ultra-Amicon	3.48	6	20.88	19.73

Yield of purified protein = 20.88 mg x 1000ml/ 200ml

= **104.4 mg/L of culture**

3.3. Removal of MBP from MBP-beta-lactamase fusion proteins

3.3.1. Cleavage of MBP by Factor Xa

MBP was cleaved and removed from the purified MBP-beta-lactamases by Factor Xa according to the method described in Section 2.4. Samples were withdrawn from the reaction mixture after incubation of 6 and 24 h, respectively, and were analyzed by SDS/PAGE (Figure 3.5). Lane 2 refers to the uncleaved MBP-PenP beta-lactamase, which shows the protein band with uncleaved protein size of approximately 75,000 Da. From the other lanes, it could be seen that the cleavage reaction resulted in two protein bands, with molecular size of approximately 42,500 Da and 30,000 Da, representing MBP and MBP-cleaved beta-lactamase, respectively. The fact that the band, corresponded to the uncleaved protein, disappeared in the sample withdrawn after 24 h of incubation, indicated that complete cleavage was achieved. All the cleaved proteins were in fully soluble form.

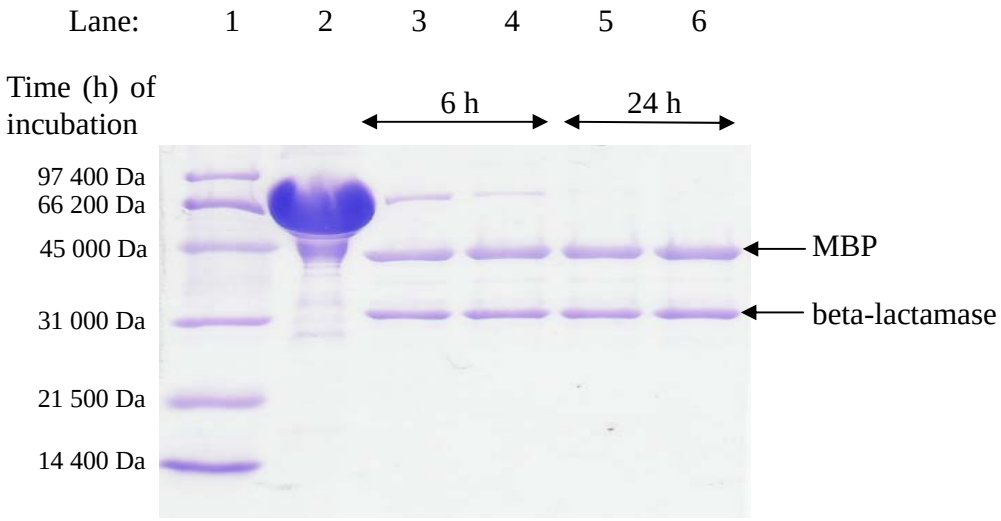

Figure 3.5. 12% SDS/PAGE analysis of MBP-cleaved beta-lactamases by Factor Xa at different incubation time points. Lane 1 is the low range molecular weight marker; lane 2 is the uncleaved MBP-PenP beta-lactamase; lanes 3-6 refer to the samples withdrawn from the cleavage reaction at 6 and 24 h, in which lanes 3 and 5 are obtained from cleavage reaction of MBP_PenP_E166C, whereas lanes 4 and 6 are from cleavage reaction of MBP_ PenP_E166C/N170Q.

3.3.2. Purification of cleavage product by DEAE ion-exchange chromatography

Following the cleavage by Factor Xa, cleavage products were purified by running the DEAE column. The corresponding purification profiles are shown in Figure 3.6. It could be seen that three peaks were resulted in each separation, and samples in different fractions were analyzed by SDS/PAGE (Figure 3.7). It was found that only MBP could bind to the column and appeared in the second peak of the profiles, while the MBP-cleaved beta-lactamases came out as unbound proteins and appeared in the earlier fractions. Purification tables of the MBP-cleaved beta-lactamases are shown in Tables 3.3 and 3.4, respectively. It could be seen that only 2.3-2.6 mg of MBP-cleaved beta-lactamases was obtained from the cleavage of 10 mg of fusion protein.

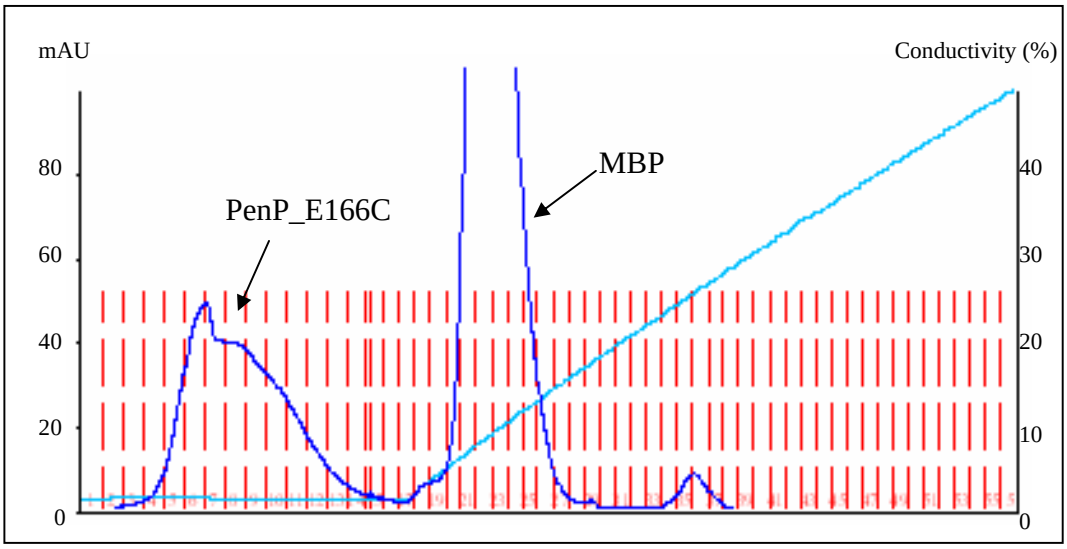

(a)

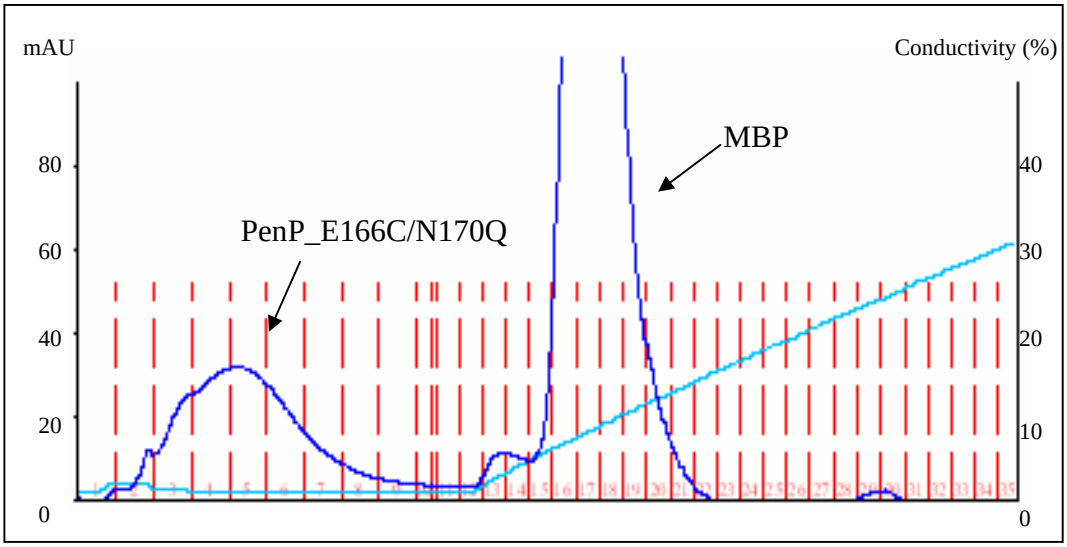

(b)

Figure 3.6. Elution profiles of MBP-cleaved PenP_E166C (a) and MBP-cleaved PenP_E166C/N170Q (b) from DEAE ion exchange chromatography. Column was washed with 12-column volume of Tris-HCl buffer to remove unbound proteins. Elution was performed with a gradient of 25 mM NaCl to 500 mM NaCl in 25-column volume of buffer. Protein concentration was determined by absorbance at 280 nm and the unit was mAU (milli absorption unit). Elution salt concentration was determined by the conductivity flow cell, and it was represented by conductivity, i.e. 40% = 215 mM NaCl.

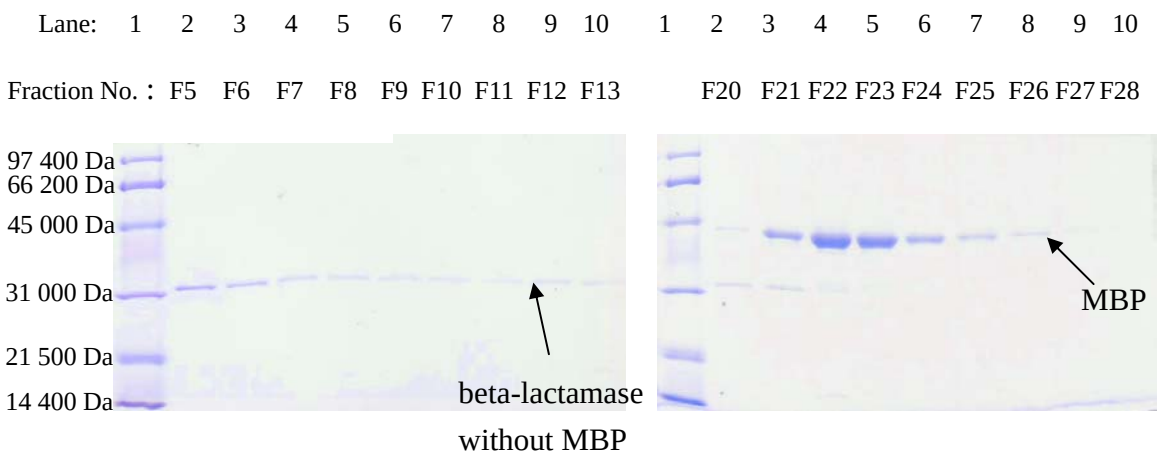

(a)

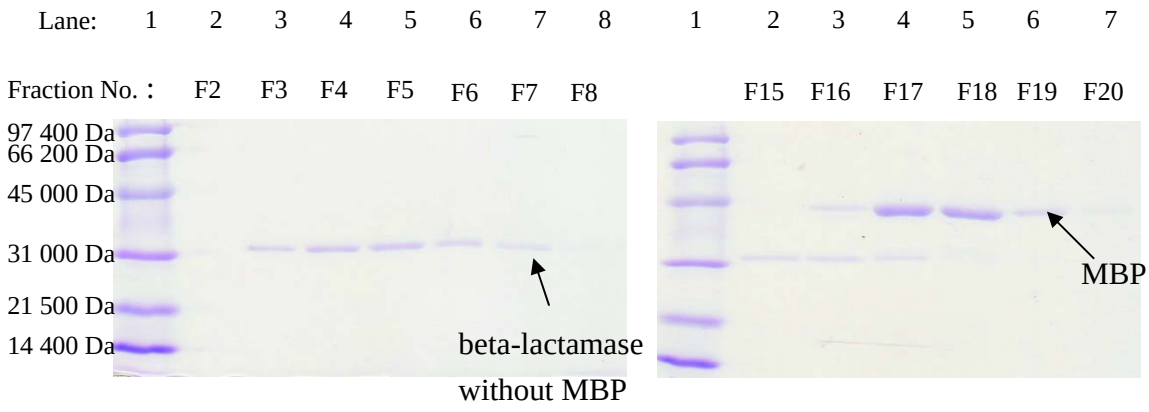

(b)

Figure 3.7. 12% SDS/PAGE analysis of the column fractions from the DEAE ion-exchange chromatography for MBP-cleaved E166C (a) and MBP-cleaved E166C/N170Q (b). Lane 1 is the MW marker; lanes 2-10 represent different column fractions as indicated by the numbers with the letter “F”.

Table 3.3. Purification table of MBP-cleaved PenP_E166C beta-lactamase. Data was based on 10 mg of uncleaved MBP_PenP_E166C protein.

Purification Step	Protein Concentration (mg/ml)	Total Volume (ml)	Total Protein (mg)	Percentage Protein Recovery (%)
Starting material	/	/	10	100
DEAE Ion-exchange Column	Not measurable	30	N/A	N/A
Concentration by Ultra-Amicon	2.6	1	2.6	26

Protein Yield = 2.6 mg of MBP-cleaved enzyme/ 10 mg of uncleaved enzyme

= **0.26 mg of MBP-cleaved enzyme/mg of uncleaved enzyme**

Table 3.4. Purification table of MBP-cleaved PenP_E166C/N170Q beta-lactamase. Data was based on 10 mg of uncleaved MBP_PenP_E166C/N170Q protein.

Purification Step	Protein Concentration (mg/ml)	Total Volume (ml)	Total Protein (mg)	Percentage Protein Recovery (%)
Starting material	/	/	10	100
DEAE Ion-exchange Column	Not measurable	40	N/A	N/A
Concentration by Ultra-Amicon	2.3	1	2.3	23

Protein Yield = 2.3 mg of MBP-cleaved enzyme/ 10 mg of uncleaved enzyme

= **0.23 mg of MBP-cleaved enzyme/mg of uncleaved enzyme**

3.4. Modification of E166C and E166C/N170Q with fluorophores

The beta-lactamase mutants were labeled with fluorophores according to the method described in Section 2.5. The SDS/PAGE analysis of the labeled and unlabeled mutants and the corresponding fluorescence image are shown in Figure 3.8. It could be seen from the image that the labeled mutants fluoresced under UV illumination. In this thesis, the biosensors were named according to: (1) the type of mutant and (2) the type of fluorophore used in their construction. For example, the E166C mutant, which was labeled with fluorescein-5-maleimide, was named “E166Cf”. For the E166C/N170Q mutant, which was labeled with badan, was named “E166Cb/N170Q”. As confirmed by mass spectrophotometric analysis, only the samples showing >95% labeled with fluorophores were used in the study (refer to Appendix II for the mass spectra).

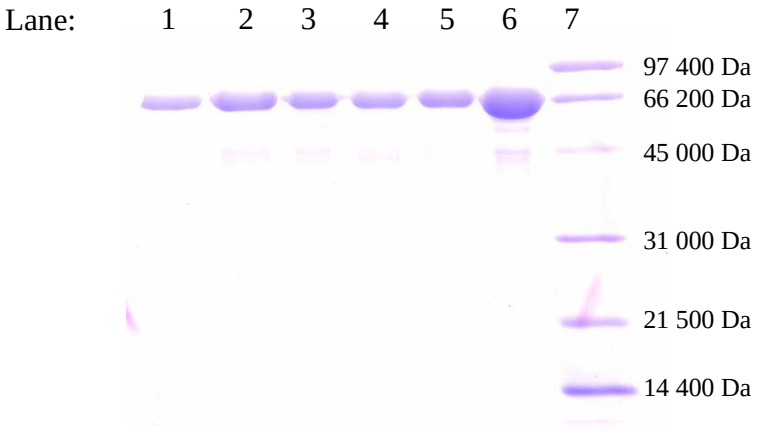

(a)

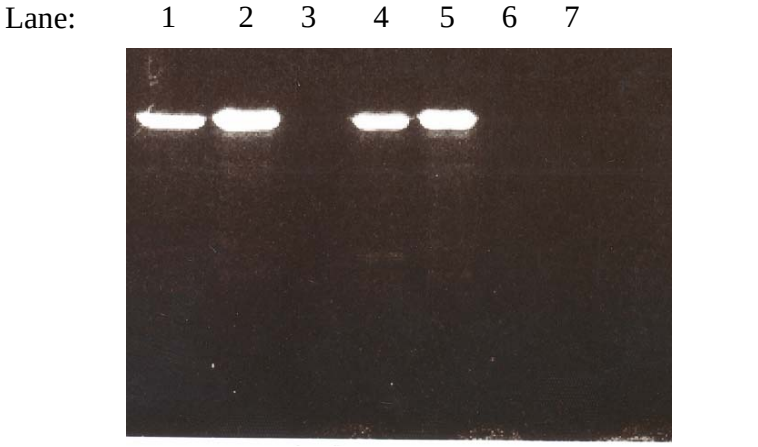

(b)

Figure 3.8. (a) 12% SDS/PAGE analysis of MBP_PenP_E166C, MBP_PenP_E166C/N170Q and their fluorophore-labeled derivatives. Lane 1 is MBP_PenP_E166Cb; lane 2 is MBP_PenP_E166Cf; lane 3 is unlabeled MBP_PenP_E166C; lane 4 is MBP_PenP_E166Cb/N170Q; lane 5 is MBP_PenP_E166Cf/N170Q; lane 6 is unlabeled MBP_PenP_E166C/N170Q and lane 7 is the low range molecular weight marker. (b) Corresponding fluorescence image under UV.

3.5. Kinetic characterization of PenP mutants and their fluorophore-labeled derivatives

The hydrolytic activities of the PenP beta-lactamase and mutants against nitrocefin were determined using the method described in Section 2.6. Nitrocefin was chosen as the substrate because of the large difference in absorbance (at 500 nm) associated with the hydrolysis of this cephalosporin. It is hence ideal for studying the kinetics of mutants displaying very low catalytic activity, i.e. the PenP mutants developed in our project. Indeed, other substrates such as penicillin G and penicillin V were used in the trial experiments, but activities of the PenP mutants towards these substrates were too low that no detectable hydrolysis could be recorded. Therefore, nitrocefin was the only substrate used in the kinetic study of the project.

According to the kinetic parameters listed in Table 3.5, it was found that the mutations E166C and N170Q caused a dramatic decrease in the activity of the PenP beta-lactamase, in which the catalytic efficiency of the E166C and E166C/N170Q were about 4 x 10^4-fold and 1.2 x 10^5-fold lower than that of the wild type, respectively. The k_{cat} of the E166C mutant was approximately 4 x 10^5-fold lower than that of the wild type, and the addition of N170Q mutation even caused further decrease in k_{cat} by five times. Apart from the reduction in the k_{cat}, the K_m values of the mutants were also lowered by the mutations, in which the K_m of E166C and E166C/N170Q were 10-fold and 16-fold lower, respectively, when compared to the wild type enzyme. Since the PenP beta-lactamase mutants exhibited very low hydrolytic capabilities and large quantities of protein samples were required for the determination of kinetic constants, only specific activities of the

fluorophore-labeled enzymes were measured and compared to their unlabeled counterparts (Table 3.6). In general, the specific activities of the fluorophore-labeled beta-lactamases were comparable to those of the unlabeled counterparts, but the fluorescein-labeled mutants showed slightly higher activities. When compared to the wild type enzyme, it was found that the single mutant and its fluorophore-derivatives generally showed over 3.6 x 10^5-fold lower in activity, whereas the double mutant and its fluorophore-derivatives showed over 5.8 x 10^5-fold smaller in the activity.

Table 3.5. Kinetic parameters of wild-type PenP beta-lactamase, E166C and E166C/N170Q against nitrocefin. Conditions: 20 ^{o}C in 50 mM potassium phosphate buffer at pH 7.0. Experiments were done in duplicate. Nitrocefin concentrations: 3-40 µM. Enzyme concentrations: E166C, 0.91 µM; E166C/N170Q, 6.92 µM. Nitrocefin hydrolysis was monitored at 500 nm.

	K_m (µM)	k_{cat} (s^{-1})	k_{cat}/K_m ($\mu M^{-1}s^{-1}$)
E166C	4.24 ± 0.23	(2.7 ± 0.05) x 10^{-3}	(6.37 ± 0.36) x 10^{-4}
E166C/N170Q	2.52 ± 0.266	(0.54 ± 0.01) x 10^{-3}	(2.14 ± 0.23) x 10^{-4}
PenP wild-type beta-lactamase*	41.0	1088	26.54

*Kinetic constants of PenP wild-type beta-lactamase was determined by Escobar *et al.*, 1991) and the assay buffer condition was 50 mM potassium phosphate, pH 7, containing 0.5 M KCl (30 ^{o}C). Nitrocefin concentration: 2-62 µM. Wild-type enzyme concentration: 1.35 nM.

Table 3.6. Specific activities of PenP E166C and its fluorophore-labeled derivatives (a); PenP E166C/N170Q and its fluorophore-labeled derivatives (b). Conditions: 20 ^{o}C in 50 mM potassium phosphate buffer at pH 7.0. Experiments were done in duplicate. Nitrocefin concentrations: 40-100 μM. Enzyme concentrations: wild-type, 0.04 nM; E166C and its fluorophore-labeled derivatives, 0.56-1.1 μM; E166C/N170Q and its fluorophore-labeled derivatives, 1.3-2 μM. Nitrocefin hydrolysis was monitored at 500 nm.

(a)

	Wild-type	**E166C**	**E166Cb**	**E166Cf**
Specific Activity (U/mg)	$(5.75 \pm 0.3) \times 10^5$	0.87 ± 0.21	0.96 ± 0.12	1.58 ± 0.22

(b)

	Wild-type	**E166C/ N170Q**	**E166Cb /N170Q**	**E166Cf /N170Q**
Specific Activity (U/mg)	$(5.75 \pm 0.3) \times 10^5$	0.23 ± 0.07	0.39 ± 0.08	0.99 ± 0.12

1 Unit of Enzyme (U) is defined as the amount of enzyme to hydrolyze 1 nmole of nitrocefin per minute at 20 ^{o}C in 50 mM potassium phosphate buffer at pH 7.0.

3.6. Protein structural and thermostability studies

3.6.1. Study of protein secondary structure

In this study, far-UV CD spectra of purified PenP beta-lactamase, E166C, E166C/N170Q and different fluorophore-labeled mutants were measured, according to the method described in Section 2.7.1. The spectra of purified PenP beta-lactamase, E166C and E166C/N170Q were compared and outlined in Figure 3.9(a). It could be seen from the figure that the spectra of the three beta-lactamases were superimposable on each other. Besides, the calculated secondary structures of the three beta-lactamases are listed in Table 3.7 and shown to be very similar. The results indicated that these 3 candidates shared very similar overall folding and no significant difference was found in their protein structures.

Whereas for measurements of E166Cb, E166Cf, E166Cb/N170Q and E166Cf/N170Q, the results are shown in Figure 3.9(b) and (c), respectively. These spectra are compared to that of the corresponding unlabeled enzyme. It is suggested that the labeled enzymes exhibit similar structure as the unlabeled counterparts as all spectra overlapped with each other. However, according to the calculated secondary structures, the fluorophore-labeled beta-lactamases were shown to have slightly less amount of α-Helix (38-39%) and turn (0-2%) than that of the unlabeled counterparts (with around 42-44% of α-Helix and 2-3% of turn). The lower amounts of α-Helix and turn were compensated by higher amount of β-Sheet in the fluorophore-labeled derivatives. To conclude, the four beta-lactamases seem to show only little alterations in the protein secondary structures, but still share very similar overall folding.

(a)

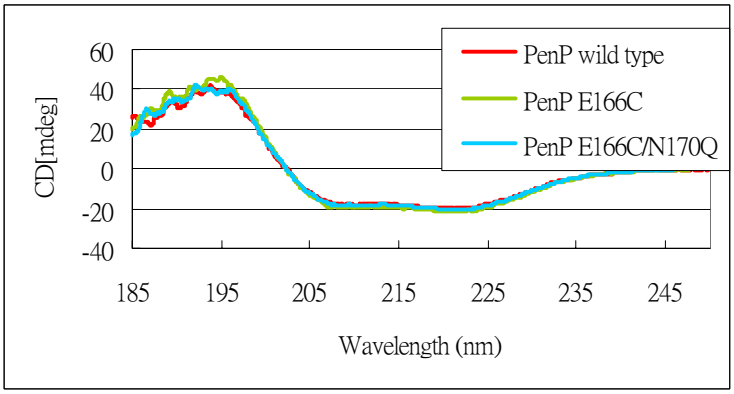

(b)

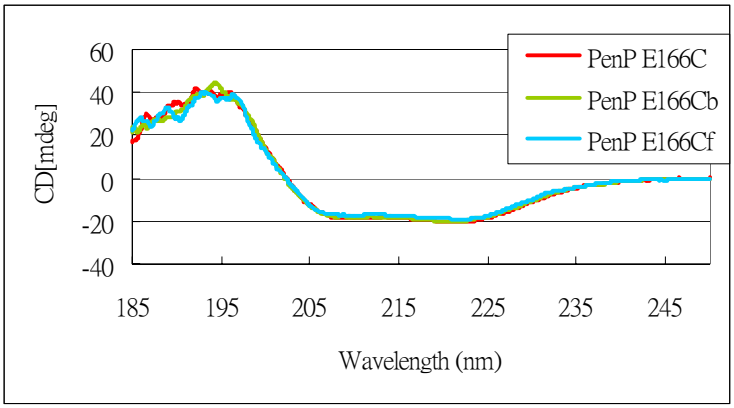

(c)

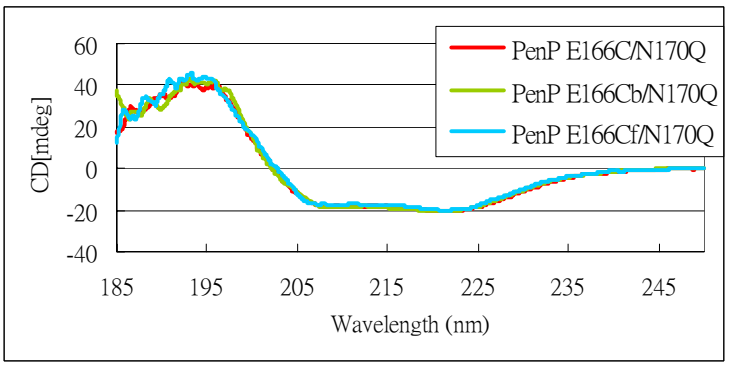

Figure 3.9. Far-UV circular dichroism spectra of PenP beta-lactamase, E166C and E166C/N170Q (a); E166C, E166Cb and E166Cf (b); E166C/N170Q, E166Cb/N170Q and E166Cf/N170Q (c). Scanning were done at a scan speed of 50 nm/min at 25 ^{o}C over the range of 185-250 nm, with the protein samples (150-200 μg/ml) buffered in 5 mM potassium phosphate (pH 7.0).

Table 3.7. The calculated secondary structure of different PenP beta-lactamases and their fluorophore-labeled derivatives.

	α-Helix (%)	**β-Sheet (%)**	**Turn (%)**	**Random (%)**
PenP wild type	43.1	39.8	2.4	14.7
E166C	42.3	42.7	1.9	13.1
E166Cb	38.7	47.9	0.1	13.3
E166Cf	38.4	46.4	1.5	13.7
E166C/N170Q	44.2	38.7	2.6	14.5
E166Cb/N170Q	38.4	48.5	1.2	11.9
E166Cf/N170Q	39.2	49.3	0.3	11.2

3.6.2. Thermal-denaturation of PenP and PenPC beta-lactamases

Thermal denaturation of PenP and PenPC beta-lactamases was carried out by circular dichroism, using the method described in Chapter 2.7.2. Changes in the enzyme folding were recorded as a function of increasing temperature, over the range of 20-85 ^{o}C. Melting curves obtained for PenP and PenPC beta-lactamases, as well as their fluorophore derivatives, are displayed in Figure 3.10. The temperature at which the relative ellipticity is dropped to 50% is regarded as the melting temperature (T_m). From the figure, it was found that the melting temperatures of different PenP biosensors ranged from 56 to 57 ^{o}C, which were much greater than that of the PenPC E166Cf (40 ^{o}C). The unlabeled PenP beta-lactamase mutants, which were also included in the study, also showed higher melting temperatures (around 59 ^{o}C) than that of the unlabeled PenPC E166C (43 ^{o}C). The results reflected that the PenP beta-lactamase confer better thermostability than the PenPC enzyme

For the PenP wild type beta-lactamase, it was found to have the highest T_m of around 64 ^{o}C. Due to the little drop of T_m in PenP E166C, it could be deduced that the mutation E166C may disturb the enzyme folding in little degree (perhaps by interfering the intrinsic interactions within the enzyme itself), but with no significant change in the overall enzyme structure (as suggested by the structural studies in the previous section). However, the mutation N170Q seems not to have such effect as the T_m of the two mutants were very similar. In addition, the attachment of fluorophore to enzyme was also found to cause a slight decrease in the T_m, and it might be attributed to the fact that the fluorophore attachment leads to a slight alternation to the protein structure.

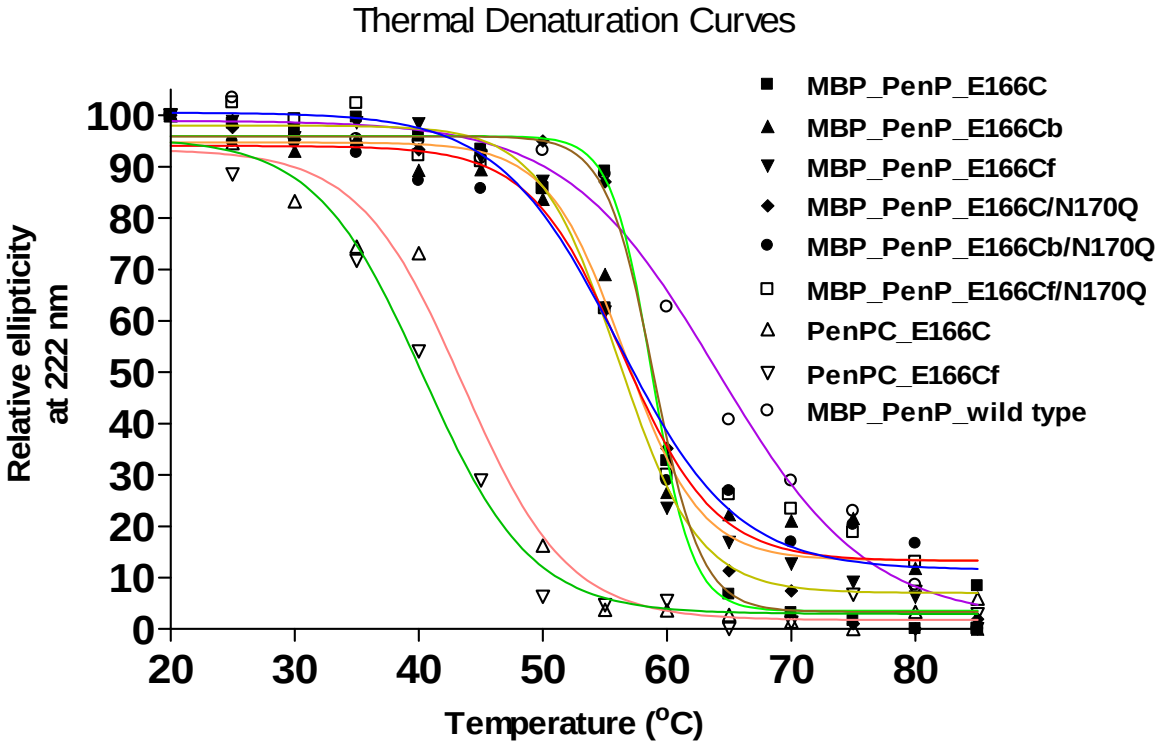

Figure 3.10. Thermal denaturation curves for PenP beta-lactamases, PenPC beta-lactamase and their fluorophore-labeled derivatives. Data was collected as a function of increasing temperature with a rate of 1 °C/min over the range of 20-85 °C in 5 mM potassium phosphate buffer (pH.7.0).

3.6.3. Thermal-inactivation of PenP and PenPC beta-lactamases

To study the effect of heat stress on the activities of beta-lactamases, heat inactivation study was performed according to the method described in Section 2.7.3. The residual activities of the enzymes, upon incubation at 50 ^{o}C for different periods of time, were measured and results are shown in Figure 3.11. The results indicated that the activity of PenPC E166C mutant dropped rapidly upon the incubation of enzyme at 50 ^{o}C, while the PenP mutants showed no change in the activities and remained very active upon an incubation of an hour. The corresponding fluorophore-labeled counterparts were also included in the study and similar observations were found. Since the badan-labeled PenP beta-lactamases behaved similarly as the fluorescein-labeled counterparts, their curves were not shown in the figure.

The rapid decrease in the activity of PenPC beta-lactamase could be attributed to its low thermostability. According to the previous section, the melting temperatures of the PenPC beta-lactamases were found to be at around 40 ^{o}C to 43 ^{o}C. Exposing to high temperature such as 50 ^{o}C, the active-site structure creased easily and the activity hence decreased. In contrast, the higher thermostability of PenP beta-lactamase, with melting temperatures at around 56 ^{o}C to 59 ^{o}C, allowed the enzyme to maintain a well-defined active-site structure at 50 ^{o}C. Therefore, the PenP enzymes kept functioning properly and 100% of the residual activities could be retained.

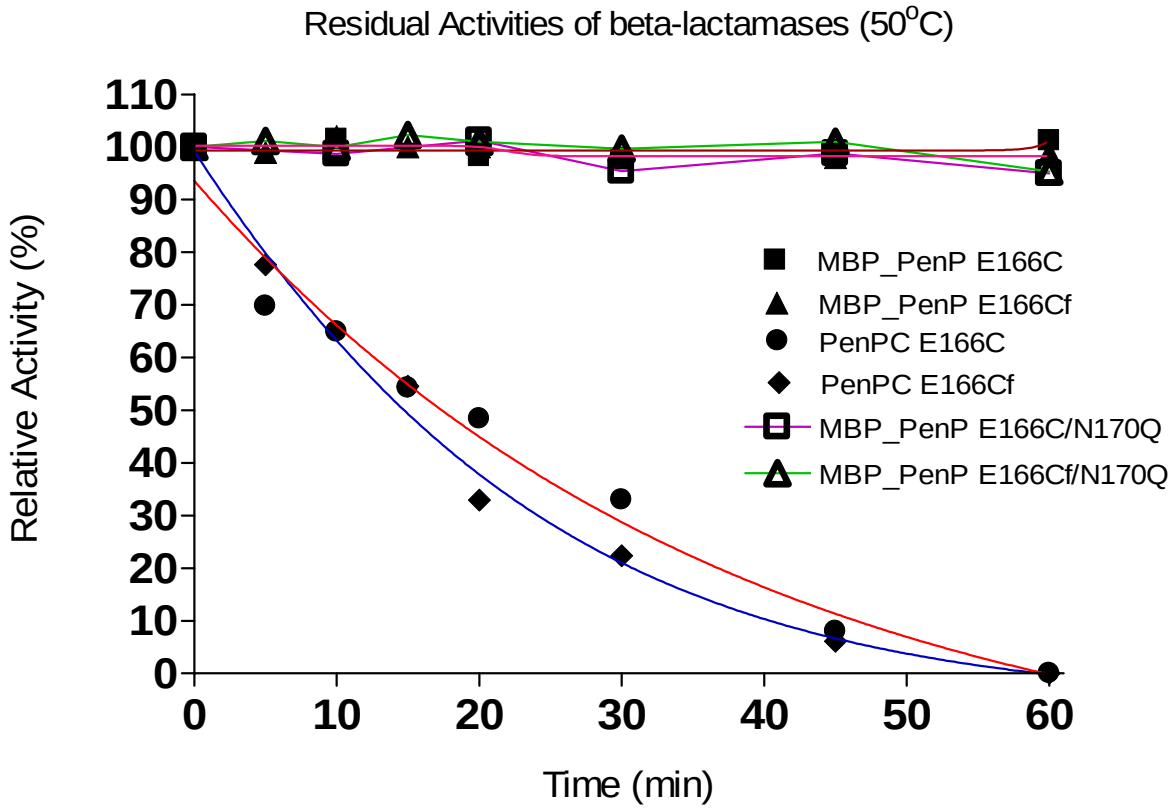

Figure 3.11. Relative activities of PenP beta-lactamases, PenPC beta-lactamase and their fluorophore-labeled derivatives as a function of incubation time. Enzymes were incubated at 50 °C in 50 mM potassium phosphate buffer at pH 7.0. Sample was withdrawn after various periods of time and immediately cooled on ice. Residual activities of the enzymes in hydrolyzing nitrocefin were determined at 20 °C.

3.7. Fluorescence studies of fluorophore-labeled beta-lactamases

3.7.1. Fluorescence spectra scanning upon addition of antibiotics

In this project, a total of three different thiol-reactive fluorophores were tested in the biosensor construction: fluorescein-5-maleimide, 6-iodoacetamidofluorescein (IAF) and 6-bromoacetyl-2-dimethylaminonaphthalene (badan). Changes in fluorescence scanning spectra of different fluorophore-labeled PenP_E166C mutants, before and after the antibiotic addition (penicillin G and cefotaxime) are outlined in Figure 3.12. In general, the PenP_E166C mutants labeled with any of these three fluorophores showed an increase in fluorescence intensity after the antibiotic addition. However, among the three labeled mutants, the magnitudes of increase in fluorescence intensity for the IAF-labeled mutant were relatively small. For example, for the badan- and fluorescein- labeled derivatives, addition of antibiotic caused at least 50% increase in the fluorescence intensity. However, the IAF-labeled counterpart only showed approximately 5% and 25% increase upon the addition of penicillin G and cefotaxime, respectively.

Regarding to the pattern of the fluorescence spectra, it was found that both fluorescein-labeled and IAF-labeled mutants only showed an increase in the fluorescence intensity upon the antibiotic addition. However, increase in fluorescence intensity was accompanied by a small shift of the emission maximum in the badan-labeled counterpart, in which the emission maximum was slightly shifted to the left (blue-shift) in the presence of antibiotics. This might be due to a change in the polarity around the badan fluorophore after substrate binding.

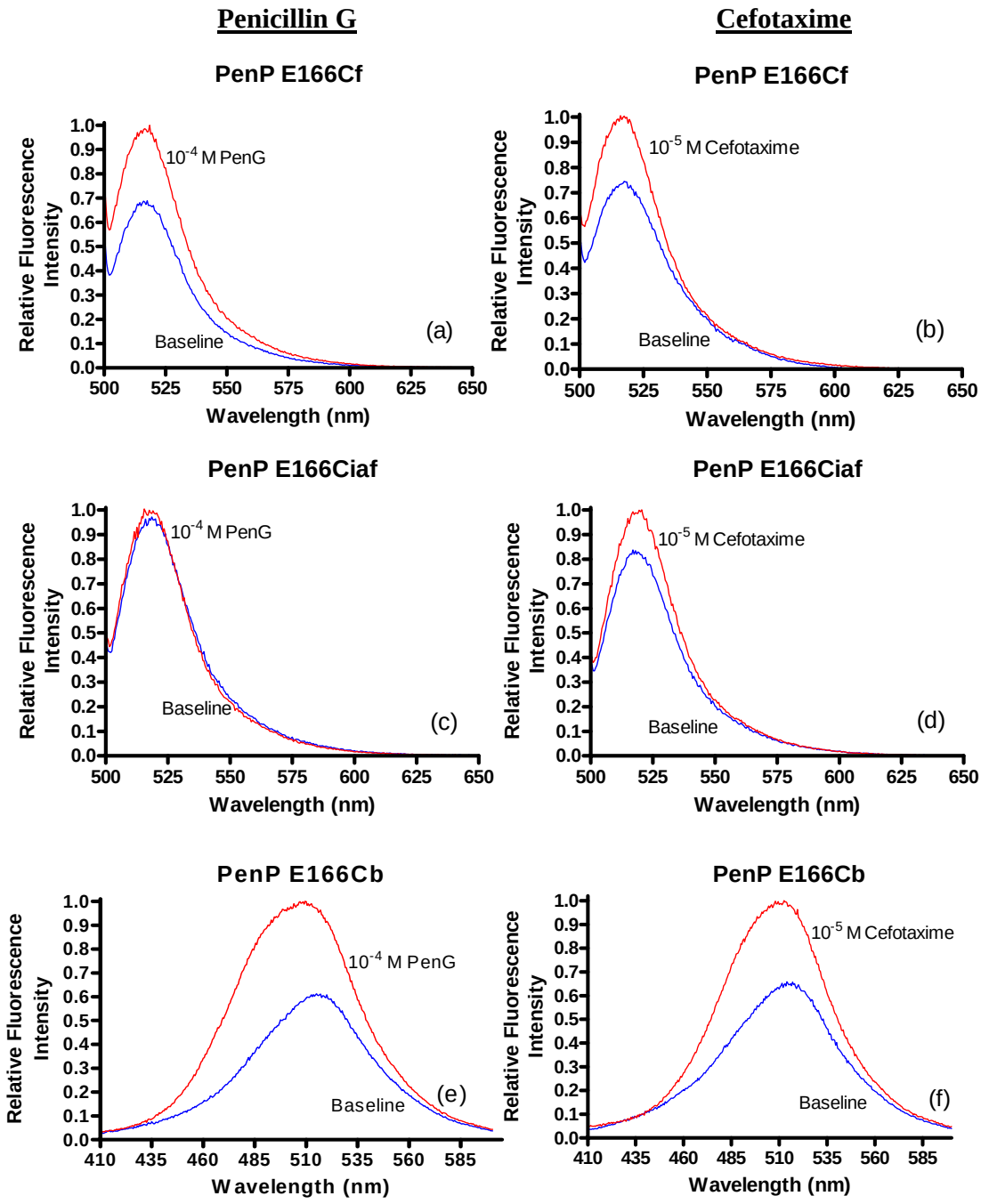

Figure 3.12. Fluorescence scanning spectra of PenP_E166Cf upon addition of Penicillin G (a), Cefotaxime (b); PenP_E166Ciaf upon addition of Penicillin G (c), Cefotaxime (d); and PenP_E166Cb upon addition of Penicillin G (e), Cefotaxime (f).

3.7.2. Time-resolved fluorescence measurement

Time-resolved fluorescence measurement was performed according to the description in Section 2.8. Fluorescence spectra were traced for an hour at a fixed emission wavelength: fluorescein-labeled mutants were monitored at 515 nm and badan-labeled mutants were monitored at 500 nm. These emission wavelengths were chosen as they were the wavelengths at which maximum changes in fluorescence intensity were observed after the addition of antibiotics. A total of 6 beta-lactam antibiotics, including both penicillins and cephalosporins (structures shown in Figure 5.9), were tested in the study. They were penicillin G, peniciilin V, ampicillin, cefoxitin (2^{nd} generation of cephalosporins), cefotaxime (3^{rd} generation of cephalosporins) and moxalactam (3^{rd} generation of cephalosporins). Time-resolved fluorescence spectra of the four PenP-based biosensors in these beta-lactam antibiotics in 50 mM potassium phosphate buffer (pH 7.0) are shown in Figures 3.13 to 3.16. Some of the spectra were absent for the badan-labeled biosensors, due to the lack of measurable signal changes in detecting some of the substrates. Both PenP_E166Cb and PenP_E166Cb/N170Q failed in showing fluorescence enhancement in the presence of ampicillin, and the former one also failed in the cefoxitin case. The four biosensors, in general, gave two different patterns of fluorescence spectra, depending on the type of beta-lactam antibiotics added.

<u>Detection of penicillin-type antibiotics</u>

For the penicillin-type antibiotics such as penicillin G and penicillin V, at low antibiotic concentrations (e.g. 10^{-7} and 10^{-8} M), the fluorescence intensity first increased rapidly and reached the maximum, and then quickly declined. At higher antibiotic

concentrations, the rising phase was too fast to be observed, and the fluorescence signal remained steady for a period of time and declined slowly. The time period, in which the signal remained steady, depends on the antibiotic concentration. The higher the antibiotic concentration, the longer would be the steady signal. This kind of spectral pattern was observed for all the penicillins being tested.

Detection of cephalosporin-type antibiotics

For cephalosporins such as cefoxitin and cefotaxime, the fluorescence signal, when compared with the penicillins, took longer time to reach the maximum value, but the signal was relatively stable, and some even showed no decline within an hour. This kind of spectral pattern was observed for all the cephalosporins being tested.

Single mutant biosensors and Double mutant biosensors

The four PenP-based biosensors can be classified into two groups based on the type of mutant used in the biosensor construction: i) Single mutant biosensors (E166Cf and E166Cb), and ii) Double mutant biosensors (E166Cf/N170Q and E166Cb/N170Q).

The two groups of biosensors showed the same detection limit towards all the substrates tested (except for those could not be detected by the badan-labeled enzymes). In general, the PenP-based biosensors can detect antibiotics with concentration as low as 10^{-8} M. Regarding to the signal stability, the double mutant biosensors generated longer detectable signal than that of the single mutant biosensors, especially in detecting the penicillin-type antibiotics. Taken penicillin G as an example, at the antibiotic concentration

of 1 μM, the fluorescence signals of the single mutant biosensors started to drop at 2000-2200 s after the antibiotic addition, while for the double mutant biosensors, the fluorescence signals remained steady for longer period of time and started to drop at 2800-3000 s after the addition of antibiotic. Similar observations were found in other penicillin-type antibiotics being tested. However, for the cephalosporin-type antibiotics, the two groups of biosensors showed no significant differences in terms of signal stability, in which both groups of the biosensors showed similar fluorescence spectral pattern.

Biosensors labeled with fluorescein-5-maleimide and biosensors labeled with badan

The four PenP-based biosensors can also be classified into another two categories based on the type of fluorophore used in the biosensor construction: i) Biosensors labeled with fluorescein-5-maleimide (E166Cf and E166Cf/N170Q), and ii) Biosensors labeled with badan (E166Cb and E166Cb/N170Q).

By comparing the fluorescence spectra generated from the two groups of biosensors, similar spectral pattern and detection limits were found. However, while all fluorescein-labeled biosensors showed significant fluorescence enhancement in all the antibiotics tested, the badan-labeled PenP_E166C and E166C/N170Q mutants only showed very little changes in fluorescence intensity (close to none) upon the addition of ampicillin (data not shown). In addition, the badan-labeled E166C also failed to generate measurable signal change in the presence of cefoxitin.

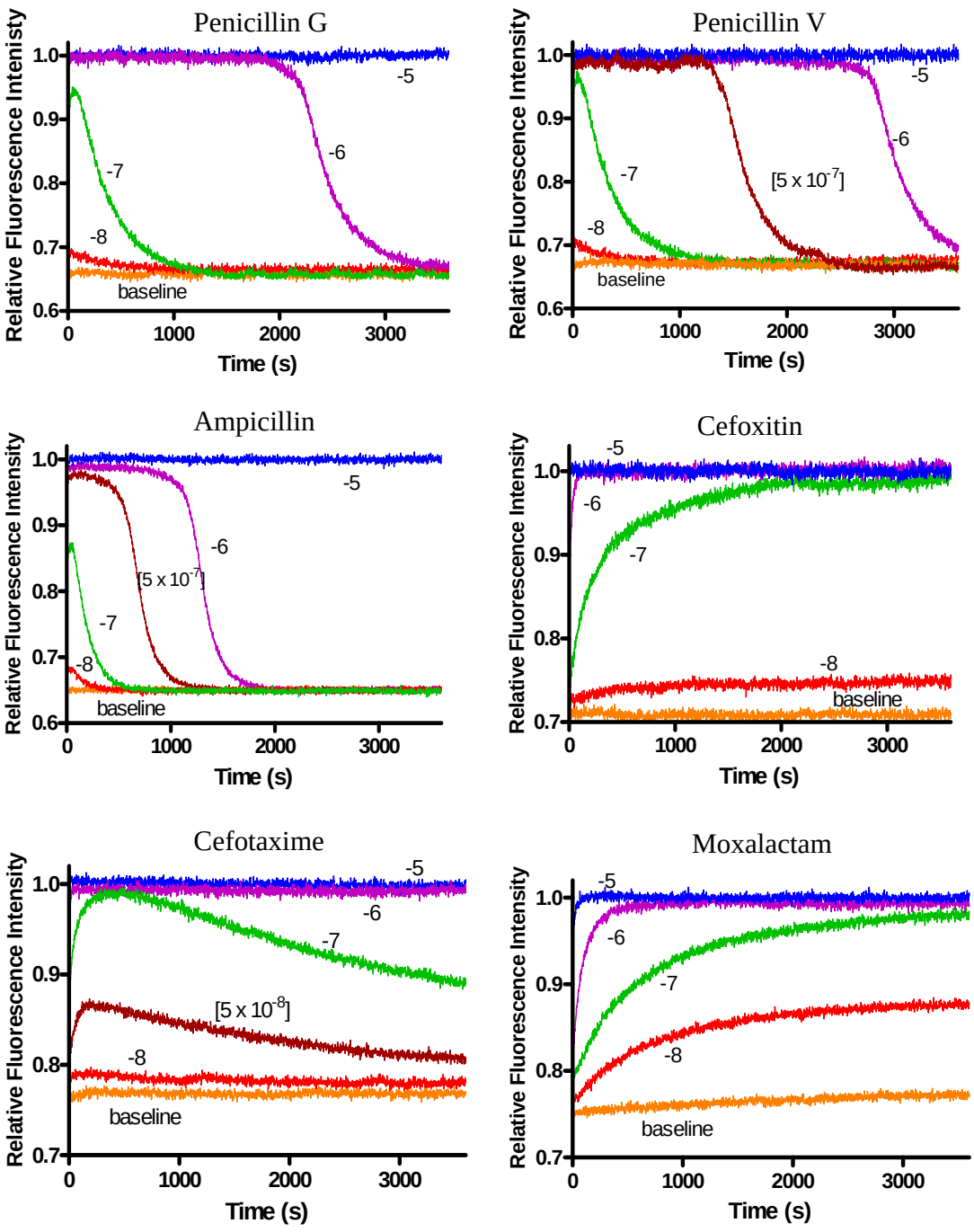

Figure 3.13. Time-resolved fluorescence spectra of MBP_PenP_E166Cf (1 x 10^{-7} M) in different beta-lactam antibiotics in 50 mM potassium phosphate buffer (pH 7.0). The numbers without brackets next to the curves denote log (antibiotic concentration), while numbers with brackets denote the actual antibiotic concentrations.

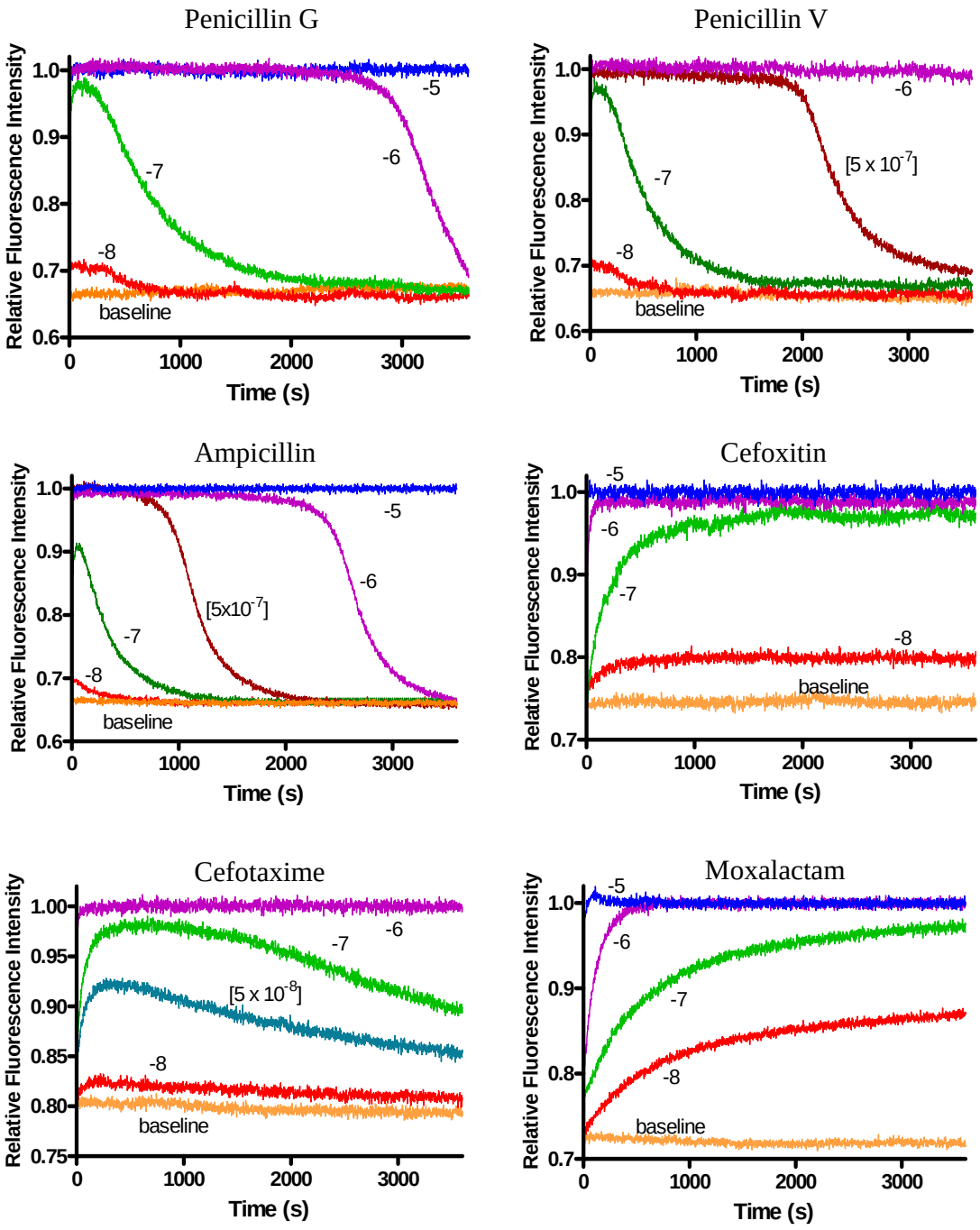

Figure 3.14. Time-resolved fluorescence spectra of MBP_PenP_E166Cf/N170Q (1 x 10^{-7} M) in different beta-lactam antibiotics in 50 mM potassium phosphate buffer (pH 7.0). The numbers without brackets next to the curves denote log (antibiotic concentration), while numbers with brackets denote the actual antibiotic concentrations.

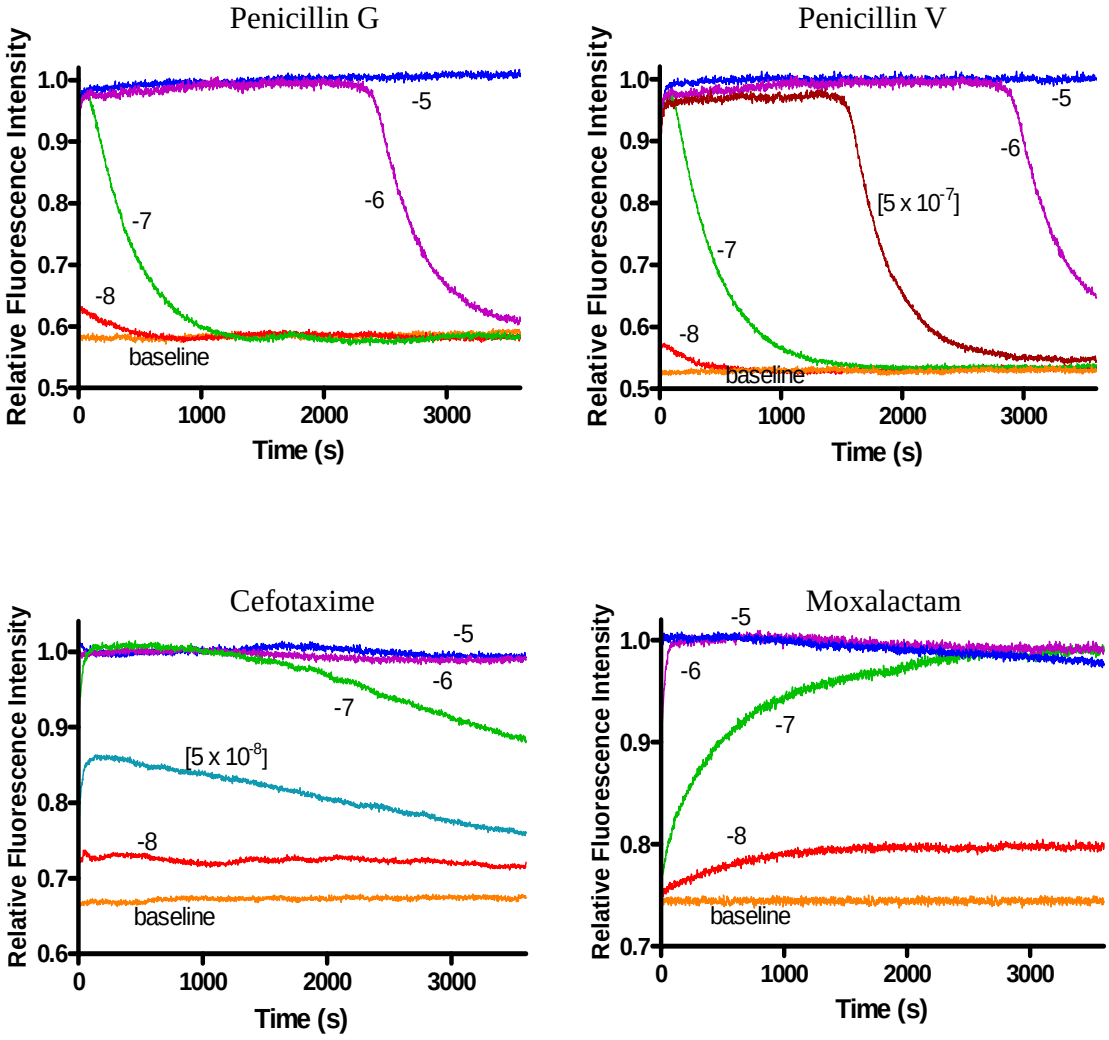

Figure 3.15. Time-resolved fluorescence spectra of MBP_PenP_E166Cb (1 x 10^{-7} M) in different beta-lactam antibiotics in 50 mM potassium phosphate buffer (pH 7.0). The numbers without brackets next to the curves denote log (antibiotic concentration), while numbers with brackets denote the actual antibiotic concentrations.

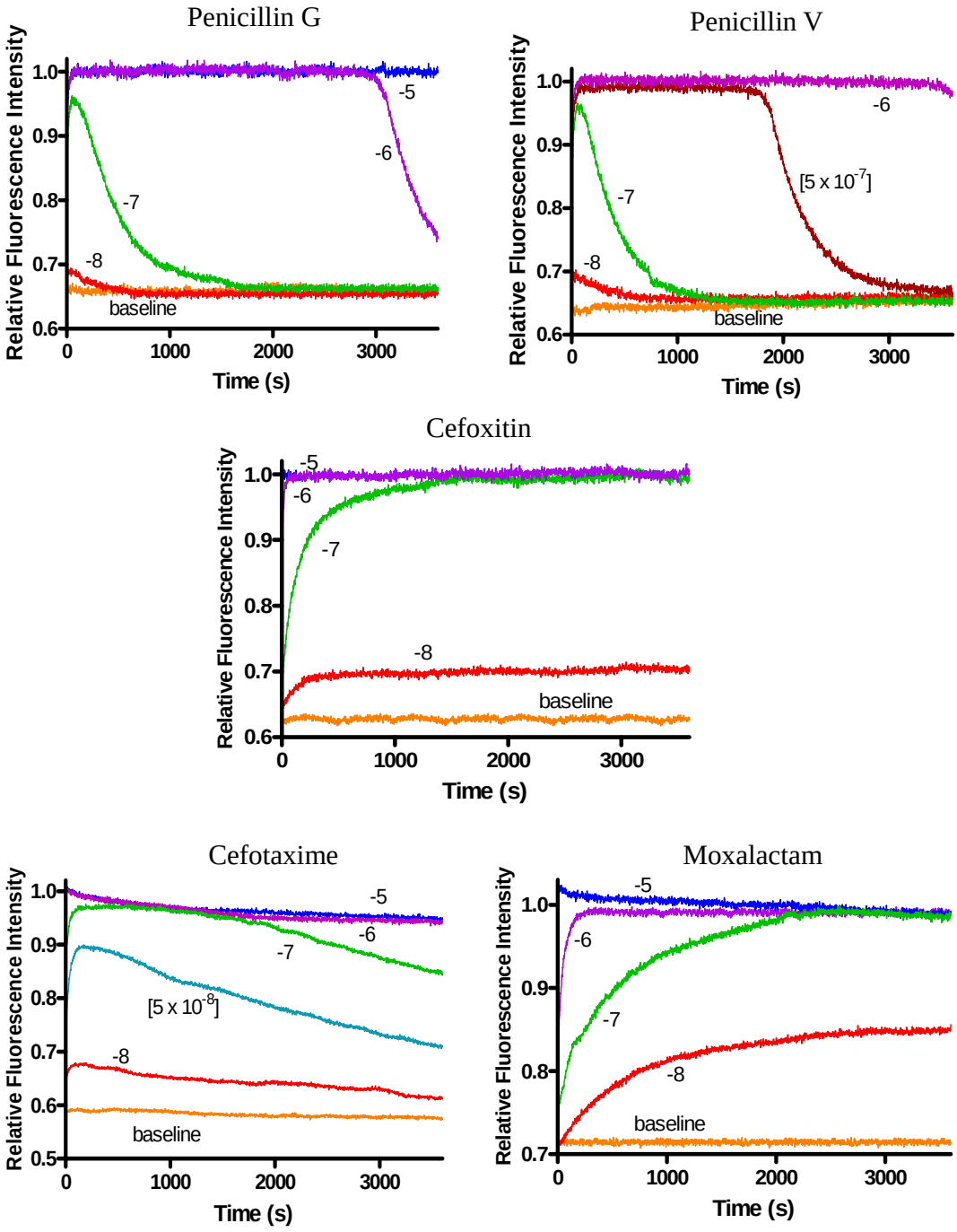

Figure 3.16. Time-resolved fluorescence spectra of MBP_PenP_E166Cb/N170Q (1 x 10^{-7} M) in different beta-lactam antibiotics in 50 mM potassium phosphate buffer (pH 7.0). The numbers without brackets next to the curves denote log (antibiotic concentration), while numbers with brackets denote the actual antibiotic concentrations.

3.7.3. Fluorescence spectra scanning upon addition of inhibitors

Changes of fluorescence scanning spectra of PenP-based biosensors upon the addition of some common beta-lactamase inhibitors were recorded and shown in Figures 3.17 and 3.18. Inhibitors such as sulbactam, tazobactam and clavulanate were included in the study (structures shown in Figure 5.10). They were added to the sample solutions at a high concentration of 10^{-4} M, which was 1000-fold greater than the biosensor concentration, to ensure the emission maxima at the steady state of reaction were obtained. From the results, all the four biosensors showed fluorescence enhancement upon the addition of all the inhibitors being tested. While the fluorescein-labeled biosensors showed an increase in fluorescence intensity only, the badan-labeled biosensors showed fluorescence enhancement accompanied by a blue-shift of emission maximum. In addition E166Cb mutant gave particularly weak signal upon the addition of tazobactam, in which only around 20% of increase in fluorescence intensity was achieved, compared to around 40% of increase in the other three biosensors.

(a) Sulbactam

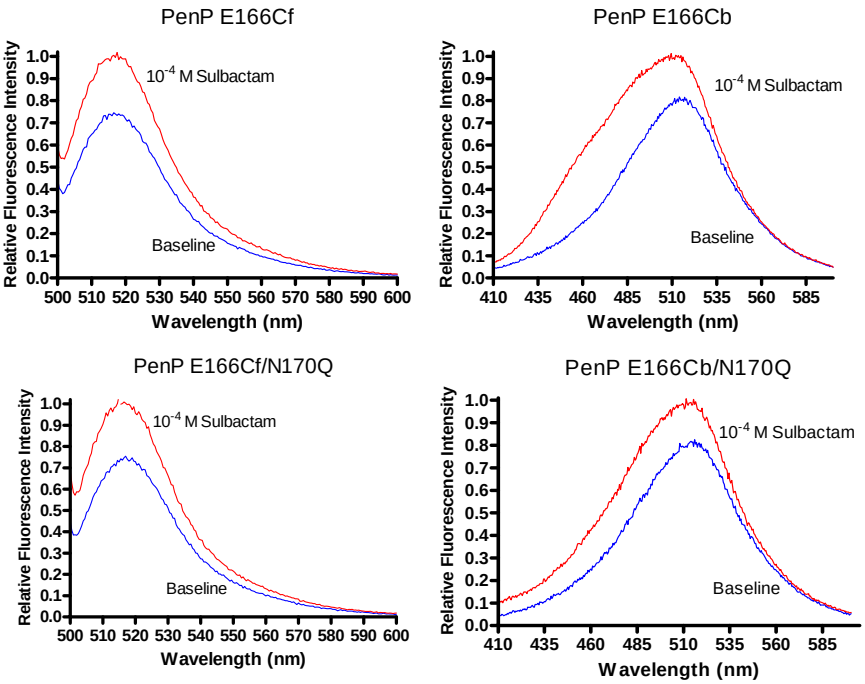

(b) Tazobactam

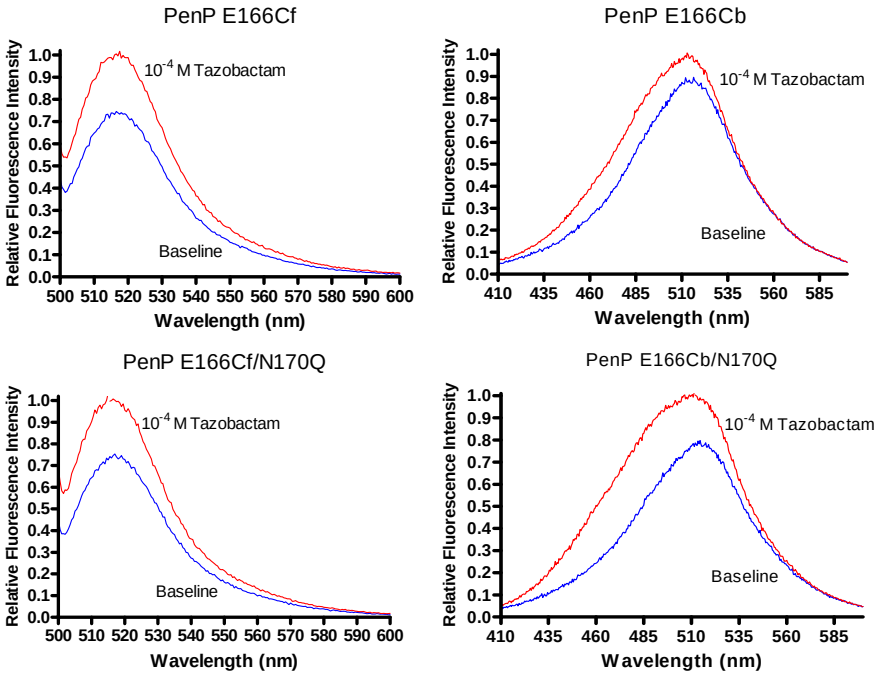

Figure 3.17. Fluorescence spectra of different fluorophore-labeled beta-lactamases (1×10^{-7} M) in 50 mM potassium phosphate buffer (pH 7.0) in the presence of 10^{-4} M of sulbactam (a) and tazobactam (b).

Clavulanate

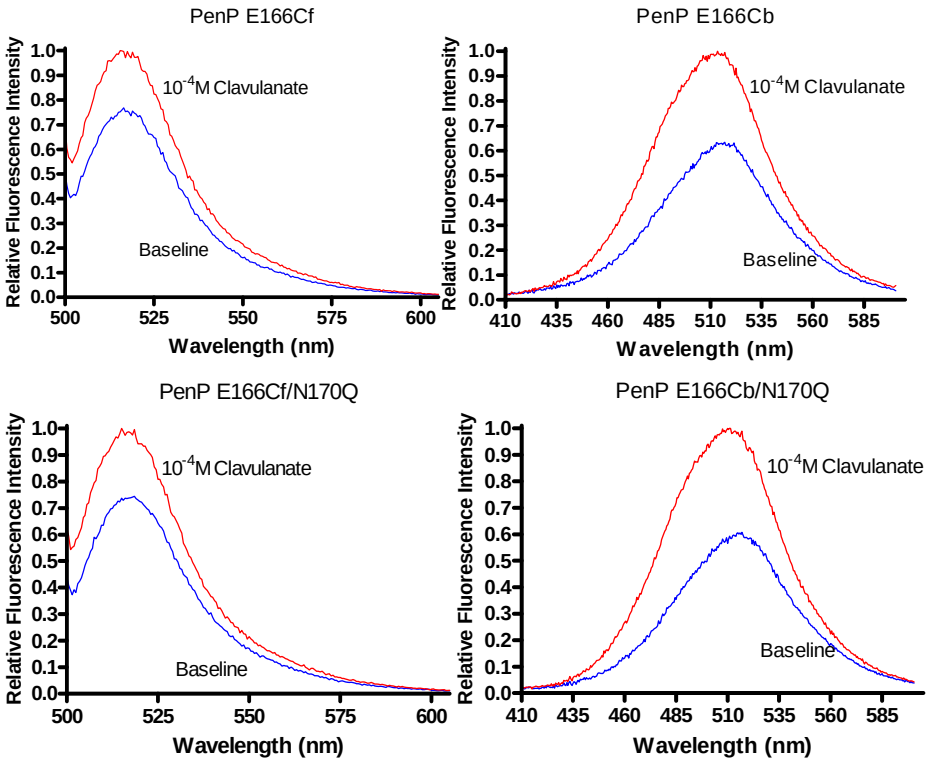

Figure 3.18. Fluorescence spectra of different fluorophore-labeled beta-lactamases (1×10^{-7} M) in 50 mM potassium phosphate buffer (pH 7.0) in the presence of 10^{-4} M of clavulanate.

3.8. Detection of acyl-enzyme intermediate in the hydrolysis of penicillin G by fluorophore-labeled beta-lactamases

Binding and hydrolysis of penicillin G by MBP_PenP_E166Cf/N170Q was monitored by electrospray ionization mass spectrometry (ESI-MS) combined with rapid quench-flow method, and the corresponding time-resolved fluorescence spectrum was recorded by stopped-flow apparatus, according to the methods described in Section 2.9. The studies were done in parallel at room temperature with identical mutant and substrate concentrations of 5×10^{-7} M.

3.8.1. Time-resolved fluorescence measurement by stopped-flow studies

Since the binding of penicillin G to the PenP mutants occurred very rapidly, tracing of fluorescence changes was assisted by the stopped-flow apparatus. Changes in the fluorescence intensity of MBP_PenP_E166Cf/N170Q in the first 100 s of the reaction with penicillin G were recorded and the corresponding fluorescence spectrum is shown in Figure 3.19(a). The spectrum showed that the fluorescence intensity increased and reached the plateau within one minute of the reaction.

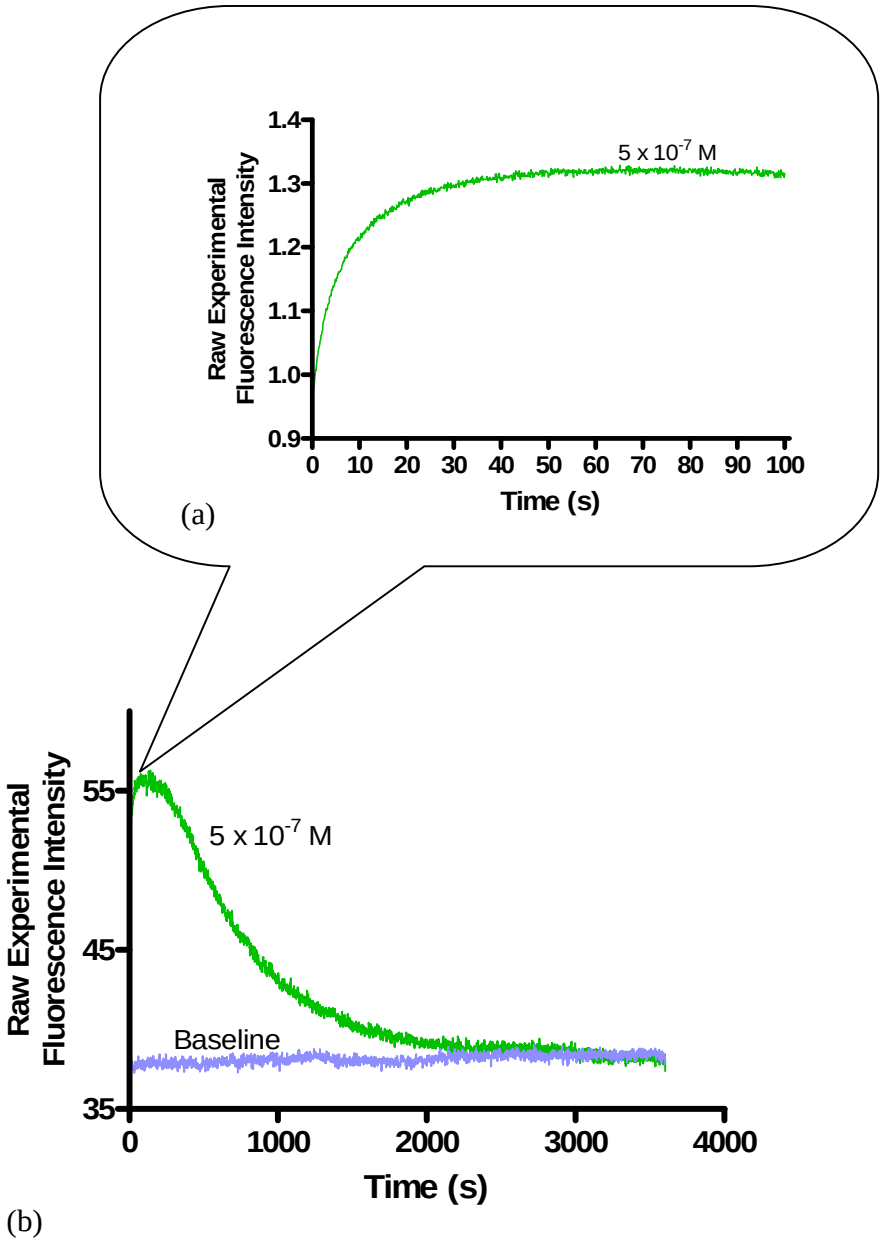

Figure 3.19. Time-resolved fluorescence spectra of MBP_PenP_E166Cf/N170Q upon addition of penicillin G, with biosensor to substrate ratio of 1:1 at concentration of 5 x 10^{-7} M. (a) Spectra showing fluorescence signal enhancement in the first 100 s. (b) Spectra showing the fluorescence signal changes throughout an hour experiment.

3.8.2. Detection of reaction species by ESI-MS

MBP_PenP_E166Cf/N170Q was allowed to react with penicillin G for desired time interval, and the reaction was quenched by formic acid. The reaction mixture was then analyzed by ESI-MS and the spectra as a function of reaction time are shown in Figure 3.20. Two peaks are in each spectrum. The first peak was measured with a molecular mass of approximately 73,003 Da, which was consistent with the calculated mass of the MBP_PenP_E166Cf/N170Q (73,002.1 Da), within the experimental uncertainty limit. The calculated mass was determined based on the primary amino acid sequence of the enzyme. For the second peak, it should be the adduct complex of the penicillin G and MBP_PenP_E166Cf/N170Q, in which the measured molecular mass (approximately 73,333 Da) was consistent with the calculated mass of the two (334.4 Da + 73,002.1 Da = 73,336.5 Da), within the experimental uncertainty limit. Since the formic acid in the ESI-MS sample solution would break any non-covalent associations, the detected adduct complex should be the covalently-bound adduct complex, i.e., acyl-enzyme intermediate (EC*), instead of a non-covalent enzyme substrate complex (EC).

The amount of each reaction species could also be indicated by the peak heights in the de-convoluted mass spectra. It could be seen from the spectra that, the amount of free enzyme (first peak) decreased in the first two minutes of the reaction, while that of the substrate-enzyme adduct complex (second peak) increased. Whereas in the mass spectra at the 30-minute, the enzyme peak restored the height as that at the beginning of the reaction, and the peak corresponded to EC* disappeared.

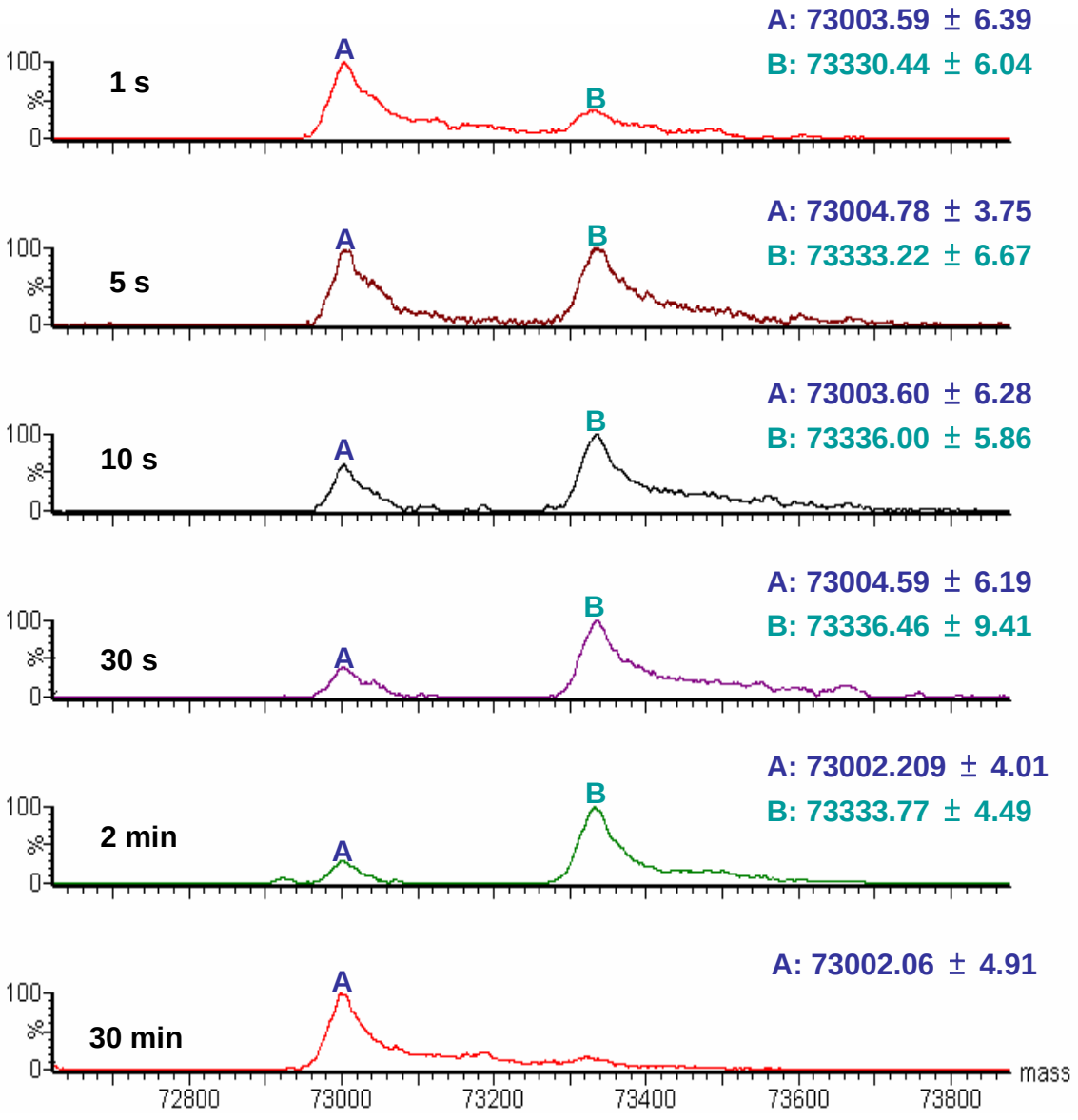

Figure 3.20. Mass spectrometry spectra of the reaction between MBP_PenP_E166Cf/N170Q and penicillin G at different time intervals.

Chapter Four: Discussion

4.1. Preparation of MBP-PenP fusion proteins using a *E.coli* expression system

4.1.1. *E. coli* Expression System

Many expression systems are now available for heterologous protein production. One of the most attractive tools is the usage of the Gram-negative bacterium *Escherichia coli* (Baneyx, 1999). There are various benefits of using *E. coli* as the production host, for example, the growth and manipulation of this organism are easy with the use of simple laboratory equipment. Moreover, a variety of vectors and host strains are readily available for the protein production. Besides, there is also a wealth of well understood knowledge of the genetics and physiology of the microbe, as well as the knowledge about the effects of genetic and environmental factors on the expression of heterologus proteins. All of these advantages make *E. coli* a popular host for the heterologus protein production.

E. coli BL21(DE3) was used for the expression of the PenP beta-lactamase in this project. It was chosen because this *E. coli* strain lacks the cytoplasmic Lon protease and ompT outer membrane protease. Therefore, the target proteins, not all but at least some of them, should be more stable during purification than in other host strains which contain these proteases. However, as the *E. coli* BL21(DE3) does not transform well, an alternate strain (TOP10) was used for the maintenance of the plasmids.

4.1.2. Maltose binding protein as a fusion partner

According to a previous work done by our research group, PenP beta-lactamase was highly expressed in *E. coli* as His-tagged proteins and found to be highly soluble (work not shown). However, some of the His-tagged PenP beta-lactamase mutants were either only partially soluble or expressed as inclusion bodies (data not shown). Such conditions were believed to be related to the improper protein folding resulted from the mutation(s). To avoid such phenomenon from happening, an alternate protein-fusion system was used to facilitate the production of fully soluble proteins.

MBP was found to be an effective solubilizing agent in enhancing the solubility of polypeptides with which it is fused (Kapust and Waugh, 1999). Studies using the MBP-fusion system for the target protein expression found that such system could achieve high-level expression, high solubility and easy purification of the expressed proteins (Bach *et al.*, 2001; Ishii *et al.*, 1998; Park and Sancar, 1993). Because of the above advantages, the beta-lactamase gene in this project was subcloned into the pMAL-c2X vector (New England Biolabs) and expressed as N-terminal fusion with MBP protein. Protein expression from the vector was under the control of a tac promoter, which was induced using the lactose analog isopropyl beta-D-thiogalactoside (IPTG). Both mutants, MBP_PenP_E166C and MBP_PenP_E166C/N170Q, were expressed in a fully soluble form in *E. coli* (Figure 3.2), and were easily purified by a simple one-step affinity chromatography by the amylose column.

4.1.3. Expression and purification of MBP-PenP mutants

Results for the expression and purification of MBP-PenP mutants are shown in Sections 3.1 and 3.2. According to Figure 3.2, maximal yields of the MBP-PenP mutants were achieved upon growing the culture for 3-4 h, indicating that it was the right time to harvest. As the PenP beta-lactamases are expressed in the form of MBP fusion proteins, they were easily purified by the one-step affinity chromatography using the amylose column. This purification system separates the MBP fusion protein by protein-carbohydrate interaction between the MBP fusion and amylose resin, followed by the elution with maltose (Chu *et al.*, 1988).

The purification profiles of the MBP-PenP in amylose affinity column are shown in Figure 3.3. A single peak resulted from the purifications of both the single and double mutants, and samples in fractions of the elution peaks were analyzed by SDS/PAGE (Figure 3.4).Very pure fusion protein was found in the fractions 45-53. The small amount of impurities in the fractions within the elution peak might be the single MBP or due to the protein degradation by the host proteases. The results indicated that the purification step was very efficient. SDS/PAGE analysis of the concentrated purified samples are also outlined in Figure 3.8. More than 95% pure MBP fusion protein was obtained by the one-step affinity chromatography for both mutants, and this enzyme purity was sufficient for further studies. The production yields for the two PenP mutants were good, in which the yield for MBP_PenP_E166C was approximately 160 mg/L of culture and that of MBP_PenP_E166C/N170Q was approximately 104 mg/L of culture.

4.2. The use of MBP in biosensor development

MBP has a molecular size of approximately 42,500 Da, which is much larger than PenP beta-lactamase (approximately 30,000 Da). Fusion of PenP with MBP led to a higher molecular weight of around 72,500 Da. In order to investigate the effect of the attachment of this large MBP on the sensing properties of the biosensors, MBP was cleaved and removed from the purified MBP-beta-lactamases by Factor Xa.

4.2.1. Poor recovery of MBP-cleaved beta-lactamases

Factor Xa cleaves MBP fusion protein at the specific excision site (recognition amino acid sequence IEGR) which is located at the junction between MBP and the fusion partner (Figures 2.1, 5.1-5.2). According to the SDS/PAGE analysis shown in Figure 3.5, complete cleavage of MBP-PenP beta-lactamases could be achieved upon incubating the proteins with Factor Xa at 4 ^{o}C for 24 h. All the cleaved proteins were in fully soluble form.

Although the protein cleavage system works specifically in a short reaction time, the total recovery of the MBP-cleaved beta-lactamases was unsatisfactory. Most of the enzymes were lost during the column purification step, and only about 23-26% of the total protein could be recovered. Apart from the inevitable loss during the experimental steps, the handling of the small amount of protein and the larger molecular size of MBP might be part of the reasons. MBP is larger than the PenP beta-lactamase, which dominates a major part of the uncleaved protein. From the results, only 2.3-2.6 mg of MBP-cleaved beta-lactamases was obtained from the cleavage of 10 mg of fusion protein.

4.2.2. Negligible effects of MBP on biosensing system

Because of the well-characterized structure and folding of MBP, many experiments were carried out with the uncleaved MBP fusions, including those studies about the protein structure-function relationship (Spurlino *et al.*, 1991; Sharff *et al.*, 1992; Sachdev and Chirgwin, 2000). The attachment of MBP to the N-terminus did not interfere with the function of proteins (Ishii *et al.*, 1998; Park and Sancar, 1993). In addition, previous work showed that specific activities of the cleaved MBP-PenP beta-lactamases with various substrates, including penicillin G, penicillin V, ampicillin and nitrocefin, were almost identical to those of the uncleaved proteins (Liu, 2003). Therefore, it was believed that fusion to MBP would not have any significant effect on the catalytic functions of beta-lactamases. Nevertheless, in order to examine whether the fusion to MBP would affect the sensing properties of the biosensors, purified beta-lactamases without MBP were labeled with fluorescein-5-maleimide and their performance in detecting penicillin G was evaluated.

According to preliminary data, the fluorescence patterns generated from the PenP biosensors without MBP were almost identical to that of the corresponding uncleaved biosensors in detecting penicillin G (data not shown). These findings suggested that the sensing properties of the MBP-cleaved and uncleaved PenP biosensors were similar, i.e. fusion to MBP exhibited no significant effect on our sensing system. What is more, since the cleavage of the fusion protein and the subsequent purification steps would be rate-limiting in terms of time and cost, the whole fusion proteins were used for our studies and biosensor development.

4.3. Catalytic Deficiency of E166C and E166C/N170Q mutants

4.3.1. Sites of mutations

Two mutants, E166C and E166C/N170Q, were generated and used as the basis for the construction of the biosensors. The glutamate 166 and asparagine 170 residues were chosen as the sites for mutation, aiming to suppress the hydrolytic ability of the enzyme. Such catalytic impairment turned the enzyme to a "binding-protein" and generated detectable signal upon the binding of antibiotics. Both Glu-166 and Asn-170 residues were reported to play vital roles in the deacylation step (Chen *et al*., 2001; Escobar *et al*., 1994; Zawadzke *et al.*, 1996). As mentioned in Chapter One, interaction with Glu-166 enhances the nucleophilicity of the hydrolytic water molecule and prepares it for deacylation. Mutation of Glu-166 into cysteine was found to hinder the activation of the catalytic water molecule and reduce the enzyme activity significantly, in which the catalytic efficiency of the mutant was about 2.9 x 10^4-fold lower than those of the wild-type PenP enzyme (Escobar *et al.*, 1994).

Apart from the electrostatic interactions with Glu-166, the postulated hydrolytic water molecule was also found to interact with another residue, Asn-170 (Lamotte-Brasseur *et al.*, 1991; Zawadzke *et al.*, 1996; Guillaume *et al.*, 1997). Site-directed mutagenesis of this residue into glutamine showed that the extended side chain blocked the niche where the water molecule is normally accommodated, and hence resisted its access and impaired the deacylation (Zawadzke *et al.*, 1996). In addition, Chen and Herzberg (2001) also revealed that the double mutation, E166D/N170Q, of the PC1 beta-lactamase from *Staphylococcus aureus* resulted in a protein incapable of hydrolyzing penicillin G. In order to further

suppress the deacylation rate of PenP and improve the signal stability of our sensors in antibiotic detection, the E166C/N170Q mutant was also constructed.

4.3.2. Kinetic properties of MBP-PenP mutants and their fluorophore-labeled derivatives

The kinetic parameters of the PenP beta-lactamase and mutants against nitrocefin are shown in Table 3.5. By comparing the activities between the mutants and the wild-type PenP, it was found that the mutations E166C and N170Q caused a dramatic decrease in the activity of the PenP beta-lactamase, in which the catalytic efficiency of E166C and E166C/N170Q was about 4 x 10^4-fold and 1.2 x 10^5-fold lower than that of the wild-type, respectively. Such a large reduction in the enzyme activity indicated the importance of Glu-166 and Asn-170 in the beta-lactam hydrolysis, a feature on which a general consensus has been reached (Escobar *et al.*, 1994; Zawadzke *et al.*, 1996; Matagne *et al.* 1998; Chen and Herzberg, 2001). Besides, the mutation of N170Q was shown to cause a further decrease in the enzyme catalytic efficiency by about five times, which was in agreement with the findings when specific activities of the unlabeled mutants were used for comparison. These results hence reflected that the mutation N170Q truly further suppressed the hydrolytic ability of the enzyme. Apart from the reduction in the k_{cat}, the K_m values of the mutants were slightly lowered by the mutations, indicating that the mutants exhibited similarly good affinities to the substrates as the wild type enzyme. Similar findings were also revealed in previous report (Escobar *et al.*, 1994), in which the K_m of PenP_E166C was found to be lower than the wild-type enzyme by 4 times. In addition, while the specific activities of the badan-labeled beta-lactamases were similar to their

unlabeled counterparts, the fluorescein-labeled beta-lactamases were found to have relatively higher activities (Table 3.6). This might reflect that the attachment of fluorescein molecule to the mutants would facilitate substrate hydrolysis, perhaps by altering the orientations of some catalytic residues, or by changing the environment of the active site. However, in general, the activities of the fluorophore-labeled beta-lactamases were still comparable to those of the unlabeled counterparts, indicating that the active-site structure was conserved after the fluorophore labeling.

Taken together, these results indicated that mutations of E166C and N170Q in PenP beta-lactamase led to a great loss in the hydrolytic activity, but without hindrance on the substrate binding of the mutants. The unique kinetic change made the mutants behave similarly to the penicillin-binding proteins. Negligible effect on the K_m values of the mutants revealed that substrate binding process remained very efficient even in the absence of Glu-166. However, it was suggested that removal of Glu-166 did reduce the acylation rate of the enzyme, as evidenced by the unaffected K_m values even with a large reduction in the k_{cat}. A similar observation was reported in the PenPC E166D mutant (Gibson *et al.*, 1990). The fast substrate binding process, as revealed by the rapid fluorescence enhancement shown in the fluorescence spectra (Figure 3.13-3.16), reflected that an alternative mechanism may also be involved in activating the Ser-70 hydroxyl group without the direct participation of Glu-166. As suggested by Stynadka *et al.* (1992), the removal of the negatively charged Glu-166 carboxylate might lead to a large decrease in the Lys-73 pKa value in the TEM-1_E166N when compared with the wild-type enzyme. In that case, the Lys-73 would be unprotonated and act as the general base for assisting the

enzyme acylation (Matagne *et al.*, 1998). On the other hand, according to the recent molecular dynamics simulations of the Michaelis complex between TEM-1 and penicillin G (Diaz *et al*., 2002), results suggested that the hydroxyl Ser-130, which was shown to be bound to the substrate hydroxyl group, could accept the proton from Ser-70. It was also hypothesized that Glu-166 and Ser-130 constituted two competitive acylation pathways respectively, in which the kinetic preference for one mechanism or the other would depend on the nature of the substrate, and/or on the presence of point mutations. Nevertheless, there is not yet any general consensus on the actual acylation mechanism of class A beta-lactamase. Careful kinetic analysis of the different mutant enzymes is hence a prerequisite to any meaningful mechanistic conclusions. However, the present results do agree with the view that Glu-166 plays a more important role in deacylation than in acylation (Leung *et al*., 1994; Guillaume *et al.*, 1997).

Although the removal of the Glu-166 and Asn-170 severely impaired the enzyme activity, the PenP_E166C and PenP_E166C/N170Q mutants did hydrolyze substrate slowly. It was suggested that deacylation was accomplished by the hydrolytic water molecule, which was still present in the acyl-enzyme intermediate (Strynadka *et al.*, 1992; Knox *et al.,* 1993), though it was no longer held in the optimum position and was not as effective a nucleophile as in the wild-type enzyme for attacking the ester bond of the acyl-enzyme complex. In addition, Lys-73 and Ser-130 could also assist in the deacylation steps by providing the means in proton transfer, as evidenced by the altered deacylation rates of the various Lys-73 and Ser-130 mutants (Gibson *et al.*, 1990; Hata *et al*., 2000; Lietz *et al.*, 2000).

4.4. Studies of the protein secondary structure

Circular dichroism (CD) spectrometry is a useful technique for analyzing protein structure (Greenfield, 1999). It measures the differences in absorption between the left-handed and right-handed polarized light, which arises due to the structural asymmetry of a molecule. The protein secondary structure can be determined by CD spectroscopy in the "far-UV" spectral region (185-250 nm). Alpha-helix, beta-sheet and random coil structures are some common conformational motifs of proteins, each of which exhibits a characteristic shape and magnitude of the CD spectrum. For example, alpha-helix gives rise to a signal with negative ellipticity at 222 nm and 208 nm, and positive ellipticity at 193 nm; beta-sheet displays a broad negative band near 218 nm and a positive band near 195 nm; while the disordered extended chain exhibits a weak broad positive band near 217 nm and a negative band near 200 nm. As a result, by analyzing the spectra of a protein molecule, the composition of its conformational motifs and the protein secondary structure can be estimated.

The use of CD in determining the protein secondary structure is a valuable tool in protein studies. For example, it allows the comparison of the structures of a protein obtained from different species, or the comparison of the structures for different mutants of the same protein. Besides, the CD also allows the studying of the conformational stability of a protein under stresses such as heat, extreme pH and denaturants. In this project, CD was used to examine the secondary structures of PenP beta-lactamases, mutants and their fluorophore-labeled derivatives. Moreover, the theromstabilities of the proteins were also evaluated, which would be further discussed in Section 4.7.6.

4.4.1. Effects of mutation(s)

In order to study whether the mutation(s) introduced in the PenP mutants would lead to any significant changes in the enzyme structure, the far-UV CD spectra of the purified PenP beta-lactamase, E166C and E166C/N170Q mutants were measured and compared. The spectra of the three beta-lactamases were shown to be superimposable on each other (Figure 3.9(a)) and similar calculated secondary structures were obtained (Table 3.7). The results hence suggested that the PenP beta-lactamase, E166C and E166C/N170Q mutants share very similar protein folding, and the E166C and N170Q mutations did not perturb the enzyme secondary structures. This finding is in agreement with a similar study of PenP_E166C, in which the mutation of Glu-166 to cysteine has been found to exert minimal effects on the secondary structure of enzyme (Escobar *et al.*, 1994).

4.4.2. Effects of fluorophore-labeling reaction

During the construction of the PenP biosensors, fluorophores were attached to the PenP mutants by unfolding the proteins in 6 M GuHCl before the addition of fluorophore (Section 2.5). After the labeling reaction, the proteins were allowed to refold by removing the GnHCl by buffer exchange. In order to ensure the fluorophore-labeled enzymes could refold into their native structures, the labeled proteins were analyzed by circular dichroism. From this study, the effects of fluorophore attachment on the protein secondary structure were also estimated.

The far-UV CD spectra of E166Cb, E166Cf, E166Cb/N170Q and E166Cf/N170Q were measured and the results are listed in Figures 3.9(b) and (c). The spectra of the fluorphore-labeled mutants and their corresponding unlabeled counterparts were

superimposed on each other. However, for some unknown reasons, the fluorophore-labeled beta-lactamases were shown to have a slightly less amount of α-Helix and turn than that of the unlabeled counterparts. These changes indicated a slight alteration in the protein folding, and might lead to a small decrease in the melting temperature of the labeled mutants (as described in Section 3.6.2). Despite the slight changes in the protein structures, the four beta-lactamases still seem to share a very similar overall folding, as evidenced by their overlapped spectra. To conclude, fluorophore labeling only exerts minimal effects on the enzyme secondary structure and all labeled enzymes refolded properly after the harsh unfolding reaction.

4.5. Characterization of fluorophore-labeled PenP mutants

Due to the catalytic-defective property of the PenP beta-lactamase mutants, the sufficiently stable enzyme-substrate complex can accumulate and allows the enzyme to function as a biosensor. Since the residue 166 is located at the flexible omega loop, by site-selectively labeling this residue with a fluorescent reporter group, the binding of the substrate will induce a conformational change of the loop, hence move the reporter group. As a result, the fluorescence properties will change accordingly and serve as the basis of the signal (Gilardi *et al.*, 1994; Marvin *et al.*, 1997). In order to label the residue 166 specifically, the glutamate at that position was mutated into a cysteine residue, so that a thiol-reactive fluorescent probe could couple to it (Post *et al.*, 1994; Marvin *et al.*, 1997; Marvin and Hellinga, 1998; Salins *et al.*, 2001; Schindel *et al.*, 2001). Since both MBP and the wild-type PenP did not posses any cysteine residue, the cysteine residue introduced by mutation was the unique cysteine in the entire molecule and the fluorescent probe could hence be attached to the enzyme site-selectively.

4.5.1. Spectral properties of fluorophore- labeled mutants

A total of three thiol-reactive fluorophores were tried in the biosensor construction: fluorescein-5-maleimide, 6-iodoacetamidofluorescein (IAF) and 6-bromoacetyl-2-dimethylaminonaphthalene (badan). In order to assess their abilities in developing a sensitive biosensor, changes in fluorescence scanning spectra of different fluorophore-labeled E166C mutants before and after the antibiotic addition were studied and outlined in Figure 3.12. Penicillin G and cefotaxime were chosen as the testing substrates as they represented the two different classes of the beta-lactam family. Results

showed that the PenP_E166C mutants labeled with any of these three fluorophores could show fluorescence enhancement after the antibiotic addition. However, among the three labeled mutants, the magnitudes of increase in the fluorescence intensity for the IAF-labeled mutant were particularly small. Besides, while the IAF-labeled mutants and the mutants labeled with fluorescein-5-maleimide showed an increase in the fluorescence intensity only, the badan-labeled mutants showed an increase in fluorescence intensity accompanied by the shifts of the emission maxima. Such observations were also observed in the PenPC biosensors (unpublished work), and the situation might be explained by the differences in structures and spectral properties of the three fluorophores.

In addition, molecular modeling of the PenPC biosensors has been done previously (Siu *et al.*, unpublished work). Both PenPC and PenP beta-lactamases belong to the same class of beta-lactamase and they show extensive similarities in their amino acid sequences (for details please refer to Section 4.7). Due to the high homology of the two beta-lactamases and the unavailability of X-ray crystal structure of PenPC beta-lactamase, the modeling of the PenPC biosensors were constructed by using the X-ray crystal structure of the PenP beta-lactamase as the starting model. Hence, these models are believed to be very useful in explaining the conditions of the PenP biosensors as well. Results of the modeling and the computational results of the overall changes in the solvent accessible area (SAA) of the fluorescence probes attached to the E166C mutant before and after pencillin G binding based on ten stable conformations are shown in Figures 4.2 to 4.3 and Table 4.1 (Siu *et al.*, unpublished work).

Fluorescein-5-maleimide and IAF

Fluorescein derivatives are the most common fluorescent derivatization reagents for covalently labeling proteins. Apart from their high absorptivity and excellent fluorescence quantum yield, their good water solubility and low susceptibility of the corresponding protein conjugates make them very useful in the preparation of green-fluorescent thiol conjugates of biomolecules. Both fluorescein-5-maleimide and IAF are common derivatives of fluorescein. They react readily with the thiol groups of proteins to yield thioethers via the reactions shown in Figure 4.1.

According to Figure 3.12, the PenP_E166C mutant labeled with fluorescein-5-maleimide or IAF showed an increase in the fluorescence intensity after antibiotic addition. The observation reflected that the binding of antibiotic triggered some changes in the local environment of fluorophore, which made the fluorophore fluoresce more strongly. According to the molecular models of E166Cf and E166Ciaf (Figures 4.2 and 4.3), the SAA of the fluorescein-5-maleimide and iaf increased by 73 $Å^2$ (+13%) and 62 $Å^2$ (+11%), respectively, when the substrate (penicillin G) was bound to the labeled enzyme (Table 4.1). This infers that the fluorophore, which is originally buried inside the enzyme pocket, moves outside upon the binding of the substrate. Once the fluorophore becomes more solvent-exposed, the label fluoresces more strongly and hence an increase in the fluorescence intensity could be detected (Klonis *et al.*, 1888; Klonis and Sawyer, 2000; Chan *et al.*, 2004).

However, although the PenP_E166C mutant labeled with either

fluorescein-5-maleimide or IAF showed fluorescence enhancement after antibiotic addition, a weaker signal (i.e. smaller magnitude of increase) was observed in the latter case. Such a difference might be related to the length and the nature of the linker between the protein and the attached fluorophore. For the case of fluorescein-5-maleimide, the linker (succinimidylthioether linkage) is relatively rigid so that the fluorescein molecule moves according to the movement of the linker, i.e. the whole molecule (loop + linker + fluorescein) moves together. For the IAF, the linker (acetamidothioether linkage) is comparatively more flexible and should have more rotational freedom. Hence, when the linker moves, the fluorescein molecule moves accordingly but may orient itself in a different position because of the flexibility of the linker. Since the experimental result showed that there was a smaller increase in the fluorescence signal in the IAF case, it was inferred that the fluorescein molecule of the IAF arranged itself in a relatively less exposed environment than that encountered in the case of fluorescein-5-maleimide, after the binding of antibiotics. This was evidenced by the smaller increase in SAA (62 $Å^2$) found in the model of E166C_iaf. The differences observed in the E166Cf and E166Ciaf cases also reflected that the nature of the linker between the protein and fluorophore might be one of the significant factors in effecting the movement of fluorophore, hence the quality of the fluorescence signal.

Badan

Badan is one of the most useful thiol-reactive probes for protein structure studies because its fluorescence emission peak and intensity are particularly sensitive to conformational change and ligand binding. It reacts with the protein thiol groups to form

very strong thioether bonds via the reaction shown in Figure 4.1.

Unlike the fluorescence spectra generated by mutants labeled with fluoresceins, it was found that the badan-labeled mutant showed an increase in fluorescence intensity accompanied by a small shift of the emission maximum upon the antibiotic addition. According to Figure 3.12, the emission maxima, which originally took place at 513 nm, was shifted slightly to 500 nm in the presence of antibiotics. The shifting was believed to be caused by the change in the polarity around the badan upon the substrate binding. According to the solvatochromic property of badan, when the label encounters a less polar environment, the emission wavelength would be shifted to the higher energy side (blue-shift) because of the larger energy gap between the excited state and the ground state. Therefore, the blue-shift of the emission maximum upon the binding of substrate reflected that the badan, instead of moving to a more exposed and polar environment, encountered a more hydrophobic condition (Owenius *et al.*, 1999, Schindel *et al.*, 2001, Nguyen *et al.*, 2006). Regarding to the molecular modeling of E166Cb (Figure 4.4), the SAA of badan decreased by 291 $Å^2$ (- 81%) when penicillin G was bound to the enzyme. It was hence suggested that upon the binding of the substrate, the flexibility of the omega loop allowed the label either to be buried in a hydrophobic pocket of the acylated enzyme or shielded by the penicillin G moiety, instead of moving out of the pocket. This might be driven by the hydrophobic nature of the badan structure. Since badan fluoresces more strongly in a non-polar condition, once the substrate enters the enzyme active site and the badan is buried in the hydrophobic pocket or shielded by the substrate, the fluorescence intensity detected would increase.

From the results, it could be concluded that when the PenP_E166C was labeled with fluorescein-5-maleimide and badan, significant changes in fluorescence signals were generated upon substrate bindings, while only small changes were observed in the IAF-labeled enzymes. Therefore, we concentrate on studying the properties of mutants labeled with fluorescein-5-maleimide and badan in this project. In the later chapters, the fluorophore “fluorescein-5-maleimide” would be described as “fluorescein” for simplicity.

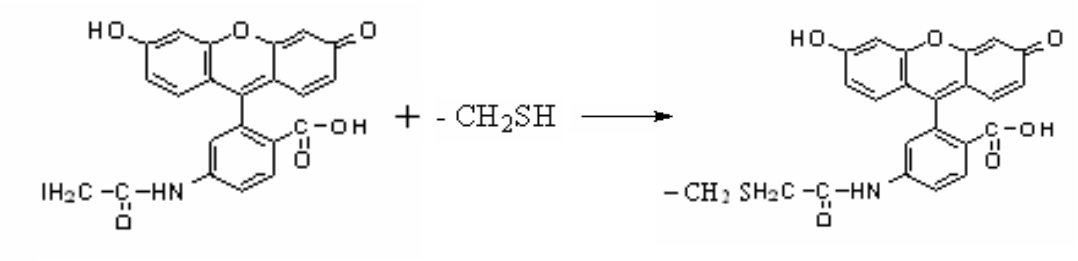

6-iodoacetamidofluorescein thioether

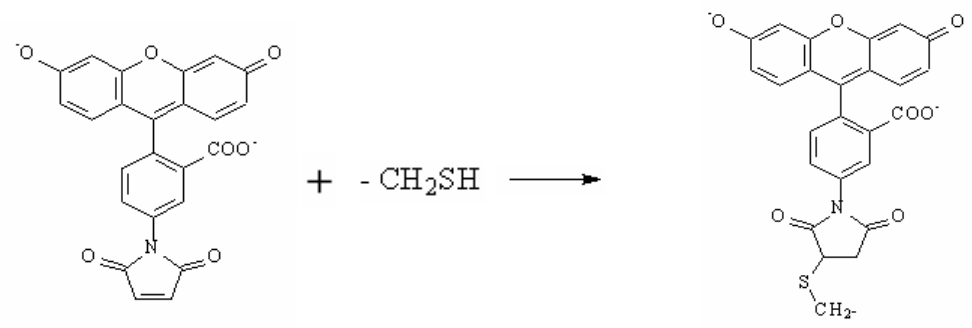

Fluorescein-5-maleimide thioether

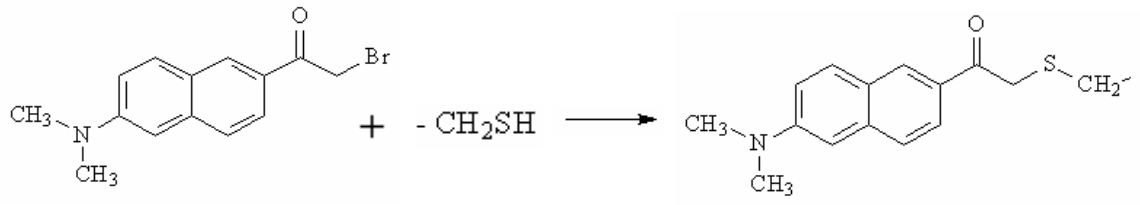

Badan thioether

Figure 4.1. Reaction of a thiol with 6-iodoacetamidofluorescein (a), fluorescein-5-maleimide (b), and badan (c).

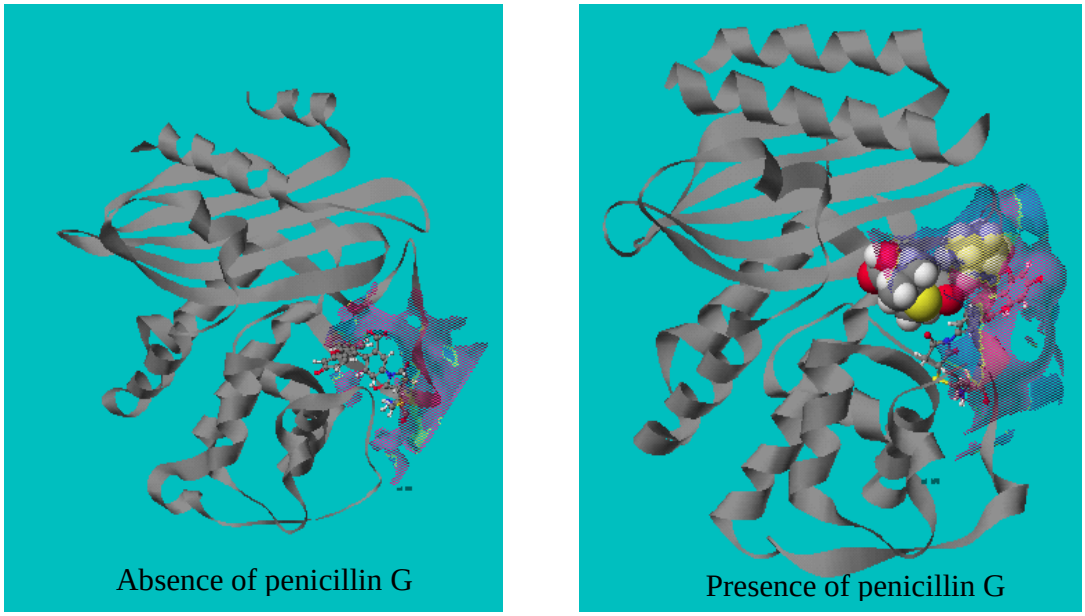

Figure 4.2. Molecular model for E166Cf before (left) and after (right) binding with penicillin G. (Siu *et al.*, unpublished work).

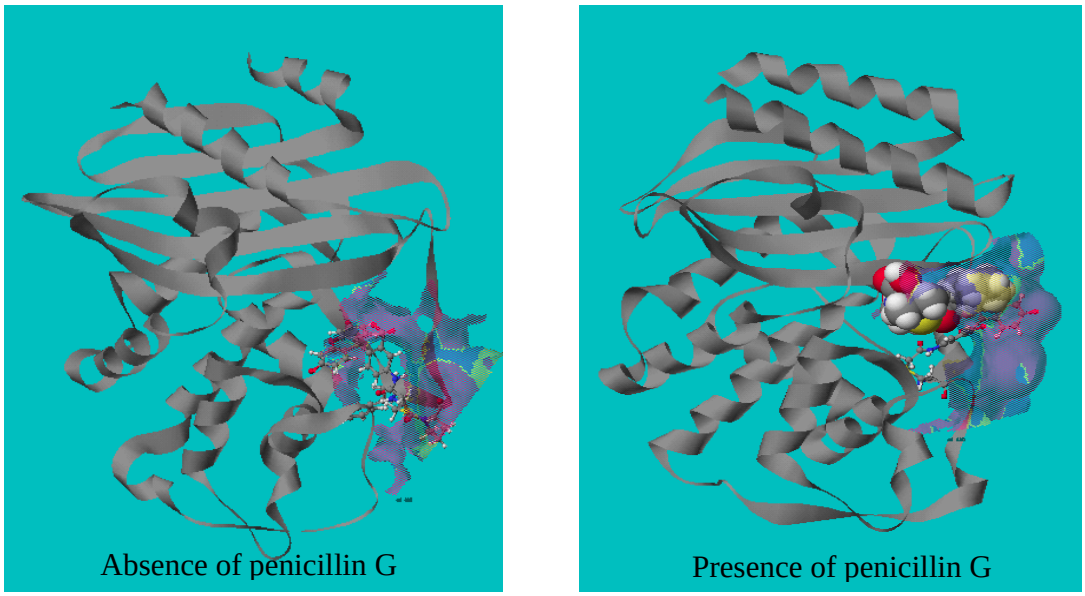

Figure 4.3. Molecular model for E166Ciaf before (left) and after (right) binding with penicillin G. (Siu *et al.*, unpublished work).

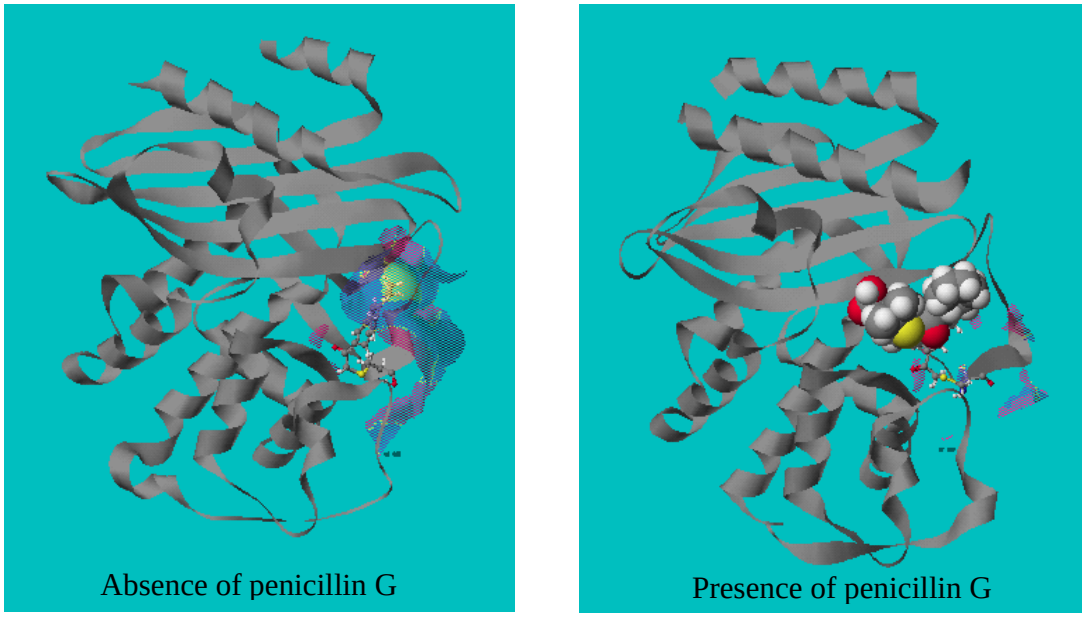

Figure 4.4. Molecular model for E166Cb before (left) and after (right) binding with penicillin G. (Siu *et al.*, unpublished work).

Table 4.1. Calculated solvent accessible areas of different fluorescence reporter groups covalently linked to E166C before and after penicillin G binding (Siu *et al.*, unpublished work).

Solvent Accessibility ($Å^2$) of fluorescence probes	Before substrate binding	After substrate entry	Difference	Percentage change (%)
E166Cf	559	632	+73 (±4)	+13
E166Ciaf	566	628	+62 (±3)	+11
E166Cb	355	64	-291 (±23)	-81

4.5.2. Detection of beta-lactam antibiotics

Time-resolved fluorescence measurement was performed according to the description in Section 2.8.1. Two groups of antibiotics, including penicillins and cephalosporins, were studied. The time-resolved fluorescence spectra of the four PenP biosensors in these beta-lactam antibiotics are shown in Figures 3.13 to 3.16. The signals detecting cephaolsporins gave better stabilities (longer detectable signals) than that of penicillins. However, steady signals could be achieved at a shorter time in the latter case. The differences in the spectral pattern might be explained by the nature of the biosensor.

PenP is a kind of class A beta-lactamase, which binds and hydrolyzes penicillins more effectively than cephalosporins (Matagne *et al.*, 1998; Matagne *et al.* 1999). When detecting penicillins, the enzyme binds to the substrate rapidly and a signal is generated within a short time. However, once the substrate is hydrolyzed by the enzyme, the fluorescence intensity will drop and return to the baseline (original intensity), whereas for the cephalosporins, which are poor substrates of the PenP beta-lactamase (Matagne *et al.* 1999), the slower increase in the fluorescence intensity may be attributed to the slow binding of substrate to the enzyme. However, the fluorescence signal can remain stable for a longer time, as long as the substrate is not hydrolyzed. In the cases of cefoxitin and moxalactam, the signals were very stable and no decline was observed within an hour. It indicated that no hydrolysis was observed. This kind of spectral pattern was observed for all the tested antibiotics under the cephalosporin family.

In that case, apart from testing the presence of antibiotics, analysis of the fluorescence

spectral pattern from the biosensors also allows classification of the types of antibiotic being tested (provided that only one type of substrate is present). In addition, it is also worth noting that the emission maxima and signal stability indeed display a dose-response relationship with the initial substrate concentration. At low antibiotic concentrations, increase in the substrate concentration gave a higher fluorescence signal, hence a higher fluorescence emission maximum. However, at high antibiotic concentrations in which the substrate was in excess, the emission maximum saturated and would not increase further with the increase in the substrate concentration. Instead, the fluorescence intensity would remain at the maximum value and appeared as a plateau. In that case, increase in the substrate concentration gave a longer stable signal, hence better signal stability.

Comparisons between the single mutant sensors and double mutant sensors indicated that both groups showed the same detection limit towards all the substrates tested (except for those which could not be detected by the badan-labeled mutants). However, the double mutant biosensors generated longer detectable signal than that of the single mutant biosensors, especially in detecting the penicillin-type antibiotics. This could be attributed to the fact that the second mutation (N170Q) further reduced the hydrolytic rate of the beta-lactamase and slowed down the substrate hydrolysis (Chen and Herzberg, 2001). The double mutant sensors hence gave longer detectable signals, until all the substrates were hydrolyzed. However, for the cephalosporin-type antibiotics, the two groups of biosensors showed no significant differences in terms of signal stability, in which both of them gave similar fluorescence spectral pattern. This might be due to the fact that any differences in their hydrolytic rates could not be easily observed as this class of antibiotics are poor

substrates of the PenP beta-lactamases and hydrolysis are very slow (Matagne *et al.* 1999).

Comparisons between the fluorescein-labeled biosensors and badan-labeled biosensors showed that the two groups gave similar spectral pattern and detection limits. However, it was surprising to find that the badan-labeled biosensors only showed very little changes in fluorescence intensity (close to none) upon the addition of ampicillin. In addition, the badan-labeled E166C failed to give any measurable signal enhancement in the presence of cefoxitin. For the latter case, the same observation was previously found in the PenPC_E166C biosensor which was labeled with acrylodan (unpublished work). One possibility for this was that the fluorophore might be arranged in an orientation that the fluorescence was quenched by the sulphur group of cefoxitin (see Figure 5.9 for the antibiotic structures). However, further studies, such as molecular modeling, have to be carried out in order to confirm the reason. For the case of ampicillin, there is no known fluorescence quenching group in its structure and it is unknown why the badan-labeled biosensors showed no significant changes in the fluorescence intensity in the presence of this antibiotic. Nevertheless, since such a lack of detection signal was only observed in the badan-labeled PenP mutants so far and not the fluorescein-labeled counterparts, the badan molecule seems to be more susceptible to quenching because of its new orientation after substrate binding.

Apart from the lack of detection signal for certain types of antibiotics, the badan-labeled biosensors also suffered from the problem of poor quantum yield. Since the quantum yield of badan is low, the signal to noise ratio is relatively large, especially when

using a spectrofluorimeter with low or fair sensitivity. Therefore, the badan-labeled biosensors may be more susceptible to false signals and may cause one to arrive at a wrong conclusion. In contrast, fluorescein confers excellent quantum yield and even small changes in the fluorescence intensity would be detected with relative ease. Hence the fluorescein-labeled biosensors seem to give more reliable results. However, the problem of the poor quantum yield of badan may be overcome simply by using a spectrofluorimeter with better sensitivity.

Taken together, the double mutation (E166C/N170Q) of the beta-lactamase further suppressed the hydrolytic ability of the enzyme, and the double mutant biosensors conferred better signal stability and gave longer detectable signals than the single mutant counterparts in detecting penicillins. In addition, the biosensors labeled with fluorescein-5-maleimide performed better than the ones labeled with badan, with the former generated fluorescence signals in all the tested antibiotics in this study and less susceptible to false results. Moreover, it is interesting to note that when penicillin G and penicillin V were used as the substrates, substrate hydrolysis by the PenP mutants could not be detected by the UV/VIS spectrophotometric method (see Section 3.5). However, the drop in signal shown in the fluroesence spectra indicated that substrate hydrolysis did occur. In consequence, the PenP biosensor developed in this study might provide an alternative approach to detect substrate hydrolysis.

4.5.3. Detection of beta-lactamase inhibitors

Apart from detecting beta-lactam antibiotics, PenP biosensors showed changes in fluorescence intensity in the presence of beta-lactamase inhibitors. Changes of fluorescence scanning spectra of PenP biosensors upon the addition of some common beta-lactamase inhibitors were recorded and shown in Figures 3.17 and 3.18. All the four biosensors showed fluorescence enhancement upon the addition of sulbactam, clavulanic acid and tazobactam. However, the relatively weak signal given by the PenP_E166Cb in tazobactam once again suggested that the badan-labeled biosensors seem to be less suitable in the biosensor development.

The ability of signal generation allows the PenP biosensors to find their applications in drug discovery, in which they have the potential of developing an important tool for high-throughput screening of new beta-lactamase inhibitors.

4.6. Biosensing process of PenP biosensors

In order to illustrate the biosensing process of the PenP biosensors more clearly, the time-resolved fluorescence measurement and electrospray ionization mass spectrometry (ESI-MS) were performed in parallel. Since the rapid acylation of the PenP mutants could not be followed by manual mixing methods, the binding and hydrolysis of penicillin G by MBP_PenP_E166Cf/N170Q was monitored by ESI-MS coupling with the rapid quench-flow method, and the corresponding changes in the fluorescence intensity were traced by the stopped-flow spectrophotometer. Penicillin G and MBP_PenP_E166Cf/N170Q were chosen for the study as penicillin G can be hydrolyzed quite efficiently by our PenP beta-lactamase mutant, so that the whole binding and hydrolysis process could be easily monitored within a short incubation time. On the other hand, because of the high quantum yield of fluorescein and low catalytic rate of the double mutant, MBP_PenP_E166Cf/N170Q seemed to be the best candidate in the biosensor development and it was hence used in this study. By doing this study, the actual species which were involved in the fluorescence enhancement could be determined.

Since the binding of penicillin G to the PenP mutants occurred very rapidly, in order to monitor accurately the changes in the fluorescence intensity at the beginning of the reaction, the fluorescence spectrum was followed by the stopped-flow apparatus. The time-resolved fluorescence spectrum of MBP_PenP_E166Cf/N170Q in the first 100 s of the reaction was recorded in Figure 3.19(a) and the changes were described in Section 3.8.1.

4.6.1. Detection of acyl-enzyme intermediate in penicillin G hydrolysis

ESI-MS has been a popular method for studying the products or intermediates of the enzyme reactions. Characterization of acyl-enzyme intermediate in the catalytic hydrolysis of beta-lactam antibiotics by mass spectrometry was firstly demonstrated by Aplin *et al*. (1990). Binding reaction between penicillin G and MBP_PenP_E166Cf/N170Q was handled by the assistance of a quench-flow device and the corresponding ESI-MS spectra are shown in Figure 3.20. The results indicated that the amount of free MBP_PenP_E166Cf/N170Q decreased in the first two minutes, while that of the penicillin G-MBP_PenP_E166Cf/N170Q adduct complex increased. The changes in the amount of the two species indeed indicated the binding action of penicillin to the enzyme, generating the corresponding substrate-enzyme adduct complex. At the 30-minute time point, the amount of free enzyme restored to that at the beginning and the substrate-enzyme adduct complex disappeared. It implied that, all penicillin G in the reaction solution was hydrolyzed in the half-hour reaction time, products were released and the penicillin G-MBP_PenP_E166Cf/N170Q adduct complex was converted back to the native MBP_PenP_E166Cf/N170Q.

4.6.2. Correlation between fluorescence spectra and enzyme kinetics

When comparing the mass spectra from ESI-MS with the corresponding fluorescence spectra, a good correlation was observed. The amount of the penicillin adduct complex of MBP_PenP_E166Cf/N170Q at different time intervals in the mass spectra was in qualitative agreement with the enhancement of fluorescence intensity in the time-resolved fluorescence spectrum. These results provided a strong evidence that the covalently-bound

penicillin adduct complex of MBP_PenP_E166Cf/N170Q (i.e. EC*) plays a major role in fluorescence enhancement.

To give a better illustration, fluorescence changes from the biosensors can be rationalized by the enzymatic reaction shown in Figure 1.2. After adding antibiotic (C) to the enzyme (E), the antibiotic associates with the enzyme to form a non-covalent substrate-enzyme complex (EC), and later convert into a tetrahedral covalent acyl-enzyme intermediate (EC*) upon acylation. During the EC and EC* formation, because of the access of the antibiotic to the enzyme active site, the flexible omega loop moves the attached fluorophore, leading to a change in the local environment of fluorophore and hence it fluoresces more strongly. As a result, the fluorescence intensity increases. At a low [C], since the rate of EC and EC* formation is small (small k_1[E][C]), a slow increase in the fluorescence intensity is observed. When more and more EC and EC* are formed, the fluorescence intensity increases and reaches its maximum. However, once the substrate is hydrolyzed by the enzyme and converted to the product (P), the amount of EC and EC* decreases. The product (P) will leave the active site and the fluorophore is allowed to return to its original position and restore its initial weak fluorescence signal. As a result, the fluorescence intensity decreases and return to the original value.

For the cases of high [C], the high k_1[E][C] allows rapid EC and EC* formation and hence a fast increase in the fluorescence intensity is observed. Once the reaction reaches a steady state, in which the rate of EC and EC* formation is equal to the product formation rate, all the enzymes are saturated with the substrate and the fluorescence signal remains

steady and results in a plateau. However, when most of the substrates are hydrolyzed and the rate of product formation exceeds that of the EC and EC* formation, releases of products will cause the fluorescence intensity to decrease. Sometimes, especially for some cephalosporins like moxalactam, the fluorescence signal can remain stable for a very long period of time (with no decline within an hour-experiment). It corresponds to the fact that the beta-lactamase cannot hydrolyze cephalosporins effectively, and the accumulated EC and EC* allows the generation of stable fluorescence signals.

4.7. Comparison between PenP and PenPC biosensors

Both PenP and PenPC beta-lactamases belong to the class A beta-lactamases, the sequence alignment of the two demonstrates that they are very similar as they share about 52% sequence identity (Figure 4.5). The PenPC biosensors, PenPC_E166Cf and PenPC_E166Cb, have also been constructed and demonstrated the ability to generate detectable fluorescence signals upon the binding of various beta-lactams (see Appendix V for relevant data) (Chan *et al.*, 2004; Chan *et al.*, unpublished work). Although the PenP and PenPC enzymes share extensive similarities in the amino acid sequences, their fluorophore derivatives nevertheless exhibit many differences in their physical and biosensing properties. In this section, a brief comparison between the properties of the PenPC and PenP biosensors and an evaluation of them in developing a sensing system for beta-lactams are made. Only the single mutant-based biosensors were considered in the following comparison so as to study the properties of biosensors derived from the same mutant but different kinds of class A beta-lactamases.

4.7.1. Detection limit

According to a previous work, it was found that the detection limit of PenPC_E166Cb is generally lower than that of PenPC_E166Cf. The PenPC_E166Cb biosensor can detect penicillin G at a concentration as low as 5-10 nM in water, compared to 50 nM for the PenPC_E166Cf (Chan *et al.*, unpublished data). For the PenP biosensors developed in this project, all four biosensors showed similar detection limits of 10 nM in all the antibiotics tested. The results hence suggested that the PenP biosensors exhibit similar detection limits to that of PenPC_E166Cb.

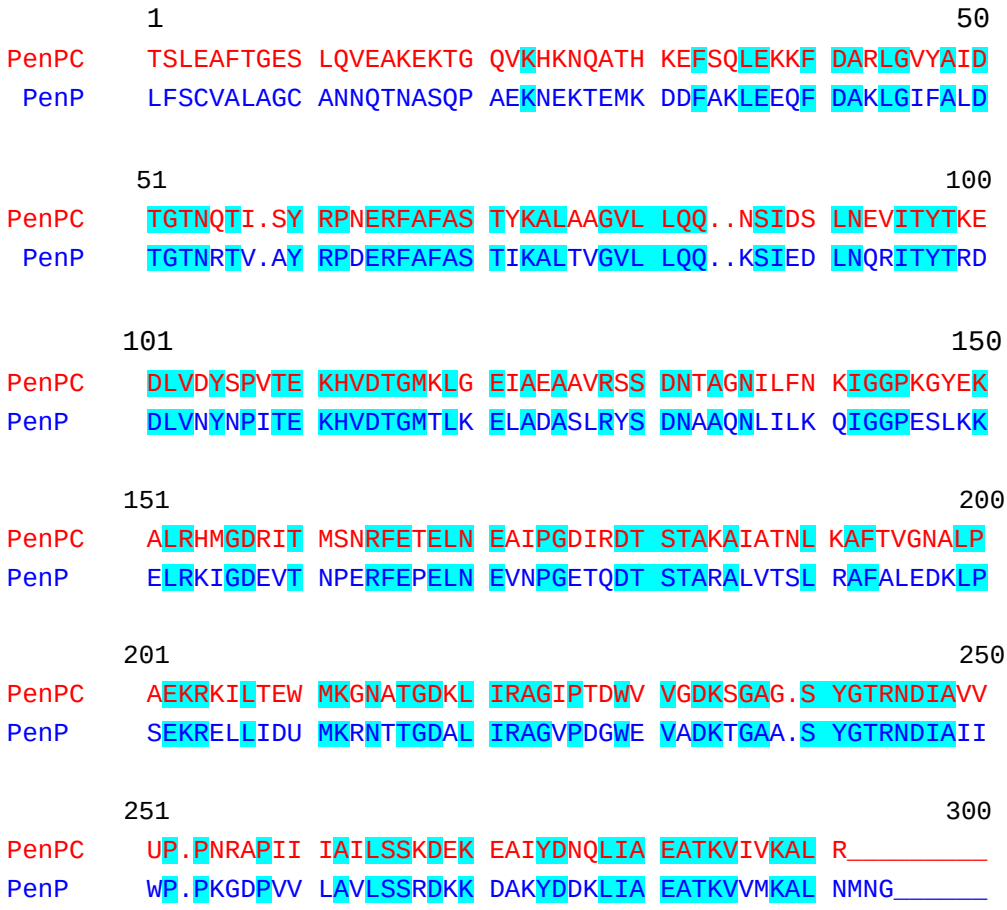

Figure 4.5. Sequence alignment of the PenPC and PenP beta-lactamase numbered according to the ABL scheme. Conserved residues are shaded in dark. The two proteins are 52% identical at the amino acid sequence level.

4.7.2. Sensitivity

While the two types of biosensor show similar detection limits, some of their spectral properties are different. In general, the maximal signal changes generated from the PenPC biosensors are greater than those of the PenP counterparts. The maximal signal change of the PenPC biosensors has been shown to be as large as 150% and 100% in detecting penicillins and cephalosporins, respectively, compared to only around 90% and 50% in the PenP cases. However, such large signal changes in the PenPC biosensors are usually observed in the case of high antibiotic concentrations, which may not be very beneficial in the sensing system aiming for the detection of trace antibiotics in food (but this property may still be advantageous in drug screening processes). At lower antibiotic concentrations, there were distinct observations for different types of beta-lactam antibiotics being tested. For example, PenPC_E166Cb was shown to generate signal changes as large as 90-110% in detecting penicillin V and penicillin G at 0.1 μM (Figure 5.12), compared to only 45-85% changes in the PenP biosensors. However, for the same concentration of cephalosporin, signals from the PenP biosensors showed around 30-50% increase whereas those of the PenPC only showed around 5-30% increase. The results suggested that PenPC_E166Cb seem to be more sensitive in the detection of penicillins, while the PenP biosensors are more sensitive in detecting low concentrations of cephalosporins. In addition, it is important to note that the PenP biosensors are the most sensitive in detecting antibiotics at concentrations in the range of 10-100 nM. Within this range, the biosensors show relatively large changes in the fluorescence intensity even there is only a small difference in the antibiotic concentrations (see Appendix III).

4.7.3. Response time

Although both PenP and PenPC biosensors show rapid fluorescence enhancement upon the binding of penicillins, the PenP biosensors seem to give a faster response than the PenPC in detecting cephalosporins. When using cefoxitin and moxalactam as the substrates, the fluorescence signals from the PenP biosensors increased relatively faster and reached the signal maxima at a shorter time when compared to the PenPC. For example, at 0.1 µM of moxalactam, the PenP biosensors generally gave a stable maximum signal at 200-500 s of the reaction. In contrast, the signals from the PenPC counterparts were still at the rising phase and could not reach a plateau within an hour of experiment. This suggested that the PenP biosensors show a faster response than the PenPC biosensors.

4.7.4. Signal stability

Regarding the signal stability of the two groups of biosensor, the situation is quite complicated. For the cephalosporins, no significant difference in signal stability was found as the signals from both biosensors were relatively stable throughout the experiments. However, at high concentrations of penicillins, the PenP biosensors showed longer steady signals than the PenPC counterparts. For example, at 1 µM of penicillin G, the single mutant PenP biosensors gave steady signals for about 2000-2200 s, but the PenPC biosensors could keep signals steady in the first 500 s only. However, that was not the case for the lower antibiotic concentrations. At 0.1 µM of penicillin G, the signals of the single mutant PenP biosensor dropped rapidly at the very beginning of the reaction and returned to the baseline (original fluorescence intensity) at 1000 s, but the corresponding signals from the PenPC biosensors dropped relatively slower, and hence longer detectable (but

unstable) signals were obtained. The situation was particularly obvious in PenPC_E166Cb, in which a detectable signal was still observed after an hour of experiment (Figure 5.12). Since our biosensors aimed for detecting residual antibiotics at trace levels, the PenPC biosensors (particularly the PenPC_E166Cb) seem to perform better in terms of signal maintenance, as they can generate longer detectable signals at low concentrations of penicillins, though the signals are not so steady.

In fact, the spectral patterns from the two kinds of biosensor gave us some ideas about the catalytic differences of the two beta-lactamases. When there is a decrease in the fluorescence intensity, the slope of decrease observed in the PenP biosensors is steeper than that of the PenPC cases. The steeper slope indeed indicates a higher deacylation rate constant (k_3) of the PenP mutants, hence faster rate of ES* decomposition. The long stable signal shown by the PenP biosensors reflects that, the rate of ES* formation is probably much greater than that of decomposition, and thus results a better accumulation of acylenzyme in the PenP mutant. Whereas for the PenPC biosensors, the shorter stable signal indicates a shorter acylenzyme accumulation, which implies the rate of ES* formation differs not too much from that of the decomposition (not as much as in the PenP). As the steeper slope of the signal drop in PenP reflects its faster rate of ES* decomposition than the PenPC, the rate of ES* formation in PenP is thus believed to be faster than the PenPC as well. As a result, when compared to PenP, the smaller k_3 (slower rate of ES* decomposition) and the slower rate of ES* formation of PenPC lead to a slower decrease in the fluorescence intensity but at an earlier time of reaction.

4.7.5. Specificity

So far, the fluorescein-labeled PenP biosensors have shown the ability to generate detectable fluorescence changes in all antibiotics tested in this study. However, the badan-labeled PenP E166C and PenP E166C/N170Q did not give any measurable signal changes in the presence of ampicillin, and the former also failed to detect cefoxitin. The lack of signal increase is probably due to fluorescence quenching (see Section 4.5.2). In contrast, for the PenPC E166C mutants, both fluorescein-labeled and badan-labeled derivatives showed significant fluorescence enhancement in all the antibiotics tested, including ampicillin and cefoxitin (Figures 5.11-5.12). The variations in specificity of the two types of biosensor suggest that the orientations of the fluorophore after the substrate binding in the two cases might be different even there is the same substrate. The fluorescence scanning spectra of PenPC_E166Cb in the presence of penicillin G might serve as a strong indicator of the phenomenon (Figure 4.6).

Upon the binding of penicillin G, the blue-shift of the emission maximum observed in PenPC_E166Cb was larger than that of PenP_E166Cb, in which the emission maximum in the former was shifted from 513 nm to 490 nm, and that of the latter was shifted from 513 nm to 510 nm. The smaller blue-shift in PenP_E166Cb indicated that although the badan molecule encounters a more hydrophobic environment after the binding of penicillin G, this new environment is comparatively less hydrophobic than that encountered in PenPC_E166Cb. Because of the distinct orientations/ positions of badan upon substrate binding in the two biosensors, it is possible that the fluorescence quenching occurs in the badan-labeled PenP E166C only, when the fluorophore is in close contact with a quenching

group of the substrate (if any), but not in the PenPC counterpart. In terms of developing a reliable sensing system, it seems that PenP_E166Cb is not a suitable candidate as false-negative results may often be generated.

4.7.6. Protein thermostability

The theromstabilities of the PenP and PenPC biosensors were examined by the thermal denaturation study. The melting curves obtained for PenP and PenPC beta-lactamases, as well as their fluorophore labeled derivatives, are shown in Figure 3.10. The melting temperatures of the PenP biosensors (56-57 ^{o}C) were much higher than that of the PenPC E166Cf (40 ^{o}C). *B. licheniformis*, the bacterial source of PenP beta-lactamase, is known to be thermophilic and most of its enzymes are thermostable (Chell and Sundaram, 1978; Hwang *et al.*, 1997; Pavlova *et al.*, 1989). It was previously reported that the melting temperature of the *B. licheniformis* beta-lactamase was 63 ^{o}C (Vanhove *et al.*, 1995), which was consistent with our finding in the present study as the MBP-PenP wild-type beta-lactamase was found to have a melting temperature of 64 ^{o}C. This result also implied that the MBP fusion to the PenP beta-lactamase did not alter the thermostability of the enzyme.

It is believed that the good thermostabilty of the PenP biosensors would facilitate their storage and handling, which is particularly useful when manipulation of samples at high temperature is required. To further test the tolerance of the PenP biosensors at high temperatures, heat inactivation study was performed at 50 ^{o}C in the assay buffer. Enzymes were incubated at 50 ^{o}C and samples were withdrawn after various periods of time and

immediately cooled on ice. The residual activities of the enzymes in hydrolyzing nitrocefin at 20 ^{o}C were then measured and the results are shown in Figure 3.11. The results indicated that the activities of the PenPC biosensors dropped rapidly upon incubation at 50 ^{o}C, while the PenP biosensors showed no change in activities and remained very active upon an incubation of an hour. This finding, which is in agreement with the heat denaturation study, suggests that the PenP biosensors exhibit higher thermostability than that of the PenPC.

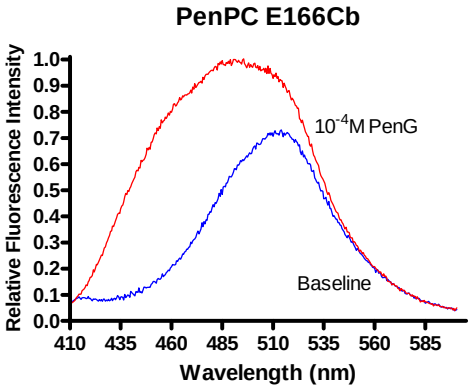

λ^{Em}_{max} (no PenG) /nm	λ^{Em}_{max} (10^{-4} PenG) /nm	Magnitude of blue-shift /nm	Monitoring Wavelength /nm
513	490	25	460

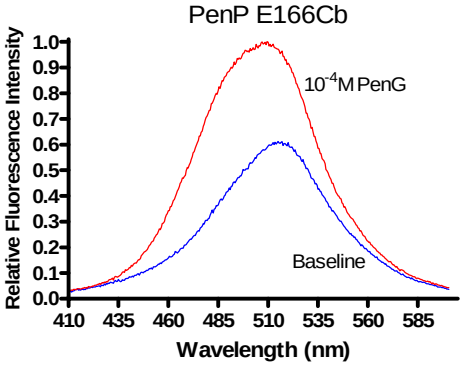

λ^{Em}_{max} (no PenG) /nm	λ^{Em}_{max} (10^{-4} PenG) /nm	Magnitude of blue-shift /nm	Monitoring Wavelength /nm
513	510	3	500

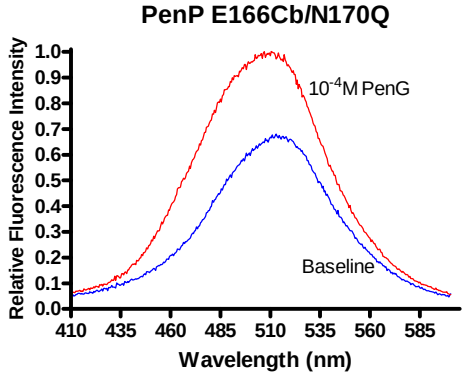

λ^{Em}_{max} (no PenG) /nm	λ^{Em}_{max} (10^{-4} PenG) /nm	Magnitude of blue-shift /nm	Monitoring Wavelength /nm
513	510	3	500

Figure 4.6. Fluorescence scanning spectra of various badan-labeled biosensors (1 x 10^{-7} M) in 50 mM phosphate buffer (pH 7.0) in the presence of 10^{-4} M of penicllin G.. Information of the blue-shift of emission maxima is listed in the tables on the right.

Chapter Five: Conclusion

Two PenP beta-lactamase mutants, E166C and E166C/N170Q, were constructed in this project. Mutations of E166C and N170Q were found to cause a dramatic decrease in the activity of the PenP beta-lactamase, in which the catalytic efficiency of the E166C and E166C/N170Q were approximately 4 x 10^4-fold and 1.2 x 10^5-fold lower than that of the wild-type, respectively. In the study, four fluorescence biosensors (PenP_E166Cf, PenP_E166Cb, PenP_E166Cf/N170Q and PenP_E166Cb/N170Q) were successfully developed from the PenP beta-lactamase. The PenP-based biosensors were able to detect various beta-lactam antibiotics at a concentration as low as 10 nM. It was shown that biosensors developed from the double mutants (E166C/N170Q) gave longer detectable signals than that developed from the single mutant (E166C). This reflected that the second mutation truly further slowed down the deacylation of the enzyme.

Apart from the detection of antibiotics, the capability of the PenP biosensors in signal generation in the presence of beta-lactamase inhibitors, such as sulbactam and clavulanate, also reveals their potentials in developing as valuable tools for drug screening.

An ideal biosensor should give a low detection limit, fast response and be able to generate significant and stable signals; likewise its detection should be sensitive and specific. In addition, it is advantageous if the biosensor can be kept in good condition by easy storage. In terms of developing a good sensing system, the PenP biosensor labeled with fluorescein-5-maleidmide seem to be more useful than the badan-labeled counterparts, as the former confers a higher quantum yield with a low incidence of false results.

By comparing our biosensors with the PenPC biosensors developed previously, PenPC E166Cb seems to be the best candidate in detecting penicillin-type antibiotics, because of its ability to generate significant and long detectable signals with a low detection limit, whereas PenP E166Cf seems to be the best in detecting cephalosporin-type antibiotics, as it can give significant and stable signals, with fast response time and a low incidence of false results. In this project, the PenP biosensors demonstrated their high thermostability, with normal activities at temperature as high as 50 ^{o}C. This property, which is absent in the PenPC counterparts, may facilitate the storage and handling of the PenP biosensors. It is believed that the biosensing properties of the biosensors, such as the signal stability and detection limit, could be continuously improved by protein engineering techniques.

APPENDIX I

MKIEEGKLVIWINGDKGYNGLAEVGKKFEKDTGIKVTVEHPDKLEEKFPQVAA

TGDGPDIIFWAHDRFGGYAQSGLLAEITPDKAFQDKLYPFTWDAVRYNGKLIAY

PIAVEALSLIYNKDLLPNPPKTWEEIPALDKELKAKGKSALMFNLQEPYFTWPLI

Maltose Binding Protein

AADGGYAFKYENGKYDIKDVGVDNAGAKAGLTFLVDLIKNKHMNADTDYSI

AEAAFNKGETAMTINGPWAWSNIDTSKVNYGVTVLPTFKGQPSKPFVGVLSAG

INAASPNKELAKEFLENYLLTDEGLEAVNKDKPLGAVALKSYEEELAKDPRIAA

TMENAQKGEIMPNIPQMSAFWYAVRTAVINAASGRQTVDEALKDAQTNSSSNN

Linker

NNNNNNNNLGIEGRISEFGSKTEMKDDFAKLEEQFDAKLGIFALDTGTNRTVAY

Factor Xa recognition site

RPDERFAFASTIKALTVGVLLQQKSIEDLNQRITYTRDDLVNYNPITEKHVDTG

166^{th}

MTLKELADASLRYSDNAAQNLILKQIGGPESLKKELRKIGDEVTNPERFCPELN

PenP_E166C

EVNPGETQDTSTARALVTSLRAFALEDKLPSEKRELLIDWMKRNTTGDALIRA

GVPDGWEVADKTGAASYGTRNDIAIIWPPKGDPVVLAVLSSRDKKDAKYDDK

LIAEATKVVMKALNMNGK

Figure 5.1. Amino acid sequence of MBP_PenP_E166C. Regions shaded in grey, green and yellow represent the maltose binding protein, Factor Xa recognition site and PenP_E166C, respectively. Region indicated by red arrow refers to the linker between maltose binding protein and beta-lactamase.

Figure 5.2. Amino acid sequence of MBP_PenP_E166C/N170Q. Regions shaded in grey, green and yellow represent the maltose binding protein, Factor Xa recognition site and PenP_E166C/N170Q, respectively. Region indicated by red arrow refers to the linker between maltose binding protein and beta-lactamase.

APPENDIX II

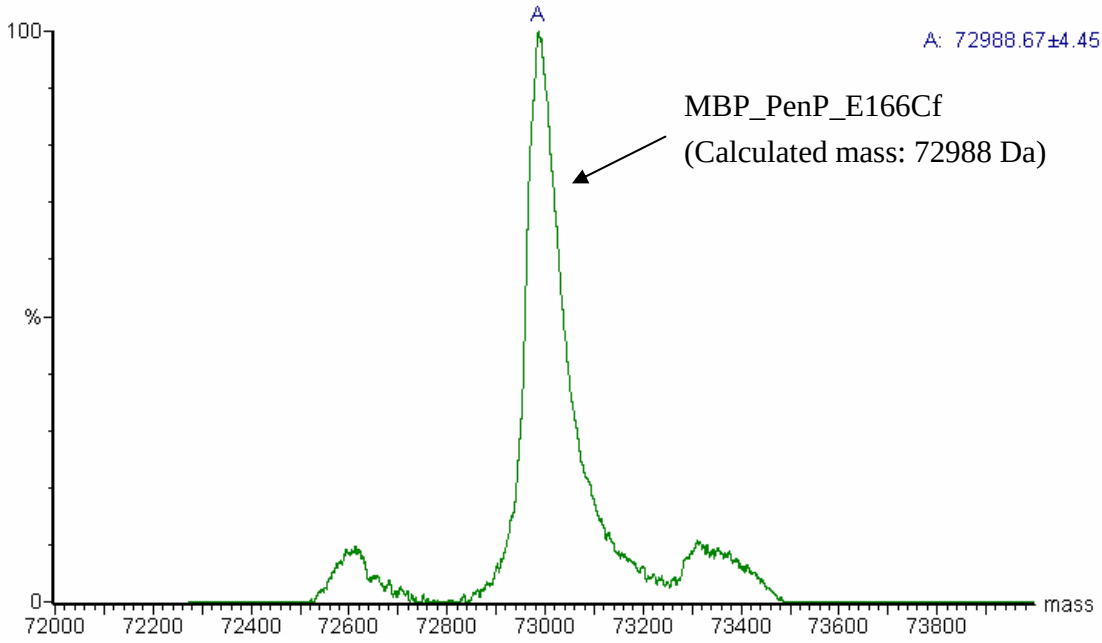

(a)

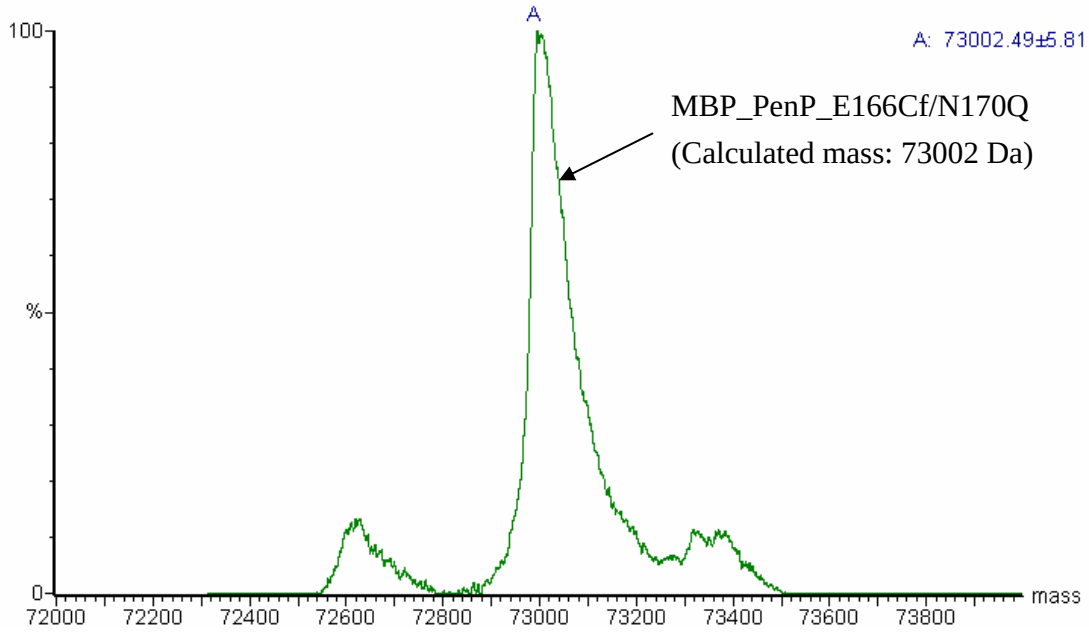

(b)

Figure 5.3. Mass spectra of MBP_PenP_E166Cf (a) and MBP_PenP_E166Cf/N170Q (b). In both cases, over 95% of enzymes were labeled with fluorophores.

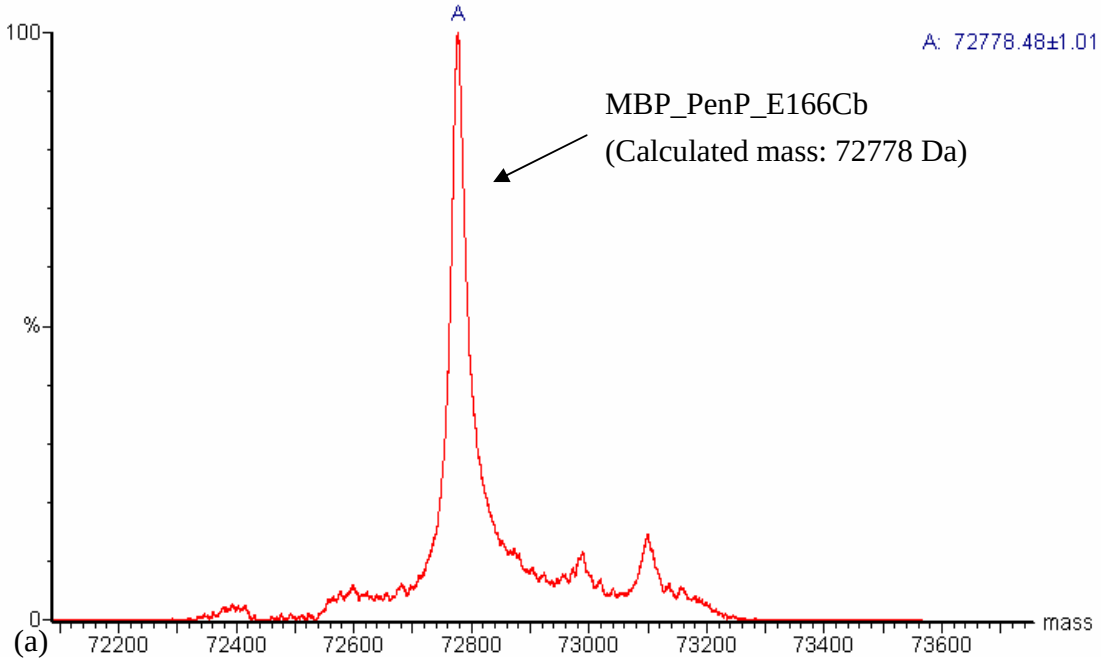

(a)

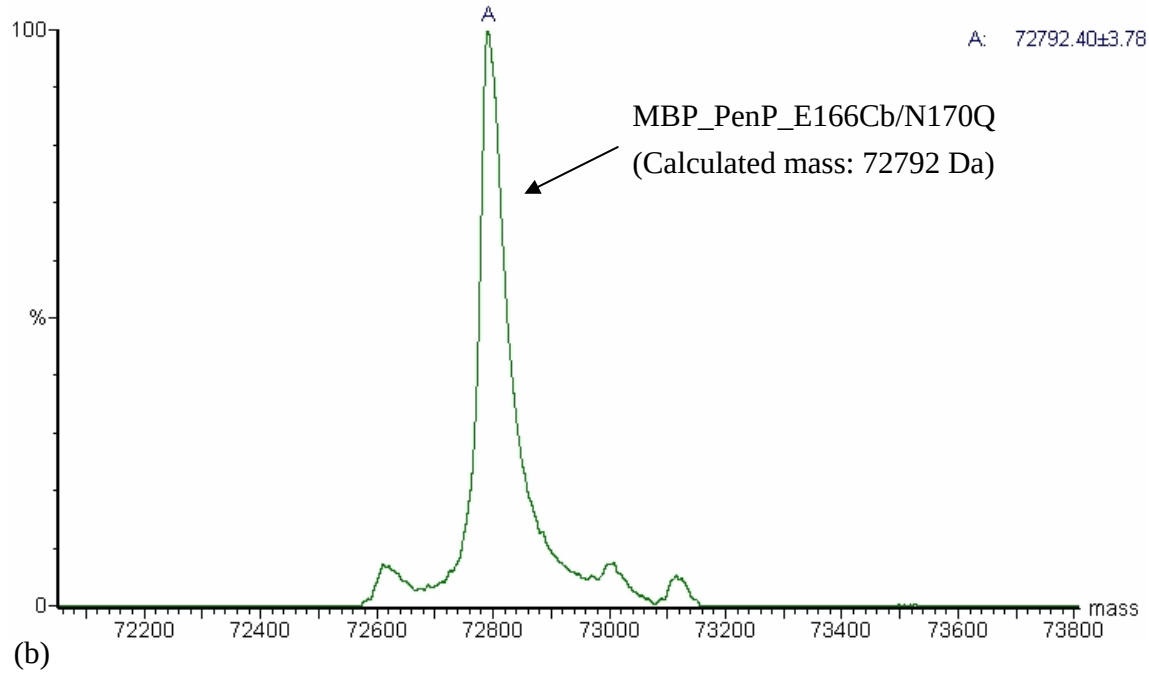

(b)

Figure 5.4. Mass spectra of MBP_PenP_E166Cb (a) and MBP_PenP_E166Cb/N170Q (b). In both cases, over 95% of enzymes were labeled with fluorophores.

APPENDIX III

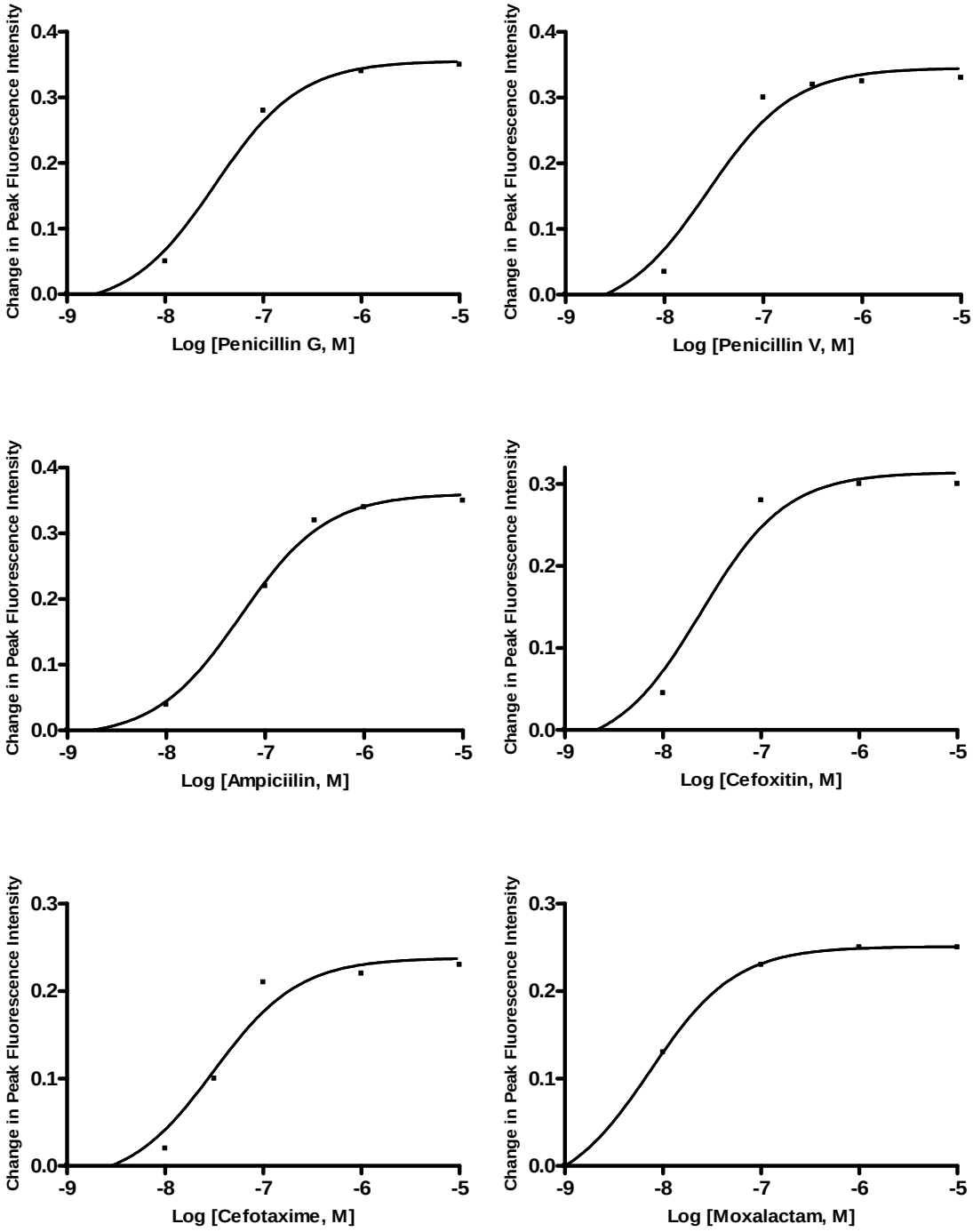

Figure 5.5. Plot of change in fluorescence intensity (at the maxima) of MBP_PenP_E166Cf as function of log [antibiotic, M].

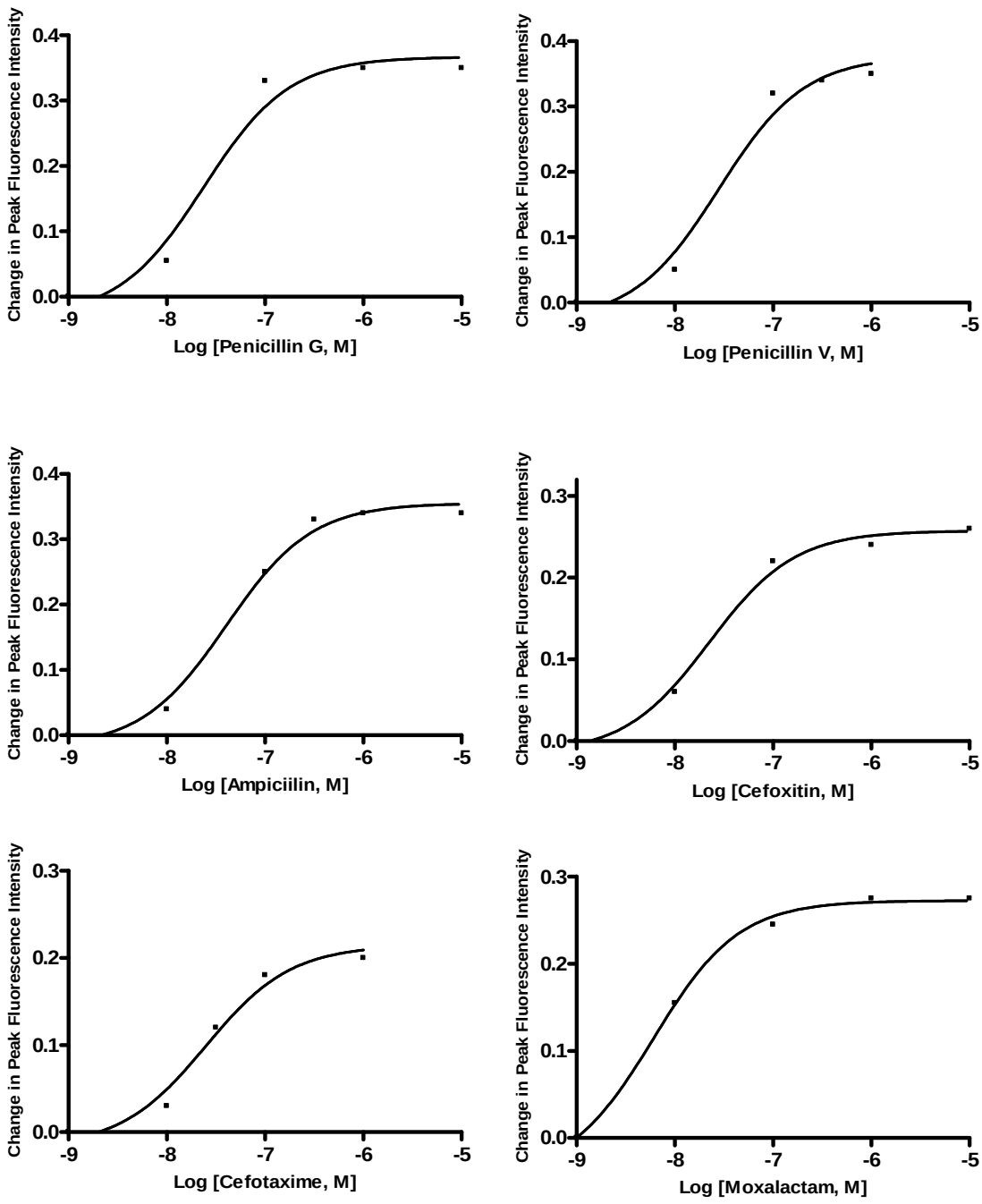

Figure 5.6. Plot of change in fluorescence intensity (at the maxima) of MBP_PenP_E166Cf/N170Q as function of log [antibiotic, M].

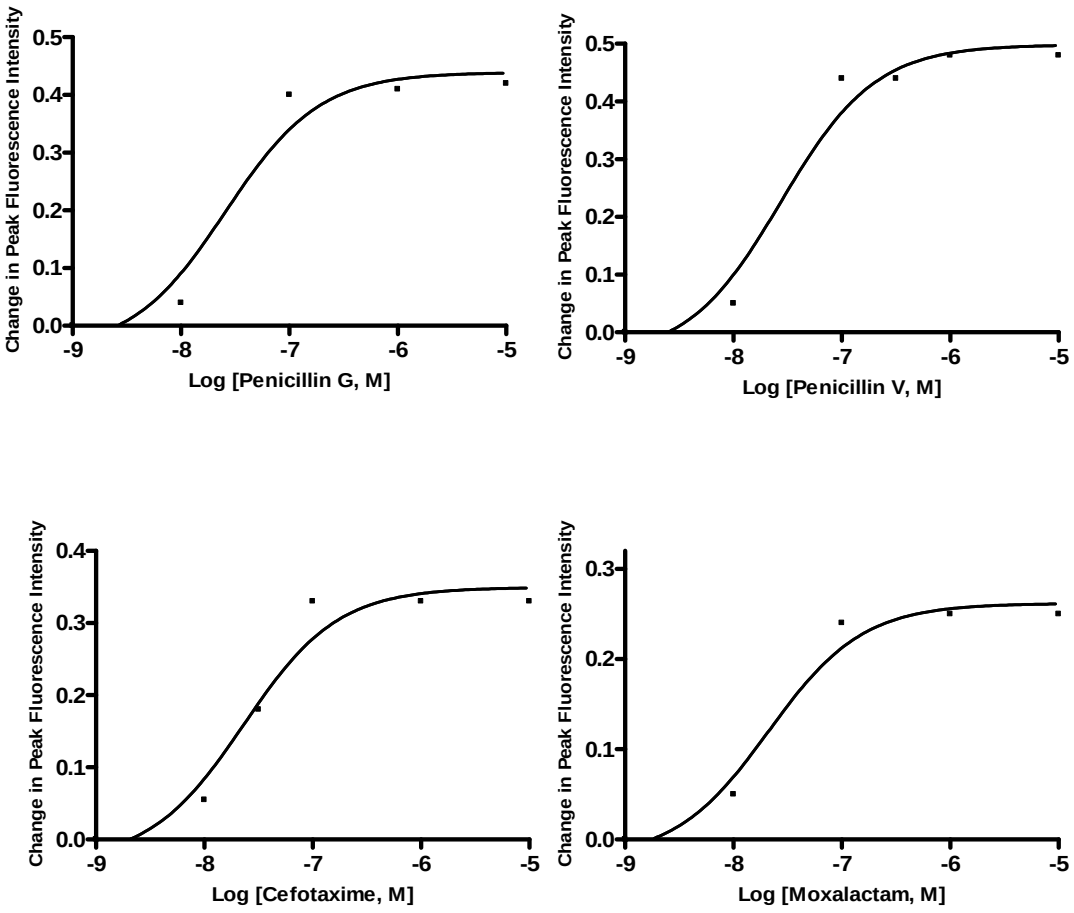

Figure 5.7. Plot of change in fluorescence intensity (at the maxima) of MBP_PenP_E166Cb as function of log [antibiotic, M].

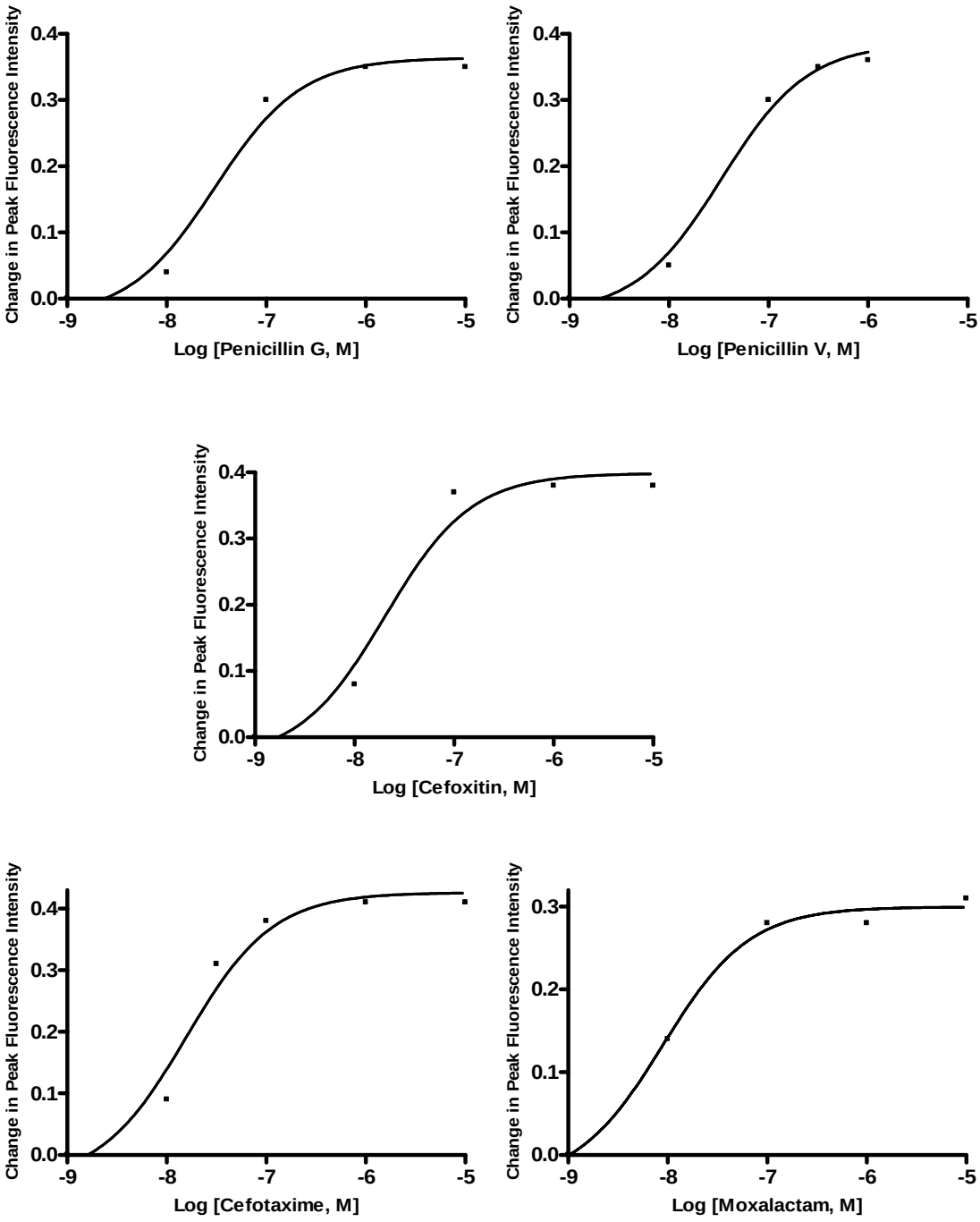

Figure 5.8. Plot of change in fluorescence intensity (at the maxima) of MBP_PenP_E166Cb/N170Q as function of log [antibiotic, M].

APPENDIX IV

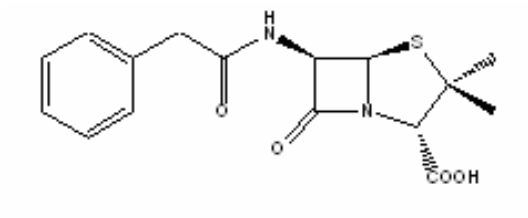

Penicillin G

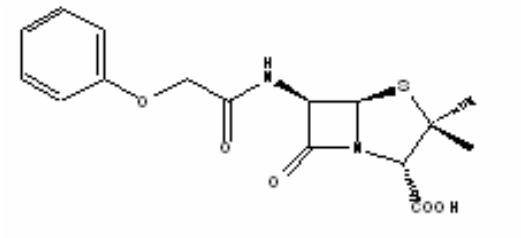

Penicillin V

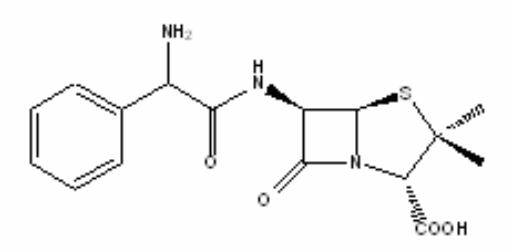

Ampicillin

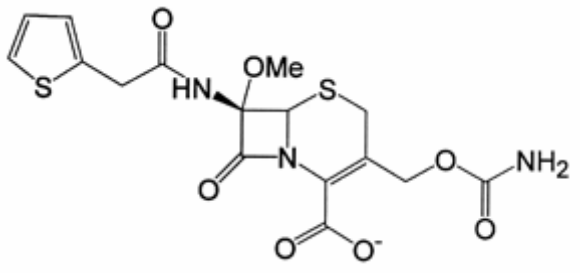

Cefoxitin

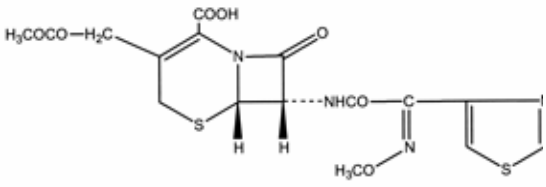

Cefotaxime

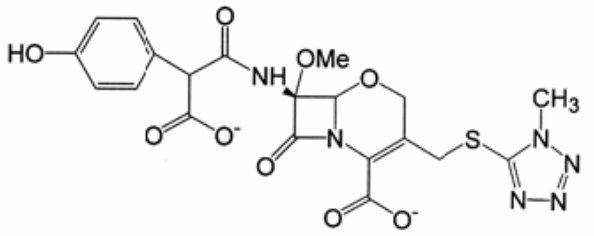

Moxalactam

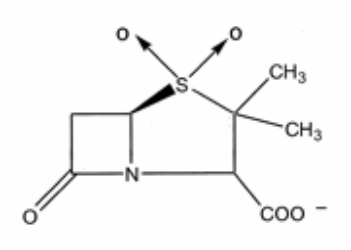

Sulbactam

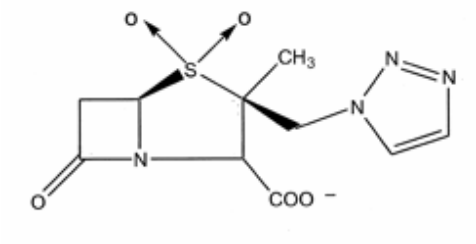

Tazobactam

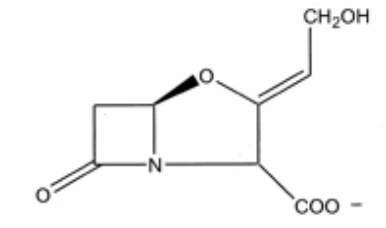

Clavulanate

Figure 5.10. Chemical structures of the beta-lactamase inhibitors used in the study.

APPENDIX V

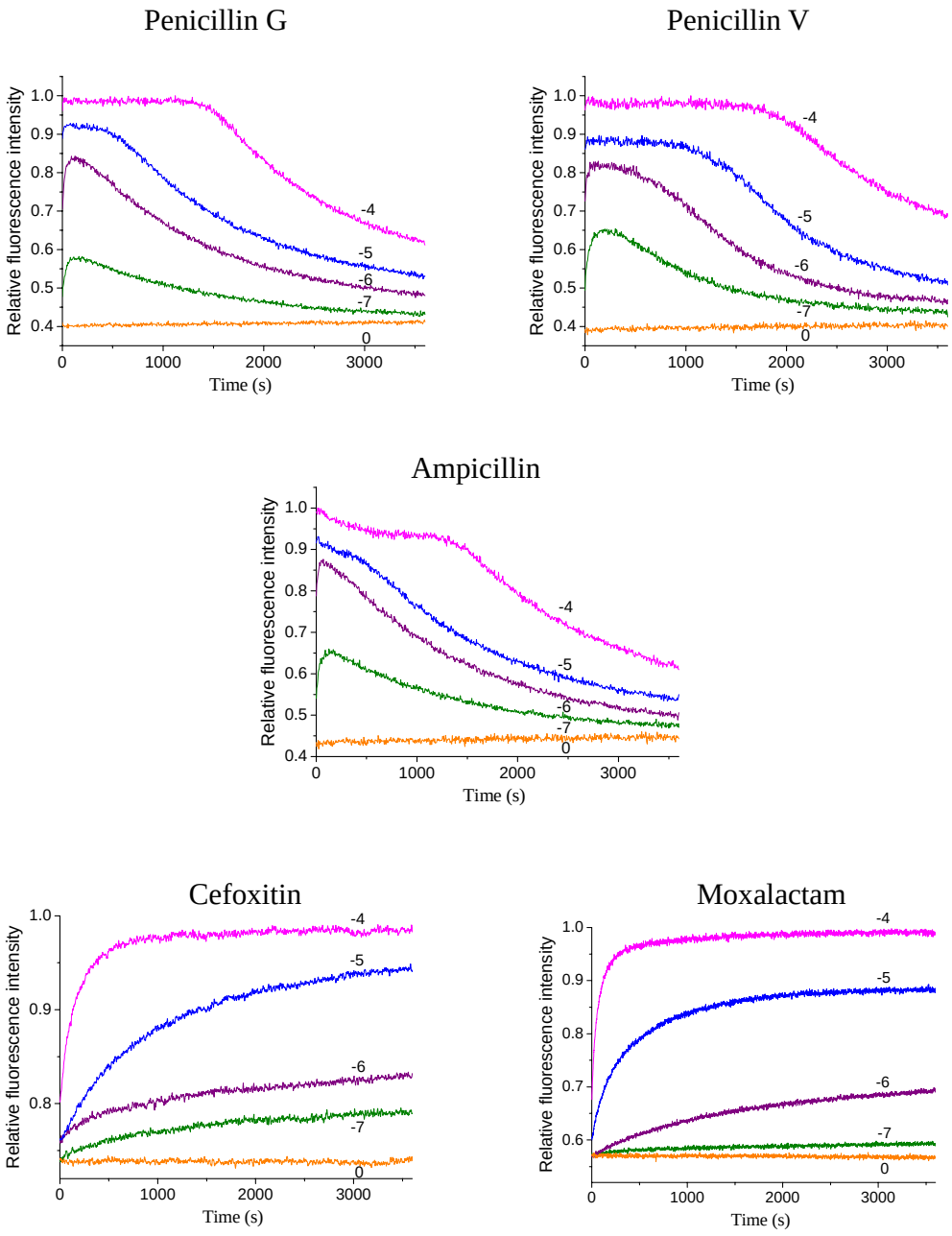

Figure 5.11. Time-resolved fluorescence spectra of PenPC_E166Cf in different beta-lactam antibiotics in 50 mM potassium phosphate buffer (pH 7.0). The numbers without brackets next to the curves denote log (antibiotic concentration), while numbers with brackets denote the actual antibiotic concentrations.

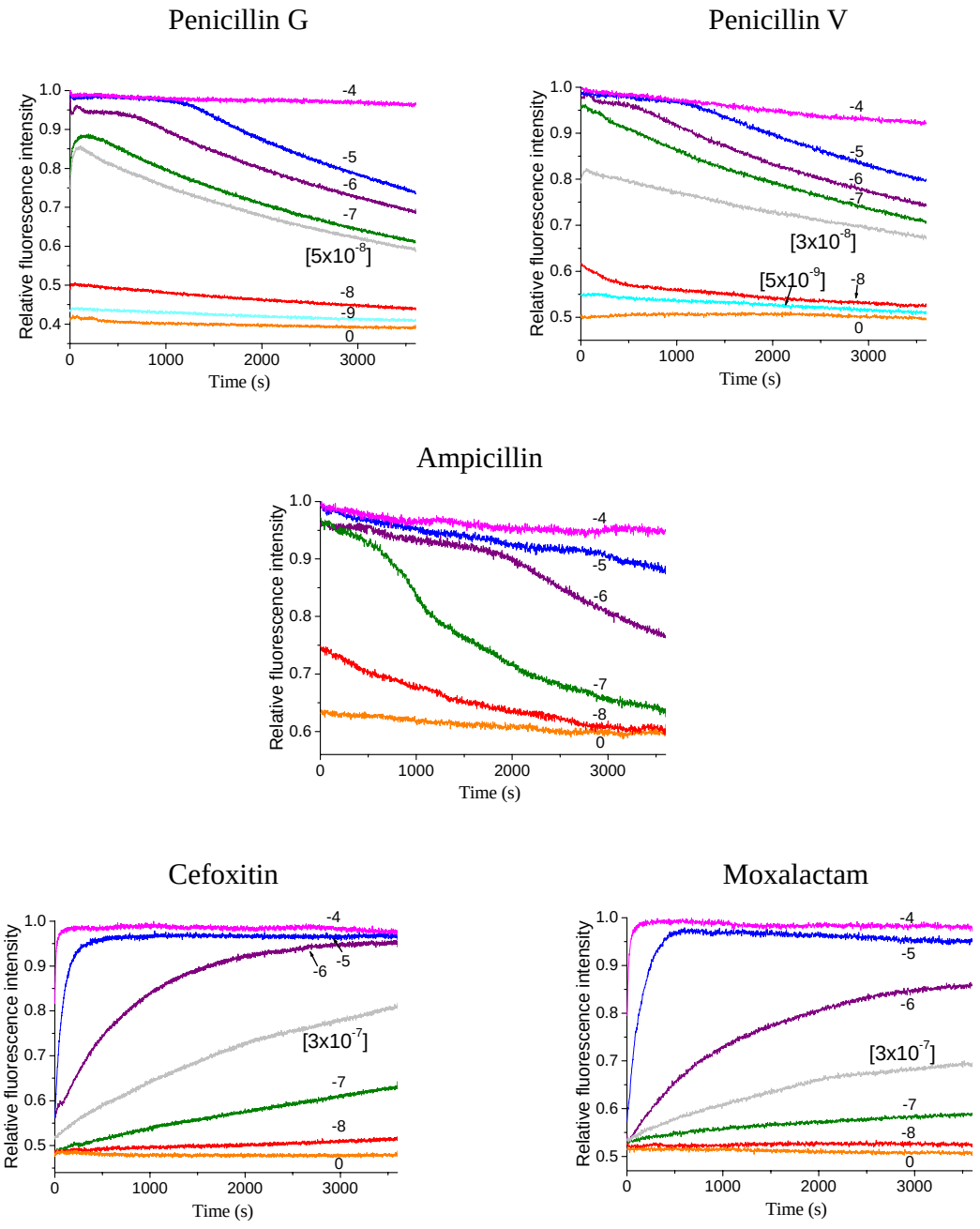

Figure 5.12. Time-resolved fluorescence spectra of PenPC_E166Cb in different beta-lactam antibiotics in 50 mM potassium phosphate buffer (pH 7.0). The numbers without brackets next to the curves denote log (antibiotic concentration), while numbers with brackets denote the actual antibiotic concentrations.

APPENDIX VI

Reagents and Solutions

(A) Media for bacterial culture and protein expression

2xTY medium (100 ml)

- Tryptone 1.6 g
- Bacto-yeast extract 1 g
- NaCl 0.5 g
- ddH_2O 100 ml

(B) Reagents for SDS-PAGE

Sample loading dye (8 ml)

- 0.5 M Tris-HCl (pH 6.8) 1 ml
- SDS 0.2 g
- Glycerol 2 ml
- 0.1% bromophenol blue 0.1 ml
- beta-mercaptoethanol 1 ml
- Total volume made up to 8 ml with ddH_2O

Staining solution (600 ml)

- Coomassie Blue R-250 1.6 g
- Acetic acid 100 ml
- Methanol 250 ml
- ddH2O 250 ml

Destain solution (500 ml)

- Acetic acid 50 ml
- Methanol 50 ml
- ddH2O 400 ml

Running buffer (10X, 1 L)

- Tris 30.5 g
- Glycine 144 g
- SDS 10 g
- Total volume made up to 1 L with ddH2O

(C) Agarose gel electrophoresis

TBE buffer (5X, 1 L)

- Tris 54 g
- Boric acid 27.5 g
- 0.5 M EDTA 20 ml
- Total volume made up to 1 L with ddH2O

(D) Buffer for purification of MBP_PenP beta-lactamase

Solubilization/ Binding buffer

20 mM Tris-HCl (pH 7.4), 0.2 M sodium chloride and 1 mM EDTA

Elution buffer

20 mM Tris-HCl (pH 7.4), 0.2 M sodium chloride, 1 mM EDTA and 10 mM maltose

(E) Buffer for purification of MBP-cleaved PenP beta-lactamase

Binding Buffer

20 mM Tris-HCl (pH 8.0) and 25 mM NaCl

Elution buffer

20 mM Tris-HCl (pH 8.0) and 500 mM NaCl

(F) Buffer for kinetic and fluorescence studies

50 mM Potassium phosphate buffer

50 mM K_2HPO_4 buffer, with pH adjusted to 7.0 by 50 mM KH_2PO_4 buffer

(G) Buffer for circular dichroism studies

5 mM Potassium phosphate buffer

5 mM K_2HPO_4 buffer, with pH adjusted to 7.0 by 5 mM KH_2PO_4 buffer

(It could be prepared from diluting the 50 mM potassium phosphate buffer.)

References

Ambler, R. P. (1980), The structure of beta-lactamases, *Philos Trans R Soc Lond B Biol Sci* 289; pp321-31.

Ambler, R. P.; Coulson A. F.; Frere J. M.; Ghuysen J. M.; Joris B.; Forsman M.; Levesque R. C.; Tiraby G. and Waley S. G. (1991); A standard numbering scheme for the class A beta-lactamases, *Biochem J*; 276; pp269-70.

Aplin R. T.; Baldwin J. E.; Schofield, C. J. and Waley S. G. (1990), Use of electrospray mass spectrometry to directly observe an acyl enzyme intermediate in beta-lactamase catalysis, *FEBS Lett.;* 227(1-2); pp212-214.

Bach H.; Mazor Y.; Shaky S.; Shoham-Lev A.; Berdichevsky Y.; Gutnick D. L.; Benhar I. (2001), *Escherichia coli* maltose-binding protein as a molecular chaperone for recombinant intracellular cytoplasmic single-chain antibodies, *J Mol Biol*; 312(1); pp79-93.

Banerjee S.; Pieper U.; Kapadia G.; Pannell LK; Herzberg O. (1998), Role of the omega-loop in the activity, substrate specificity, and structure of class A beta-lactamase, *Biochemistry;* 37(10)*;* pp3286-96.

Baneyx F. (1999), Recombinant protein expression in *Escherichia coli*, *Curr Opin Biotechnol;* 10; pp411-21.

Castillo R.; Silla E. and Tunon I. (2002), Role of protein flexibility in enzymatic catalysis: quantum mechanical-molecular mechanical study of the deacylation reaction in class A beta-lactamases, *J Am Chem Soc;* 124(8), pp1809-16.

Chan P. H.; Liu H. B.; Chen Y. W.; Chan K. C.; Tsang, C. W.; Leung, Y. C.; Wong, K. Y. (2004), Rational Design of a Novel Fluorescent Biosensor for Beta-lactam Antibiotics

from a Class A beta-lactamase, *J Am Chem Soc*; 126(13); pp4074-5.

Chen, C. C. H.; Herzberg, O. (2001), Structures of the Acyl-Enzyme Complexes of the *Staphylococcus aureus* Beta-lactamase Mutant Glu166Asp:Asn170Gln with Benzylpenicillin and Cephaloridine, *Biochemistry;* 40(8); pp2351-2358.

Chell R M. and Sundaram T. K. (1978), Structural basis of the thermostability of monomeric malate synthase from a thermophilic *Bacillus*, *J Bacteriol.;* 135(2); pp334-41.

Chu di Guana; Ping Lib;Paul D. Riggsa; Hiroshi Inouyeb (1988), Vectors that facilitate the expression and purification of foreign peptides in *Escherichia coli* by fusion to maltose binding protein. *Gene;* 67; pp21-30.

Damblon C.; Raquet X., Lian L. Y.; Lamotte-Beasseur J.; Fonze E.; Charlier P.; Roberts G. C. and Frere J. M. (1996), The catalytic mechanism of beta-lactamases: NMR titration of an active-site lysine residue of the TEM-1 enzyme, *Proc. Natl. Acad. Sci. USA;* 93(5); pp1747-52.

Datta R.; Das I.; Sen B.; Chakraborty A.l; Adak S.; Mandal C.; Datta A. K. (2005), Mutational analysis of the active-site residues crucial for catalytic activity of adenosine kinase from *Leishmania donovani, Biochem J.;* 387; pp591-600.

De Lorimier R. M., Smith J. J., Dwyer M. A., Looger L. L., Sali K. M., Paavola C. D., Rizk S. S., Sadigov S., Conrad D. W., Loew L., Hellinga H. W. (2002), Construction of a fluorescent biosensor family, *Protein Sci.;* 11(11); pp2655-75.

Diaz N.; Sordo T. L.; Merz Jr. K. M.; Suarez D. (2003), Insights into the acylation mechanism of class A beta-lactamases from molecular dynamics simulations of the TEM-1 enzyme complexed with benzylpenicillin, *J Am Chem Soc*.; 125(3); pp672-684.

Doi N. and Yanagawa H. (1999), Design of generic biosensors based on green fluorescent

proteins with allosteric sites by directed evolution, *FEBS Lett.;* 453(3); pp305-7.

Escobar WA; Tan AK; Fink AL (1991), Site-directed mutagenesis of beta-lactamase leading to accumulation of a catalytic intermediate, *Biochemistry;* 30(44); pp10783-7.

Escobar WA; Tan AK; Lewis ER; Fink AL (1994), Site-directed mutagenesis of glutamate-166 in beta-lactamase leads to a branched path mechanism, *Biochemistry;* 33(24); pp7619-26.

Fisher J. F.; Meroueh S. O. and Mobashery S. (2005), Bacterial resistance to beta-lactam antibiotics: compelling opportunism, compelling opportunity, *Chem Rev*; 105; pp395-424.

Ghuysen JM (1991), Serine Beta-Lactamases and Penicillin-Binding Protein, *Annu. Rev. Microbiol.*; 45; pp37-67.

Gibson RM; Christensen H; Waley SG (1990), Site-directed mutagenesis of beta-lactamase I. Single and double mutants of Glu-166 and Lys-73, *Biochem. J.*; 272; pp613-619.

Gilardi G.; Zhou L. Q.; Hibbert L.; Cass A. E. (1994), Engineering the maltose binding protein for reagentless fluorescence sensing, *Anal. Chem.*; 66(21), pp3840.

Guillaume G.; Vanhove M.; Lamotte-Brasseur J.; Ledent P.; Jamin M.; Joris B.; Frere J. M. (1997), Site-directed mutagenesis of glutamate 166 in two beta-lactamases. Kinetic and molecular modeling studies, *J Biol. Chem.;* 272(9); pp5438-44.

Greenfield N. J. (1999), Applications of circular dichroism in protein and peptide analysis, *Trends in analytical chemistry;* 18; pp238-42.

Hata M.; Fujii Y.; Ishii M.; Hoshino T. and Tsuda M. (2000), Catalytic mechanism of class A beta-lactamase. I. The role of Glu166 and Serl30 in the deacylation reaction, *Chem. Pharm. Bul.*; 48(4); pp447-53.

Healey B. G. and Walt D. R. (1995), Improved fiber-optic chemical sensor for penicillin, *Anal. Chem;* 67(24); pp4471-6.

Herzberg O. (1991), Refined crystal structure of beta-lactamase from *Staphylococcus aureus* PC1 at 2.0 Å resolution, *J Mol. Biol;* 217(4); pp701-719.

Hwang K. Y.; Song H. K.; Chang C.; Lee S. Y.; Kim K. K.; Choe S.; Sweet R. M. and Suh S. W. (1997), Crystal structure of thermostable alpha-amylase from *Bacillus licheniformis* refined at 1.7 Å resolution, *Mol Cells;* 7(2); pp251-8.

Ishii Y; Sonezaki S; Iwasaki Y; Tauchi E; Shingu Y; Okita K; Ogawa HI; Kato Y; Kondo A. (1998), Single step purification and characterization of MBP-DnaJ fusion protein and its utilization for structure-function analysis, *J Biochem (Tokyo);* 124(4); pp842-7.

Knox J. R. and Moews P. C. (1991), Beta-lactamase of *Bacillus licheniformis* 749/C. Refinement at 2 Å resolution and analysis of hydration, *J Mol Biol;* 220; pp435-55.

Knox J. R.; Moews P. C.; Escobar W. A. and Fink A. L. (1993), A catalytically-impaired class A beta-lactamase: 2 Å crystal structure and kinetics of the of *Bacillus licheniformis* E166A mutant, *Protein Engineering;* 6; pp11-18.

Kapust and Waugh (1999), Escherichia coli maltose-binding protein is uncommonly effective at promoting the solubility of polypeptides to which it is fused, *Protein Sc*i; 8; pp1668-74.

Klonis N.; Clayton A. H.; Voss E. W. Jr.; Sawyer W. H. (1998), Spectral properties of fluorescein in solvent-water mixtures: applications as a probe of hydrogen bonding environments in biological systems, *Photochem Photobiol.;* 67(5); pp500-510.

Klonis N. and Sawyer W. H. (2000), Effect of solvent-water mixtures on the prototropic equilibria of fluorescein and on the spectral properties of the monoanion, *Photochem*

Photobiol.; 72(2); pp179-185.

Kulp T. J.; Camins I.; Angel S. M.; Munkholm C. and Walt D. R. (1987), Polymer immobilized enzyme optrodes for the detection of penicillin, *Anal Chem.;* 59(24); pp2849-53.

Kotra L.P. and Mobashery S. (1999), Mechanistic and clinical aspects of beta-lactam antibiotics and beta-lactamases, *Arch. Immunol. Ther. Exp. (Warez)*; 47 (4); pp211-216.

Lamotte-Brasseur J.; Dive G.; Difeberg O.; Charlier P.; Frere J, M.; Ghuysen J. M., (1991), Mechanism of acyl transfer by the class A serine beta-lactamase of *Streptomyces albus G., Biochem J;* 279; pp213-221.

Leung Y. C.; Carol V. Robinson; Robin T. Aplin; Stephen G. Waley (1994), Site-directed mutagenesis of beta-lactamase I: role of Glu-166, *Biochem. J.;* 299; pp671-678.

Lietz E. J.; Truher H.; Kahn D.; Hokenson M. J.; Fink A. L. (2000), Lysine-73 is involved in the acylation and deacylation of beta-lactamase, *Biochemistry;* 39(17); pp4971-81.

Liu H. B. (2003), PhD thesis, The Hong Kong Polytechnic University

Marvin J. S.; Corcoran E. E.; Hattangadi N. A.; Zhang J. V.; Gere S. A.; Hellinga H. W. (1997), The rational design of allosteric interactions in a monomeric protein and its applications to the construction of biosensors, *Proc. Natl. Acad. Sci. U.S.A.*; 94(9); pp4366-4371.

Marvin J. S. and Hellinga H. W. (1998), Engineering biosensors by introducing fluorescent allosteric signal transducers: construction of a novel glucose sensor, *J. Am. Chem. Soc.;* 120 (1); pp7-11.

Matagne A; Dubus A; Galleni M; Frere JM (1999), The beta-lactamase cycle: a tale of

selective pressure and bacterial ingenuity, *Nat.Prod. Rep.;* 16; pp1-19.

Matagne A.; Lamotte-Brasseur J.; Frere J. M. (1998), Catalytic properties of class A beta-lactamases: efficiency and diversity, *Biochem. J.;* 330; pp581-598.

Minasov G.; Wang X.; Shoichet B. K. (2002), An ultrahigh resolution structure of TEM-1 beta-lactamase suggests a role for Glu166 as the general base in acylation, *J Am Chem Soc.;* 124(19); pp5333-40.

Miyanaga A.; Fushinobu S.; Ito K.; Shoun H.; Wakagi T. (2004), Mutational and structural analysis of cobalt-containing nitrile hydratase on substrate and metal binding, *Eur J Biochem;* 271(2); pp429-38.

Moews P. C.; Knox J. R.; Dideberg O.; Charlier P., Frere J. M. (1990), Beta-lactamase of *Bacillus licheniformis* 749/C at 2 Å resolution, *Proteins*; 7; pp156-71.

NICMS (2004), Beta lactam Test Methods For Use Under Appendix N And Section 6 Of The Grade "A" Pasteurized Milk Ordinance, *Milk Safety References.*
(Website: *http://vm.cfsan.fda.gov/~ear/m-a-85.html)*

Nguyen A. H.; Nguyen V. T.; Kamio Y.; Higuchi H. (2006), Single-molecule visualization of environment-sensitive fluorophores inserted into cell membranes by staphylococcal gamma-hemolysin, *Biochemistry;* 45(8), pp2570-6.

Niessen W. M. (1998), Analysis of antibiotics by liquid chromatography-mass spectrometry, *J. Chromatogr A.;* 812(1-2); pp53-57.

Nishizawa M.; Matsue T. and Uchida I. (1992), Penicillin sensor based on a microarray electrode coated with pH-responsive polypyrrole, *Anal. Chem;* 64(21); pp2642-4.

Owenius R, Osterlund M, Lindgren M, Svensson M, Olsen OH, Persson E, Freskgard PO,

Carlsson U. (1999), Properties of spin and fluorescent labels at a receptor-ligand interface, *Biophys J.;* 77(4); pp2237-50.

Papariello G. J.; Mukherji A. K.; Shearer C. M. (1973), A penicillin selective enzyme electrode, *Anal. Chem.*; 45(4); pp790-792.

Park and Sancar (1993), Environmental Effects on cell metabolism and recombinant protein production by *Bacillus substilis,* PhD thesis, Colorado State University

Pavlova I. N.; Rotanova T. V.; Zholner L. G. (1989), Aminopeptidase from a thermophilic strain of *Bacillus licheniformis, Mikrobiol Zh*.; 51(2)*;* pp47-52.

Post P. L.; Trybus K. M.; Taylor D. L. (1994), A genetically engineered, protein-based optical biosensor of myosin II regulatory light chain phosphorylation, *J. Biol. Chem.;* 269(17); pp12880-7.

Raquet X.; Lounnas V.; Lamotte-Brasseur J.; Frere J. M. and Wade R. C. (1997), pKa calculations for class A beta-lactamases: methodological and mechanistic implications, *Biophys. J.*; 73; pp2416.

Sachdev D.; Chirgwin J. M. (2003), Fusions to maltose binding protein: control of folding and solubility in protein purification, *Methods Enzymol*; 326*;* pp312-21.

Salins L. L. E.; Deo S. K. and Daunert S. (2004), Phosphate binding protein as the biorecognition element in a biosensor for phosphate, *Sens Actuators B Chem.;* 97(1); pp81-89.

Salins L. L. E.; Ware R. A.; Ensor C. M. and Daunert S. (2001), A novel reagentless sensing system for measuring glucose based on the galactose/glucose-binding protein, *Anal Biochem;* 294(1*)*; pp19-26.

Schindel C.; Zitzer A.; Schulte B.; Gerhards A.; Stanley P.; Hughes C.; Koronakis V.; Bhakdi S.; and Palmer M. (2001), Interaction of *Escherichia coli* hemolysin with biological membranes. A study using cysteine scanning mutagenesis, *Eur. J. Biochem.;* 268(3), pp800-808.

Sharff A. J.; Rodseth L. E.; Spurlino J. C.; Qiocho F. A.(1992), Crystallographic evidence of a large ligand-induced hinge-twist motion between the two domains of the maltodextrin binding protein involved in active transport and chemotaxis, *Biochem.;* 31; pp10657-63.

Spurlino J. C.; Lu G. and Qiocho F. A.(1991), The 2.3-Å resolution structure of the maltose- or maltodextrin-binding protein, a primary receptor of bacterial active transport and chemotaxis, *J. Biol. Chem.;* 266, pp5202-19.

Strynadka N. C. J.; Adachi H.; Jensen S. E.; Johns K.; Sielecki A.; Betzel C.; Sutoh K.; and James M. N. G. (1992), Molecular structure of the acyl-enzyme intermediate in beta-lactam hydrolysis at 1.7 Å resolution, *Nature;* 359; pp700 – 705.

Thevenot D. R.; Toth K.; Durst R. A.; Wilson G. S. (2001), Electrochemical biosensors: recommended definitions and classification, *Biosens. Bioelectron.;* 16(1-2); pp121-31.

Tsoi P. Y. and Yang M. S. (2004), Surface plasmon resonance study of the molecular recognition between polymerase and DNA containing various mismatches and conformational changes of DNA-protein complexes, *Biosens Bioelectron.;* 19(10); pp1209-18.

United State Food and Drug Administration (2003), *Grade A Pasteurized Milk Ordinance* (PMO), 2003 Revision, Department of Health and Human Services, Public Health Service, Food and Drug Administration.
(Homepage of US Food and Drug Administration (FDA)*: http://www.fda.gov)*

Vanhove, M.; Houba, S.; b1motte-Brasseur J.; Frere J. M. (1995), Probing the

determinants of protein stability: comparison of class A beta-lactamases, *Biochem J.*; 308 (Pt 3); pp859-64.

Waley, S. G. (1992), Beta-lactamases: mechanism of action, *In The Chemistry of Beta-Lactams*, M.I. Page, ed. (London: Chapman and Hall); pp198-228.

Zawadzke, L. E.; Chen, C. C. H.; Banerjee, S.; Li, Z.; Wasch, S.; Kapadia, G.; Moult, J.; Herzberg, O. (1996), Elimination of the Hydrolytic Water Molecule in a Class A Beta-lactamase Mutant: Crystal Structure and Kinetics, *Biochemistry;* 35(51); pp16475-16482.

Zor T and Selinger Z (1996), Linearization of the Bradford protein assay increases its sensitivity: theoretical and experimental studies, *Anal Biochem;* 236(2); pp302-8.